

ABSTRACT

Li, Zheng. Using Robotic Hand Technology for the Rehabilitation of Recovering Stroke Patients with Loss of Hand Power. (Under the direction of Dr. Edward Grant)

Stroke is the third leading cause of death in the United States. Nearly 700,000 people suffered from stroke last year and two thirds of them survived but were left with any number of disabilities, one such disability is upper extremity hemiplegia. If the hand and arm doesn't have therapy immediately after stroke, it will lose its power and muscle control, resulting in a claw like appearance and loss of function. Activities of the patient's daily living will be significantly affected. Current therapy on the affected limb in the hospital is expensive and difficult to manage due to the limited amount of resources compared to the number of patients. We introduce a pneumatic actuated wearable hand and forearm device in this thesis. It is designed according to the hand and arm kinematics. It can help the patients keep power on each finger and help maintain the coordination of different fingers to achieve daily living movements. It consists of forearm brace, rehabilitation glove and artificial muscles. The custom made artificial muscles also known as McKibben Artificial Muscles are used in antagonistic pairs to control the fingers flexion and extension. The rehabilitation device is small, lightweight, home-based, and has large force capabilities. It is also affordable to the patients due to the specially designed low-cost artificial muscles. The rehabilitation device was controlled by solenoid valves in conjunction with a Mitsubishi M32/83C 16-bit micro controller. Experiments on the pneumatic elbow brace have shown that it is capable of moving each finger from full extension to flexion, to perform actions like pinching and allows the coordinated movement of two fingers.

**USING ROBOTIC HAND TECHNOLOGY FOR THE REHABILITATION OF
RECOVERING STROKE PATIENTS WITH LOSS OF HAND POWER**

by
Zheng Li





A thesis submitted to the Graduate Faculty of
North Carolina State University
in partial fulfillment of the
requirements for the Degree of
Master of Science

ELECTRICAL ENGINEERING

Raleigh

November 3, 2003

APPROVED BY:

 Dr. Edward Grant (Chair of Advisory Committee)	 Dr. H. Troy Nagle
 Dr. John F. Muth	 Dr. Ola L. A. Harrysson

Dedication

To Wen...

Biography

Zheng Li, born on February 10, 1979 in Tianjin, China, received his Bachelor of Engineering in Automation from Tsinghua University, Beijing, China, in Spring 2001 and Master of Science in Electrical Engineering from North Carolina State University in Fall 2003 respectively. He is a student member of IEEE from 2001.

Acknowledgments

I thank my parents for their love, support and encouragement. I would like to express my sincere gratitude to my advisor Dr. Edward Grant for all of his guidance, advice and support during the course of my research and thesis writing. I am very thankful for the opportunities he has provided me. My respect for him will always be in my heart.

I am also honored to have Dr. H. Troy Nagle, Dr. John F. Muth and Dr. Ola L. A. Harrysson in my committee. I would like to thank them for their interest and encouragement throughout this research.

I also thank my partner Carey Merritt for his effort on the pneumatic actuated brace for the shoulder and elbow rehabilitation. His contribution on the air muscle performance and characters experiments and programming on M16/32 micro controller are invaluable to my research. I am grateful to him for his support and may helpful discussions.

I am thankful for Andrew Nelson's help of the idea to choose a mannequin as the hand model in the experiments. I would also like to acknowledge many past and present students in CRIM including Gregory Barlow, Chris Braly, Kyle Luthy, Leonardo Mattos, James Mulling and Tim Slusser for their help and many joyful discussions.

Table of Contents

LIST OF FIGURES	IX
LIST OF TABLES.....	XI
LIST OF ABBREVIATIONS	XII
CHAPTER 1. INTRODUCTION	1
1.1 Motivation.....	1
1.2 Thesis Goals.....	2
1.3 Outline of Thesis	2
CHAPTER 2. LITERATURE REVIEW.....	4
2.1 Rehabilitation for Stroke Patient	4
2.1.1 Physical therapy	5
2.1.2 Occupational therapy	5
2.1.3 Home-based rehabilitation	6
2.2 Rehabilitation for Hand and Forearm.....	6
2.2.1 Principle of hand and forearm rehabilitation	8
2.2.1.1 Range of Motion	8
2.2.1.2 Eye-hand coordination exercises	9
2.2.1.3 Activities of Daily Living (ADL), Functional Use.....	10
2.2.2 Rehabilitation strategy of forearm and hand.....	11
2.2.2.1 Rehabilitation for Forearm.....	11
2.2.2.2 Rehabilitation of Hand.....	12
2.3 Current Rehabilitation Robots and Gloves for Forearm and Hand Rehabilitation	13
2.3.1 Wrist Robot.....	13
2.3.2 Java Therapy – Joystick.....	14
2.3.3 SportsRAC	15
2.3.4 Hand Compressible Palm Glove.....	16
2.3.5 Composite Finger Flexion Glove.....	17
2.3.6 Other Exercise Gloves or Device.....	18
2.4 Virtual Reality Application on Rehabilitation Gloves.....	18
2.4.1 CyberGlove™	18
2.4.2 CyberGrasp™	19

2.4.3 CyberForce™	20
2.4.4 Rutgers Master II-ND Force Feedback Glove	21
2.5 Rehabilitation Robots Actuators:	23
2.5.1 DC Motors	24
2.5.2 Air Muscle:	25
2.5.3 Pleated Air Muscles	26
2.6 Robotic Hand Design	28
2.6.1 Utah/MIT Hand	30
2.6.2 NASA Hand (Robonaut Hand)	32
2.6.2 Shadow Hand	33
2.7 Literature Review Summary	34
CHAPTER 3. OUTLINE OF SYSTEM DESIGN	36
3.1 Kinematics of the Hand	36
3.1.1 Finger and thumb kinematics	36
3.1.2 Wrist Kinematics:	38
3.2 Hand Model in Hand Rehabilitation	40
3.3 Design of Brace, Glove and Muscles Attachment	42
3.3.1 Design Prototype Outline	42
3.3.2 Design of the brace for elbow by Carey Merritt	43
3.3.3 Design of the Brace, Glove and Air Muscles	44
3.3.3.1 Design of forearm brace with the elbow brace	44
3.3.3.2 Rehabilitation Glove	46
3.3.3.3 Muscle Attachment	48
3.4 Artificial Muscles Design	51
3.4.1 Pneumatic Circuit	52
3.4.2 Tubing and Connectors	53
3.4.3 Pneumatic Artificial Muscles (PAMs)	54
3.4.3.1 Pneumatic Artificial Muscle Assembly	56
3.4.4 Valves	58
3.4.5 Pressure Transducers	60
3.5 Hardware Design	63
3.5.1 M32C/83 Micro-controller	63
3.5.2 Solenoid Valve Driver Circuit	66
3.5.3 Pressure Transducer Circuit	67
3.6 Final Design	68
3.6.1 Phase I: Design for Experiment	68
3.6.2 Phase II: Design for Function	70

CHAPTER 4. AIR MUSCLE CONTROL AND CHARACTERS	73
4.1 Air Muscle Overview	73
4.1.1 PWM Control.....	73
4.1.2 Bang-Bang Control	74
4.1.3 Antagonistic Muscle Pair	75
4.2 Test Platform.....	75
4.2.1 Experimental Operation.....	76
4.2.2 Single Muscle Pulling a Constant Mass.....	77
4.2.3 Air Muscle Positioning a Wooden Arm.....	78
4.3 Test Platform Experiments with Air Muscles	79
4.3.1 Response Time.....	79
4.3.2 Valve Response Time	81
4.3.3 Leakage	82
4.3.4 Exhausting the valve	84
4.3.5 Flow Experiments and Results.....	87
4.4 Characteristics of the Air Muscle.....	88
4.4.1 Static Characteristics.....	88
4.4.2 Dynamic Characteristics	91
CHAPTER 5. REHABILITATION GLOVE EXPERIMENTATION.....	94
5.1 Experiment Design and Set Up.....	94
5.2 Experiment Results.....	96
5.3 Control of Pneumatic Brace.....	99
CHAPTER 6. CONCLUSIONS AND SUGGESTIONS FOR FUTURE RESEARCH.....	104
6.1 Conclusions.....	104
6.2 Suggestions for Future Research.....	105
CHAPTER 7. REFERENCE	109
CHAPTER 8. APPENDICES	113
8.1 Robot Kinematics.....	113
8.1.1 Homogeneous Transform Matrix.....	113
8.1.2 Link Transformation	114
8.2 Controller and Experiment Code.....	117

8.2.1 Main.h and Main.c	117
8.2.1.1 Main.h	117
8.2.1.2 Main.c	117
8.2.2 Serial1.h and Serial1.c	124
8.2.2.1 Serial1.h	124
8.2.2.1 Serial1.c	125
8.2.3 adc.h and adc.c	127
8.2.3.1 adc.h	127
8.2.3.1 adc.h	127
8.2.4 Board.h	128
8.2.5 Timer.h and Timer.c	129
8.2.5.1 Timer.h	129
8.2.5.2 Timer.c	129

List of Figures

FIGURE 2.1 JAVA THERAPY USING FORCE FEEDBACK JOYSTICK	14
FIGURE 2.2 THERAPY USING SPORTSRAC.....	15
FIGURE 2.3 HAND COMPRESSIBLE PALM GLOVE	17
FIGURE 2.4 COMPOSITE FINGER FLEXION GLOVE	17
FIGURE 2.5 CYBERGLOVE™	19
FIGURE 2.6 CYBERGRASP™	20
FIGURE 2.7 CYBERFORCE™	20
FIGURE 2.8 RUTGERS MASTER II-ND.....	21
FIGURE 2.9 RMII-ND HAPTIC CONTROL INTERFACE.....	22
FIGURE 2.10 AIR MUSCLE	25
FIGURE 2.11 PLEATED AIR MUSCLE AND ITS ‘PUMPKIN’ SHAPE	27
FIGURE 2.12 COMPARISON OF ROBOTIC HAND DESIGNS IN LAST TWO DECADES	30
FIGURE 2.13 UTAH/MIT HAND	31
FIGURE 2.14 NASA HAND (ROBONAUT HAND)	33
FIGURE 2.15 SHADOW HAND	34
FIGURE 3.1 SHADOW HAND’S FINGER AND THUMB KINEMATICS	37
FIGURE 3.2 MOVEMENTS OF THE HUMAN WRIST	40
FIGURE 3.3 MODEL OF HAND	41
FIGURE 3.4 HAND MANNEQUIN.....	42
FIGURE 3.5 REHABILITATION GARMENT DESIGNED BY CAREY MERRITT ..	44
FIGURE 3.6 DRAWING OF ALUMINUM ELBOW SECTION	46
FIGURE 3.7 REHABILITATION GLOVE	47
FIGURE 3.8 CONTROLLED SEGMENTS ON THE FINGERS AND THUMB	48
FIGURE 3.9 INSERTIONS AND ORIGINS OF THE AIR MUSCLES.....	50
FIGURE 3.10 A PNEUMATIC CIRCUIT FOR PNEUMATIC ARTIFICIAL MUSCLES	52
FIGURE 3.11 NEW AIR MUSCLE DESIGN	56
FIGURE 3.12 MATERIALS REQUIRED FOR NEW AIR MUSCLE DESIGN	57
FIGURE 3.13 LOOP FORMED ON PLUGGED END OF AIR MUSCLE	58
FIGURE 3.14 ISONIC 2-WAY SOLENOID VALVE AND MANIFOLD.....	59
FIGURE 3.15 MOTOROLA PRESSURE MPX5700GP-ND TRANSDUCER	60
FIGURE 3.16 PRESSURE TRANSDUCER RESPONSE TO PSI.....	63
FIGURE 3.17 MSV1632/83 - SKP STARTER KIT PLUS™	65
FIGURE 3.18 MEAD ISONIC® 2-WAY SOLENOID DRIVER CIRCUIT	66
FIGURE 3.19 RECOMMENDED POWER SUPPLY DECOUPLING AND OUTPUT FILTERING	68
FIGURE 3.20 MUSCLE’S ATTACHMENT IN PHASE I.....	69
FIGURE 3.21 PULLEY AND THE RUBBER RINGS ON THUMB	71
FIGURE 3.22 DESIGN OF REHABILITATION DEVICE ON PHASE II.....	72
FIGURE 4.1 ANTAGONISTIC PAIR	75
FIGURE 4.2 TEST PLATFORM	76
FIGURE 4.3 TEST PLATFORM OPTIONS	77

FIGURE 4.4 1 LB ZIP-LOCK BAG OF BEE-BEES.....	78
FIGURE 4.5 ANTAGONISTIC MUSCLE PAIR CONTROLLING THE WEIGHT OF BEE-BEES.....	79
FIGURE 4.6 RESPONSE TIME TO FILL MUSCLE AT 0 LB.....	80
FIGURE 4.7 RESPONSE TIME FOR DOUBLED 7 ¼" - 11" AIR MUSCLES	81
FIGURE 4.8 VALVE RESPONSE TIME 8 – 10 MS FOR VARIOUS PRESSURES AND A ZERO LOAD.	82
FIGURE 4.9 AVERAGE LEAKAGE FROM AIR MUSCLE.....	83
FIGURE 4.10 EXHAUSTING A 7 ¼" - 11" AIR MUSCLE.....	85
FIGURE 4.11 EXHAUSTING A 7 ¼" - 11" AIR MUSCLE AT 40 AND 70 PSI WITH DIFFERENT LOADS.....	86
FIGURE 4.12 EXHAUSTING DOUBLED 7 ¼" - 11" MUSCLES	87
FIGURE 4.13 FLOW RESPONSE CURVES COMBINED (0 LB, 1 LB, 5 LB).....	88
FIGURE 4.14 FORCE VS. LENGTH FOR 5 5/16" – 7 ½" AIR MUSCLE.....	90
FIGURE 4.15 FORCE VS. LENGTH FOR 7.25" – 11" MUSCLE USED ON PNEUMATIC BRACE.....	91
FIGURE 4.16 DAMPING FOR 60 PSI WITH 5 LB, 10 LB, 15 LB LOADS.....	92
FIGURE 4.17 DAMPING FOR 80 PSI WITH 5 LB, 10 LB, 15 LB LOADS.....	93
FIGURE 5.1 WOODEN BLOCK WITH SCREW IN THE TOP.....	94
FIGURE 5.2 ANGLE MEASUREMENTS.....	95
FIGURE 5.3 EXPERIMENTS FOR TESTING FLEXION AND EXTENSION.....	96
FIGURE 5.4 SINGLE FINGER TEST – RESPONSE TIME.....	97
FIGURE 5.5 SINGLE FINGER EXPERIMENT – RANGE OF MOTION.....	98
FIGURE 5.6 PRESSURE CHANGES DURING FLEXION AND EXTENSION.....	99
FIGURE 5.7 BRACE ANGLES USING ANTAGONISTIC PAIR.....	100
FIGURE 5.8 ANTAGONISTIC CONTROLLER SCHEMATIC.....	102
FIGURE 5.9 FLEXION AND EXTENSION USING CONTROL SCHEME.....	103
FIGURE 6.1 JREHABILITOR GUI USING JAVA3D	107
FIGURE 6.2 FILE MENU	107
FIGURE 6.3 OPTIONS MENU	108
FIGURE 6.4 CONNECTION DIALOG.....	108
FIGURE 8.1 FRAME TRANSFORMATION	113
FIGURE 8.2 HOMOGENEOUS TRANSFORM MATRIX.....	114
FIGURE 8.3 SYSTEM TRANSFORMATION MATRIX K.....	114
FIGURE 8.4 LINK OF TWO ADJACENT SEGMENTS.....	115
FIGURE 8.5 LINK TRANSFORMATION MATRIX.....	116

List of Tables

TABLE 2.1 HOME-BASED TRAINING IN ADL (ACCIDENT COMPENSATION CORPORATION).....	6
TABLE 2.2 AVERAGE NORMAL ROMS FOR FOREMAN AND HAND	9
TABLE 2.3 FRANZBLAU EYE – HAND TRACING SYSTEM.....	10
TABLE 2.4 ADVANTAGE OF AIR MUSCLES	26
TABLE 2.5 PLEATED AIR MUSCLE COMPARISON TO STANDARD AIR MUSCLES	27
TABLE 2.6 MAIN FEATURE OF ROBOTIC HAND DESIGNS IN LAST TWO DECADES	29
TABLE 2.7 SHADOW HAND RANGE OF MOTION.....	34
TABLE 3.1 LINK PARAMETERS OF FINGER AND THUMB.....	38
TABLE 3.2: MUSCLES DEAL WITH THE MOVEMENT OF THE WRIST.....	39
TABLE 3.3 TUBING AND CONNECTORS USED FOR PNEUMATIC CIRCUIT....	54
TABLE 3.4 SHADOW AIR MUSCLE PRICES	55
TABLE 3.5 PNEUMATIC ARTIFICIAL MUSCLE MATERIALS	56
TABLE 3.6 SPECIFICATIONS FOR ISONIC® V1B02RW1	60
TABLE 3.7 MPX5700GP-ND SPECIFICATIONS	61
TABLE 3.8 MUSCLE’S ATTACHMENT SEGMENTS AND FUNCTIONS	69
TABLE 4.1 FOUR STATES OF CONTROL FOR AN AIR MUSCLE USING TWO SOLENOID VALVES.....	74
TABLE 8.1 LINK PARAMETERS.....	115

List of Abbreviations

- ADC – Analog to Digital Converter
- ADLs – Activities of Daily Living
- DIP – Distal interphalangeal joint
- DOF – Degrees of Freedom
- fMRI – functional Magnetic Resonance Imaging
- GUI – Graphical User Interface
- MCU – Micro Controller Unit
- MP – Metacarpophalangeal joint
- NIH – National Institute of Health
- OT – Occupational Therapy
- PID – Proportional-Integral-Derivative Control
- PIP – Proximal interphalangeal joint
- PPAM – Pneumatic Pleated Artificial Muscle
- PT – Physical Therapy
- PWM – Pulse Width Modulation
- ROM – Range of Motion
- SportsRAC – Sports Rehabilitation and Coordination

Chapter 1. Introduction

1.1 Motivation

According to the National Stroke Association, more than 700,000 people suffer a stroke every year in the United States, making it the leading cause of adult disability. Two thirds of stroke patients can survive from the stroke disabilities (*Post-Stroke Rehabilitation* 2000, p.1), but require rehabilitation to compensate for the physical and neurological deficits associated with stroke. Paralysis is the most common type of stroke (*Post-Stroke Rehabilitation* 2000, p.3). Paralysis on the upper extremity, especially hand and forearm may limit the range of motions and disable their activities of daily living. The intensive rehabilitation therapy, such as physical therapists, occupational therapists, is carried out, but it is limited because of the time and money in the therapy (Reinkensmeyer 2002a, p.1). For most of the stroke patients in rehabilitation process, a low cost home based rehabilitation solution is in great demand. Previous researchers have used robotics in the rehabilitation device because the robotics can automated the traditional therapy methods repetitively. But the problems of robotics, such as the space, price and substantial workspace, especially the incompliance with the human hand movements are still the limitations of application (Reinkensmeyer 2001, p.1). As a result, a small, inexpensive hand and forearm rehabilitation device with human compliance is needed for stroke patients. This device will also follow the kinematics of the hand and forearm and could stimulate the corresponding muscles in the body to keep practicing in the rehabilitation. Frequently used hand movements in daily living are the main goals during the rehabilitation. In the future use of this device, a virtual reality rehabilitation

environment will be the interface between the patients and their hands and forearms to improve the control of brain on the hand and forearm.

1.2 Thesis Goals

The objectives of this thesis are to describe the:

- Current rehabilitative hand and forearm robotics and the need for an alternative.
- Current robotic hand design and the model of hand and forearm based on their kinematics.
- Design and construction of the pneumatically controlled glove and forearm brace.
- Design and construction of the pneumatic control interface in conjunction with the MCU.
- Development and implementation of control software for MCU control of the pneumatic rehabilitation device.
- Demonstration of the functionality of the rehabilitation device showing the range of motion and movements of daily living accomplished by the device.

1.3 Outline of Thesis

In Chapter 2, the literature on stroke rehabilitation is reviewed. In this literature review, the main focus will be on the rehabilitation of the hand and forearm because of the important uses in the activities of the patient daily living. This literary review will

discuss the principles and strategy of hand and forearm rehabilitation, current medical professionals' roles and treatments for the upper extremity, the current rehabilitation robots and human to machine interface for stroke patients, actuators for rehabilitation robots, and the current research on the robotic hand design.

In Chapter 3, the kinematics of the human hand and forearm, and the outline of the system design are discussed by describing the overall future goal of this project and the hardware involved in such a system.

In Chapter 4, different control strategies of the air muscles is discussed, the test platform and the experiments designed with the custom made air muscles are made to show the performance and characters of the air muscles.

In Chapter 5, the detailed experiment and control algorithm used in the rehabilitation glove is described, and the results drawn from the experiment and the movements achieved are discussed.

In Chapter 6, conclusions are drawn and future suggestions are made for the development of a better device.

Finally, in the appendices the construction robot kinematics, joint transformation is introduced to explain the hand and forearm model in this thesis and the software for the experiments and control algorithm are given.

Chapter 2. Literature Review

2.1 Rehabilitation for Stroke Patient

The goals of rehabilitation are to help stroke survivors become as independent as possible and to attain the best possible quality of life. During rehabilitation stroke patients are helped to relearn their lost skills when part of the brain is damaged. Rehabilitation actually starts in the hospital about 24 to 48 hours after the stroke has occurred and the patient's medical condition has stabilized (*Post-Stroke Rehabilitation* 2000, p.3, Reddy, p.1742). The first steps involve promoting independent movement because many patients are paralyzed or seriously weakened. Paralysis is the most common type of stroke. Hemiplegia, one of the most common disabilities resulting from stroke, is due to brain damage on the opposing side of the brain (*Post-Stroke Rehabilitation* 2000, p.3). It may affect the face, an arm and a hand, a leg, or the entire side of the body. Suffering from hemiplegia, a stroke patient may have difficulty with everyday activities such as walking or grasping objects. Compared with paralysis, stroke patients recover neurological functionality more rapidly within the first three months of the onset of stroke (Reddy, p.1744). The medical professionals that are the most involved with helping patients recover from hemiplegia are physicians, rehabilitation nurses, physical and occupational therapists (*Post-Stroke Rehabilitation* 2000, p.8).

There are three primary means of rehabilitation: Physical therapy, Occupational therapy and Speech language pathology. The first two are the primary methods for helping hemiplegia patients.

2.1.1 Physical therapy

Physical therapy (PT) helps restore physical functioning and skills like walking and range of movement mainly by treating the motor and sensory impairments of stroke sufferers. Physical therapy firstly assesses the stroke patient's current condition and designs a specific rehabilitation program for the patient (*Post-Stroke Rehabilitation* 2000, p.10). Each rehabilitation program involves helping the patient regain the use of impaired limbs, teaching strategies to compensate for motor impairment, and teaching ongoing exercises that help patients maintain their improved state and re-learned skills (*Post-Stroke Rehabilitation* 2000, p.10). The physical therapy is 'repetitive' movements oriented. It requires coordination and balance and activities that are goal-directed like games (*Post-Stroke Rehabilitation* 2000, p.10-11). Physical therapy works on major impairments including partial or one-sided paralysis, faulty balance and foot drop.

2.1.2 Occupational therapy

Occupational Therapy also helps improve a stroke patient's motor abilities, which is the similar to physical therapy. However, occupational therapy focuses more on the patients learning and re-learning of motor skills for everyday activities like eating, drinking, housecleaning, and personal hygiene (*Post-Stroke Rehabilitation* 2000, p.11). These therapists also teach patients how to compensate for limited movements and how to change their environment to make it safer, non-obstructive, and more physically functional for them to live in (*Post-Stroke Rehabilitation* 2000, p.12).

2.1.3 Home-based rehabilitation

Although the acute-care hospital is always the first rehabilitation place, many stroke patients, and their family, prefer to return home or move into an assisted care facility. Undergoing treatment at home gives people the advantage of practicing skills and developing compensatory strategies in the context of their own living environment. Practicing the activities and skills of daily living can help a recovering patient to achieve a return to independence and normality more quickly. Table 2.1 shows the home-based training strategy for the ADL recovery by Accident Compensation Co.

Table 2.1 Home-based training in ADL (Accident Compensation Corporation)

1	Setting goals and outcomes that restore and maintain optimal return to independence in a planned and structured manner
2	Providing motivation to achieve goals and outcomes
3	Training and coaching to achieve functional independence in the following: health and hygiene, training to enable the claimant to use public transport, shopping and meal preparation, mobility, and transitional living skills

The major disadvantage of home-based rehabilitation programs is the requirement of specialized equipment. Rehabilitation equipment that is suitable for use at both the medical facility and at home is a desirable.

2.2 Rehabilitation for Hand and Forearm

Upper limb rehabilitation is an extremely important focus for rehabilitation due to the importance of using both arms for everyday activities like eating, drinking, bathing,

and using the bathroom. Normally one side of the body is affected much more than the other side, causing hemiplegia, or one-sided weakness (*Post-Stroke Rehabilitation* 2000, p.3). Hemiplegia includes unilateral motor dysfunction in the upper extremity that can severely limit a patient's functional movement control. One result of the condition is the lack of control in the forearm, hand and fingers, with 80% of acute stroke survivors losing arm and hand movement skills (Reinkensmeyer 2002a).

Spasticity is one of the 'positive' signs that occur immediately following or soon after stroke, and is attributed to over-activity of monosynaptic muscle-stretch reflexes (Rowland, 2002). This condition creates problems with everyday tasks. Loss of fine motor control in the forearm and the digits of the hand often cause the patient to stop using the affected forearm and hand, and transfer these activities to the unaffected hand. This causes an even greater loss of control in the affected upper extremity, which makes it increasingly more impaired. As a result, some of the main goals of rehabilitation of the upper extremity are restoration of motor function in the affected limb, giving improvement in ADLs, and recovery of previously performed functions (Cerullo 1986, p.101). Methods for retraining hand function are treated separately, since recovery of hand function does not always coincide with arm recovery (Pedretti, 1985).

Stroke rehabilitation involves assessment, therapy, and testing. For upper limb rehabilitation, the therapist must assess a patient's motor control, spasticity, range-of-motion, balance, and a patient's ability to tolerate exercise (Cerullo 1986, p.99). Once a patient is assessed the therapist will design a therapy program to improve the patient's condition. Finally, the patient's recovery is tested using one or more of the standard tests

like the Fugl Meyer test (Fugl-Meyer 1980) or the Functional Independence Measure (FIM).

2.2.1 Principle of hand and forearm rehabilitation

The effect of hand and forearm rehabilitation and treatment focus on:

- Range of motion
- Strengthening and coordination exercises
- Activities of daily living
- Functional use

2.2.1.1 Range of Motion

Range of motion (ROM) is a measurement of the extent to which a joint can go through all of its normal range of movements. It is a useful index to measure the rehabilitation of all stroke patients. It is the normal amount a specific joint can be moved. Two range of motion exercises exist in rehabilitation therapy, passive and active. "Passive" range of motion exercises are those in which the therapist actively helps the patient move a limb repeatedly, whereas "active" exercises are performed by the patient with no physical assistance from the therapist.

Normal range of motion does vary with body habits, age and genetic background, but the following ranges in table 2.2 are reasonable to use as a reference:

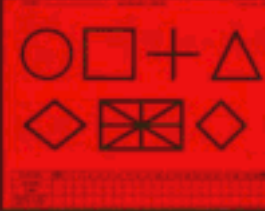
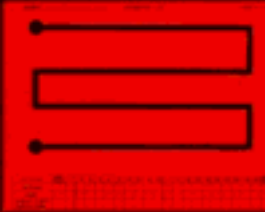
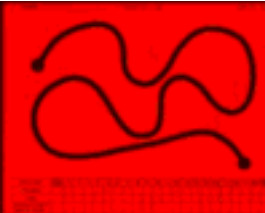

Table 2.2 Average normal ROMs for Foreman and Hand

Joint		ROM	
Elbow	Flexion	0° - 145°	
	Extension	0°	
Forearm	Pronation	0° - 70°	
	Supination	0° - 85°	
Wrist	Flexion	0° - 75°	
	Extension	0° - 70°	
	Radia	0° - 20°	
	Ulnar	0° - 35°	
Thumb	Basal joint	Palmar Adduction	0°
		Palmar Abduction	0° - 45°
		Radial Adduction	0°
		Radial Abduction	0° - 60°
	Interphalangeal	Hyperextension	0° - 15°
		Flexion	0° - 80°
	Metacarpophalangeal	Hyperextension	0° - 10°
		Flexion	0° - 55°
Fingers DIP joints	Extension	0°	
	Flexion	0° - 80°	
Fingers PIP joints	Extension	0°	
	Flexion	0° - 10°	
Fingers MCP joints	Hyperextension	0° - 45°	
	Flexion	0° - 90°	

2.2.1.2 Eye-hand coordination exercises

Eye-hand coordination is the ability to use the eyes and hands together to accomplish a given task, such as handwriting. A number of techniques can be used to do this kind of exercises. Geometric Forms or Pursuit Patterns techniques can be employed, that place one or both hands in motion simultaneously. When Geometric forms rehabilitation exercises begin, a patient is encouraged to imitate the figures on the forms. Pursuit patterns ask the patients to follow some complex curve in the graph. The error generated is the index that determines the level of control of the muscle to the hand and the patients' eye-hand coordination ability. The Franzblau Eye Hand Tracing System, table 2.3, is a product developed by Keystone View Co., for the purpose of conducting eye-hand rehabilitation (Franzblau Tracing Pattern Sheets Webpage).

Table 2.3 Franzblau Eye – Hand Tracing System

Franzblau Tracing Pattern Sheets	Use and Application
	<p>Geometric form is a convenient test of hand-eye coordination. It also aids in developing form perception by reinforcing skills learned by template tracing.</p>
	<p>Pursuits 1 sheet is useful in testing, versatile for training. Bilateral and cross patterns can be established. Targets become smaller from top to bottom.</p>
	<p>Pursuits 2 (curved lines) is for testing and training perceptual motor skills; a handy aid in amblyopia therapy. It is offered in three levels of complexity.</p>
	<p>Pursuits 3 (mazes) is for advanced skills testing and for developing binocularity, hand-eye coordination, and directionality.</p>

2.2.1.3 Activities of Daily Living (ADL), Functional Use

ADL include mobility, self-care, management of environmental hardware and devices, communication, and home management activities, such as dressing, feeding, toileting and some other basic activities. ADL is very important to stroke patients, without it they lose their independence and even experience feelings of infantilism. Training ADLs requires that the therapist tailor exercises to the patients learning style

and ability (Pedretti 1985, p.143). The therapist will break most activities down into smaller steps and slowly demonstrate and assist with each step (Pedretti 1985, p.143). During therapy these activities are repeated several times “to achieve skill, speed, or retention of learning” (Pedretti 1985, p.143). Achieving both basic and complex hand and forearm function in this method helps the patient regain their ADL. So it is very important to assess and determine problems and treatment objectives and provide training or equipment for the stroke patients to achieve their function use.

The function use of hand and forearm include: Keeping full extension, Hand Grasping, Hand Holding, Wrist Flexion and Extension, Wrist Rotation.

2.2.2 Rehabilitation strategy of forearm and hand

Rehabilitation experts commonly agree that the most important element in any rehabilitation program is a carefully directed, well-focused, repetitive practice (Woldag, 2002). This is the same kind of practice used by all people when they learn a new skill, such as playing the piano or pitching a baseball. Even when a stroke is in the "chronic" stage, individuals can be trained through repetitive motions to improve finger control, which translates into finger grasp and release, two very functional tasks. Evidence from functional Magnetic Resonance Imaging (fMRI) indicates that this increase in functionality is accompanied by brain reorganization (Carey, 2002).

2.2.2.1 Rehabilitation for Forearm

For forearm rehabilitation, the training procedures are geared to the patient’s recovery stages (Pedretti 1985, p.213).

- Stage 1: Eliciting muscle tone and the synergy patterns on a reflex basis.
- Stage 2: Passive movement, maintaining ROM of forearm and provide feedback for the desired patterns of movement.
- Stage 3: Facilitation provided through resistance to voluntary motion and repetition without facilitation
- Stage 4: Mix forearm motion with motion from the upper arm and hand
- Stage 5: Achieve ease in combinations and isolated motion and increase speed of movement.

2.2.2.2 Rehabilitation of Hand

Hand rehabilitation has a different timetable to that of arm recovery. Different goals are set in a hand rehabilitation treatment program (Pedretti 1985, p.214). Because the normal association between wrist and hand motion is disturbed, wrist rehabilitation is also considered to be part of hand recovery (Pedretti 1985, p.143).

- Goal 1: Achieve mass grasp and wrist fixation for grasp.
- Goal 2: Achieve active release of grasp.
- Goal 3: Achieve active extension for each finger with resistance.
- Goal 4: Alternate fist opening and closing and achieve voluntary hand extension and flexion.

2.3 Current Rehabilitation Robots and Gloves for Forearm and Hand Rehabilitation

In the past several decades, some rehabilitation methods and equipment have been designed especially for forearm and hand rehabilitation. Some of the designs interrelated with the whole arm rehabilitation.

- Wrist Robot
- Java Therapy – Joystick
- SportRAC
- Hand Compressible palm Glove
- Composite Finger Flexion Glove
- Other hand exercise Gloves

2.3.1 Wrist Robot

The MIT Wrist Robot is designed for the wrist rehabilitation. Because of the different kinematics of the hand and arm, the designs of rehabilitation devices typically focus on either the hand or arm. But except for placing a splint on the wrist-hand, for support, not enough attention is paid to the joint of arm and hand-wrist. This robot is still in the developmental phase and only exists as a design solution for wrist therapy. The Wrist Robot was designed to have low impedance to a free range of motion and to accommodate all the possible motions of the wrist (Krebs 2001, p.1336). The design specifies the use of brush-less DC motors. These actuators use gearing and an incremental high-resolution encoder for feedback (Krebs 2001, pp. 1337-8).

2.3.2 Java Therapy – Joystick

The Java Therapy – Joystick is a cost effective solution to robotic rehabilitation that uses a commercial force feedback joystick in combination with online games designed specifically for hemiplegic stroke rehabilitation patients. A special hand-wrist orthosis is mounted on the joystick to give the patient support for playing the games. During these games, the force feed back on the joystick is controlled through a Java applet, Immersion Corporation's provided to FEELtheWEB software, which is an ActiveX control for browsers and can receive function calls through HTML (Reinkensmeyer 2001, p.3).



Figure 2.1 Java Therapy using Force Feedback Joystick

Java Therapy tests speed, coordination, strength, and finger speed. The speed test requires the patient to move the cursor into a target as fast as they can. The coordination test requires the user to trace a figure eight while software measures the tracing error. The strength test requires the user to hold the joystick still while the software applies forces to the joystick and measures the distance moved. The Java Therapy games are: Breakout therapy (Pong), Blackjack card game, Othello, and TailGunner (Reinkensmeyer 2001,

p.4). The patient's progress is monitored throughout their playing of these games and is displayed in several progress reports.

Java Therapy testing consisted of several stroke patients using the Joystick from home three times a week for four weeks (Reinkensmeyer 2001, p.3). One patient improved his movement speed by 40% and performed over 1600 targeted movements in the speed test (Reinkensmeyer 2001, p.5). Since this rehabilitator is web-based and uses a low-cost commercially available force feedback joystick, large populations now have access to exercise programs for stroke rehabilitation and testing.

2.3.3 SportsRAC

Sports Rehabilitation and Coordination (SportsRAC) is a commercial product of Performance Health Technologies, Co. (SportsRAC Webpage). It consists of a brace whose height can be adjusted, and an exoskeleton garment for wearing on the forearm. The garment connects to the brace using a rotational joint. It can change the angle between the flat of patients forearm and hand and the horizontal level in $[-90^\circ, 90^\circ]$. A goniometer is attached on the joint to measure the movement of forearm and hand.



Figure 2.2 Therapy using SportsRAC

When using the SportsRAC, patients are positioned so that the injured limb is supported throughout the training process, thus eliminating stress to the injured or surgically treated area. Patients use their limbs and joints with controlled, limited-range movements to manipulate a pointer that moves across a computer's display. This exercise activates and stimulates neural pathways between the joint and the brain at a time when they would otherwise remain inactive. The SportsRAC Joint Rehabilitation System is its "non-resistive" therapy, allowing for pain- and stress-free joint exercise during all phases of post-operative and non-operative rehabilitation.

A computer can be also used with SportsRAC to memorize and analyze the recorded data. It is connected with the exoskeleton garment by cable interface. Along with virtual reality technology, it can simulate the movement of the forearm and hand.

2.3.4 Hand Compressible Palm Glove

This kind of Hand Rehabilitation Glove has a compressible substance coupled to the palm portion. It provides resistance to the closing or grasping motion of the hand. There are also small compressible substances on the back of the hand and fingers, which provides resistance to the hand extension. The device is instrumented to provide signals proportional to the movement of the digits of the hands. A means is also provided to measure the pressure applied by one or more of the digits of the hand using the compressible substance. Figure 2.3 shows the design sketch of the glove.

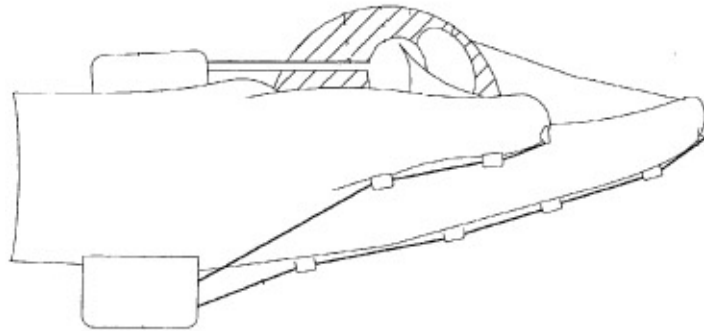


Figure 2.3 Hand Compressible Palm Glove

2.3.5 Composite Finger Flexion Glove

The finger flexion glove forces are applied to the fingers of a human hand to achieve improved hand function. The glove has tabs attached to its fingertips and a removable attachment to a crossbar. The orientation of the outrigger in reference to the longitudinal axis of the crossbar may be selectively fixed at one end of the crossbar, providing ease of force adjustment during the time the device is worn by the patient. Figure 2.4 shows the design sketch of the glove.

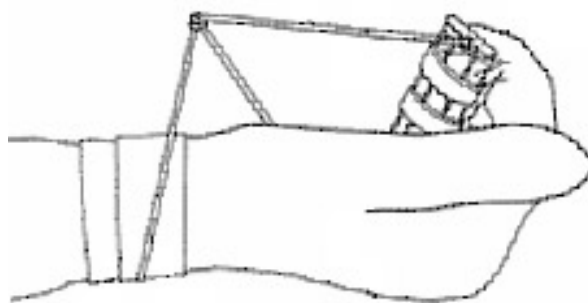


Figure 2.4 Composite Finger Flexion Glove

2.3.6 Other Exercise Gloves or Device

There are also other types of devices called Hand Exercise Devices. These devices are applied to a minor injury stroke patient or to the non-stroke humans for the purpose of exercising maintain flexibility and power.

2.4 Virtual Reality Application on Rehabilitation Gloves

CyberGlove™, CyberGrasp™, and CyberForce™ are a three-in-one device based on the virtual reality technology that senses the position of individual fingers and to give hand and arm force feedback. These products are from Immersion Corporation (Immersion 2002).

2.4.1 CyberGlove™

The CyberGlove™ is a fully instrumented glove that provides up to 22 high-accuracy joint-angle measurements. It uses proprietary resistive bend-sensing technology to accurately transform hand and finger motions into real-time digital joint-angle data. The VirtualHand™ Studio software converts the data into a graphical hand which mirrors the subtle movements of the physical hand (Immersion 2002).



Figure 2.5 CyberGlove™

2.4.2 CyberGrasp™

The CyberGrasp™ is a lightweight, force-reflecting exoskeleton that fits over a CyberGlove™ and adds resistive force feedback to each finger. With the CyberGrasp™ force feedback system, users are able to feel the size and shape of computer-generated 3D objects in a simulated “virtual world.”

Grasp forces are produced by a network of tendons routed to the fingertips via the exoskeleton. There are five actuators, one for each finger, which can be individually programmed to prevent the users’ fingers from penetrating or crushing a virtual solid object. The high-bandwidth actuators are located in a small actuator module, which can be placed on a desktop. Additionally, since CyberGrasp™ does not provide grounded forces, the actuator module can also be worn as a GraspPack™ backpack, for portable operation, dramatically increasing the effective workspace.

The device exerts grasp forces that are roughly perpendicular to the fingertips throughout the range of motion, and forces can be specified individually. The CyberGrasp™ system allows for a full range-of-motion of the hand and does not obstruct the wearer's movements. The device is fully adjustable and designed to fit a wide variety of hands.



Figure 2.6 CyberGrasp™

2.4.3 CyberForce™

CyberForce™ is a force feedback armature that not only conveys realistic grounded forces to the hand and arm but also provides six-degree-of-freedom positional tracking that accurately measures translation and rotation of the hand in three dimensions. CyberForce™ is an option designed to work with CyberGrasp™, the award-winning, lightweight, force-reflecting exoskeleton that fits over a CyberGlove™ and adds resistive force feedback to each finger. Using CyberForce™ together with CyberGrasp™, one can literally "hang his hand" on a virtual steering wheel, sense weight and inertia while picking up a "heavy" virtual object, or feel the impenetrable resistance of a simulated wall. CyberForce™ allows user to intuitively explore and interact with simulated graphical objects via the most natural interface possible – the human hand.



Figure 2.7 CyberForce™

Using the CyberForce™, stroke patients can practice some ADLs with the virtual objects. This device can also be used as a rehabilitation device to the patients' hand recovery. All products from Immersion Co. are designed to be a use together, the price of all the equipment using for rehabilitation is high and may not be affordable by most stroke patients.

2.4.4 Rutgers Master II-ND Force Feedback Glove

The Rutgers Master II-ND (RMII-ND) is an improved version of the Rutgers Master II force feedback glove. Since all the mechanics of the RMII-ND are placed in the palm, the RMII-ND is limited to a virtual environment i.e. rehabilitation using real objects is not an option.

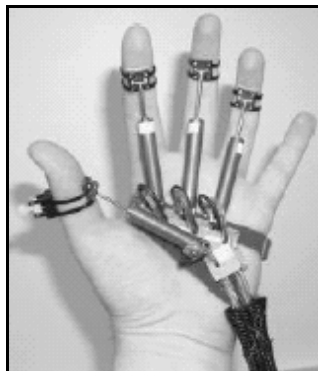


Figure 2.8 Rutgers Master II-ND

The RMII-ND connects custom pneumatic actuators between the palm and thumb, index, middle, and ring fingers as shown in figure 2.8 (Bouzit 2002). These actuators can apply up to 16 N of force when pressurized at 100 PSI and are driven by

pneumatic pulse-width modulated servo-valves, which result in better force control (Bouzit 2002, Jack 2001, p.308).

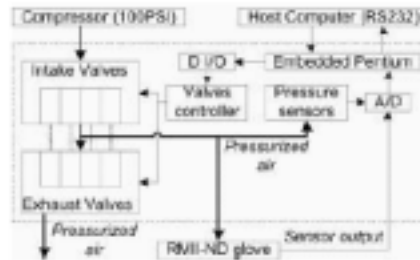


Figure 2.9 RMII-ND Haptic Control Interface

Sensors are placed in the palm measure the finger-actuator positions for feedback control. The RMII-ND uses two Hall-effect sensors to measure flexion, abduction, and adduction angles and one infrared sensor to measure piston translation inside the air cylinder for each actuator (Bouzit 2002). Since these sensors are non-contact sensors, they do not produce any oppositional frictional forces that may prevent the user from moving freely (Bouzit 2002).

The haptic control interface (figure 2.9) utilizes an embedded 233MHz Pentium PC with a PC104 bus. This embedded computer uses Pulse-Width Modulation (PWM) running at a frequency of 500 Hz to control the solenoid valves that are connected to the pneumatic actuators on the fingers (Bouzit 2002). The embedded computer communicates with a host computer using an RS-232 serial port that runs at baud-rates from 38,400 to 115,200 bps (Bouzit 2002). The host computer sends action commands and receives sensor data to and from the embedded computer. The sensor readings are

used to relate the physical environment to the virtual environment displayed on the computer screen.

2.5 Rehabilitation Robots Actuators:

In order to help patients moving in the rehabilitation process, actuators are used to drive the movement or rotation of parts of rehabilitation robots. Current rehabilitation robots use revolute joints to connect two links of the body. According to the current actuators, we could choose from different types of actuators such as pneumatic, hydraulic, piezoelectric, and DC motors. But since our application is used for the hand and forearm rehabilitation of the stroke patients, the actuator needs to have the following characters:

- Light weight and portable
- Home-based, easy to get the resources
- Small and easy to implement for the hand and finger
- No potential harm to the human body or circumstance
- Input-output linearity and low hysteresis
- Compliance

The hand and forearm rehabilitation robots are needed to be small, light weight and portable in order to make the equipment comfortable to implement on the hand and forearm (Daerden 2001a, p.738). In order to make the design more useful, the design allows use outside the hospital or recovery center. The resources to drive the actuator need to be readily available. In this situation, low voltage or pneumatic actuators are good choices. The hand and forearm have the most joints in the human's body. Actuators

should provide good input-output linearity and low hysteresis to guarantee every finger or ever joint on a finger can reach the desired position every time whenever flexion or extension (Daerden 2001a, p.738). Compliance is also an important characteristic in actuators for hand and forearm rehabilitation when the actuator needs to store and release energy, i.e. the actuator can make the robot responds to the patient more naturally and its movement needs to let the patient feel comfortable. According to the above discussion, two main actuators will be examined for hand and forearm rehabilitation.

2.5.1 DC Motors

The DC motor is a universal controller and can be used for rotational displacement. For the rehabilitation application, the requirements of low velocity and high force/torque are well suited to DC motor use. But DC motor power is a trade-off because power $P = \tau \cdot \omega$, where τ is torque and ω is rotational speed. To give high power at (1) slow rotational speeds, torque must be large, and (2) high rotational speeds, torque must be small. This will limit the torque with a desired rotational velocity and an upper limit of the motor power. The ability to manually drive a robot without any opposing force, with substantial actuator power is hard to achieve because adding gears to a motor increases the frictional resistance of the gear train (Reinkensmeyer 2002b, p.12). So, in order to achieve the desired velocity and power, it needs to have a larger motor. But this will also make the DC motor big and heavy, which will make the design to have less application.

DC motor also has the problem of the compliance. It has the shortage of the movement like a human being since the inner design of it is rigid. If a patient continues to

have the rehabilitation on a DC motor, he may have more muscles at the end, but still can not hold a cup to drink coffee because DC motor is not precise enough (Daerden 2001a, p.738).

DC motors not only have trouble with meeting the ideal requirements for a robotic rehabilitator but they are also difficult to control. Force control is a major complication for DC motors because they require “complicated and state-of-the-art feedback control and sensory equipment to achieve this” (Daerden 2001a, p.738).

2.5.2 Air Muscle:

Air Muscles consist of a rubber tube contained within a braided sleeve. Figure 2.10 shows the air muscle filled with high pressure air. When inflated the rubber tube balloons, and is eventually constrained by the braided sleeve, this action causes the air muscle to shorten in length, and as such it replicates, in part, the action of the human muscle. Air Muscles have a power-to-weight ratio as large as 400:1, vastly outperforming both pneumatic cylinders and DC motors, which can attain a ratio approximately 16:1 at best. Air Muscles are normally operated using compressed air in the 0-60psi (0-4 bar) range.



Figure 2.10 Air Muscle

Table 2.4 Advantage of Air Muscles

Advantage	Description
Lightweight	Weigh as little as 10g - particularly useful for weight-critical applications.
Low cost	Cheaper to buy and install than other actuators and pneumatic cylinders.
Smooth Movement	Air muscles have no 'stiction' and have an immediate response. This results in smooth and natural movement.
Flexible	Can be operated when twisted axially, bent round a corner, and need no precise aligning.
Powerful	Produce an incredible force especially when fully stretched
Damped	Air Muscles are self-dampening when contracting (speed of motion tends to zero), and their flexible material makes them inherently cushioned when extending.
Compliant	Can be used to store and release energy during separate phases of running due to gas compressibility and the dropping force-displacement characteristics (Daerden 2001a, p.738, Daerden 2001b, p.1958).
High Force/Low Speeds	Can operate with high forces at low speeds (Daerden 2001a, p.738).
Easy to install	Loops in the ends of the air muscle can attach to just about anything. Can connect directly to the joint without any gears (Daerden 2001b, p1958).

*Table adapted from Shadow Robot Company Website

The high power/weight ratio apart air muscles have shortcomings. Air muscles use high air pressure, so there is always friction existing between the inner rubber tubing and outer braiding when the tubing expands. This is particularly so at the ends of the muscle, where friction can be more random and unpredictable. Such friction can wear the rubber tubing and may even cause sudden bursting. Friction also causes hysteresis during the air muscle expansion and extraction. No linear relationship exists between force and displacement of air muscles, only pressure and force has linear relationship. Friction can be reduced by paying attention to air muscle design, making process and maintaining to air muscles. Pressure sensors can be used for a feedback in the motion control system (Shadow Robot Co. 2002).

2.5.3 Pleated Air Muscles

Pleated Air Muscles (PPAMs) were recently developed by the Department of Mechanical Engineering at Vrije Universiteit Brussel (Daerden 2001b, p.1958). PPAMs

are an enhancement of the standard air muscle and are distinguished by their pleated design for the hollow outer netting. The pleated membrane or sleeve is made out of Kevlar®49 quasi-unidirectional fabric lined with a polypropylene film which gives it a high tensile stiffness and makes the muscle gas-tight (Daerden 2001a, p.740). Since this pleated membrane has its fold faces laid out in a radial pattern, there is no friction byproduct during the folding-unfolding stage (Daerden 2001a, p.739). This unfolding of the membrane makes the PPAM looks like a pumpkin when it is fully contracted and allows for maximum displacements of up to 50% of the initial length (figure 2.11) (Daerden 2001a, p.739, Daerden 2001b, p.1958). The benefits of removing the friction component compared to standard air muscles are listed in table 2.5 below.



Figure 2.11 Pleated Air Muscle and its ‘pumpkin’ shape

Table 2.5 Pleated Air Muscle comparison to Standard Air Muscles

Pleated Air Muscles	Standard Air Muscles
No hysteresis	Hysteresis
Maximum displacement 50%	Maximum displacement 20%-30%
Wide range of gas pressures 10 kPa - 300 kPa/1.45 PSI - 43.5 PSI	Threshold at 90 kPa/13 PSI if hard rubber Only low pressures if soft rubber
Requires simple PI control	Requires more complex control algorithms

No rubber tube necessary	Rubber tube wears out
--------------------------	-----------------------

*Comparison derived from Daerden's "Pleated Pneumatic Artificial Muscles: Compliant Robotic Actuators 2001"

2.6 Robotic Hand Design

There is a long history of robot hand research. As early as 1965, an artificial hand (Belgrade Hand) was developed by Rajko Tomovic at the University of Belgrade, Yugoslavia. It was one of the earliest attempts to equip an artificial limb with a sense of touch. Its fingertips had pressure-sensitive switches that were activated by contact with an object. In cooperation with the University of South California (USC), a new Belgrade Hand was developed in 1988 and is now named the Belgrade/USC Hand.

From the 1980s, there was an increased activity on robotic hand development, and this trend continues today. Several robotic hands have been developed over the past two decades. They are designed differently and the results are not easily comparable for the purpose of declaring one design better than another. Table 2.6 shows some of the noticeable examples of robotics hands and the main features of the mechanical designs.

Table 2.6 Main feature of Robotic Hand designs in last two decades

Column 1: Design name	Column 2: Research institute	Column 3: Year	Column 4: Number of Fingers (Thumb)	Column 5: Number of Joints	Column 6: Degree of freedom	Column 7: Actuation Type	Column 8: Reference
1	2	3	4	5	6	7	8
Okada Hand	Electro-technical laboratory, Japan	1979	4 (Y)	11	11	Electrical revolute motors	Okada 1986
Stanford/JP L Hand	Stanford University	1983	3 (N)	9	9	Electrical revolute motors (DC)	Salisbury 1983 Chase 1997 Fearing 1987
Utah/MIT Hand	Utah University	1985	4 (Y)	16	16	Pneumatic actuator	Jacobsen 1986 McCammon 1990 Johnston 1996
Belgrade/USC Hand	University of Belgrade	1988	5 (Y)	18	4	DC Motors	Bekey 1990
Barret Hand	Barret Technology, Inc	1988	4 (N)	8	4	Electrical revolute motors (Brushless)	Townsend 2000 Barret hand webpage
UB Hand II	Bologna University	1992	4 (N)	13	13	Electrical revolute motors	Melchiorri 1992 Melchiorri 1993 Bonivento 1993
DLR Hand I	DLR-German Aerospace Center	1997	4 (Y)	16	13	Electrical revolute motors	Butterfass 1999 Liu 1999
LMS Hand	Université de Poitiers	1998	4 (Y)	17	16	Electrical revolute motors	Gazeau 2001
DIST Hand	DIST-Università di Genova	1998	5 (Y)	16	16	Electrical revolute motors	Caffaz 1998 Dist hand webpage
Robonaut Hand	NASA Johnson Space Center	1999	5 (Y)	22	14	Electrical revolute motors (Brushless)	Lovchik 1999 Ambrose 2000 Robonaut webpage
Tokyo Hand	University of Tokyo	1999	5 (Y)	16	12	Pneumatic muscles	Lee 1999
DLR Hand II	DLR-German Aerospace Center	2000	4 (Y)	17	13	Electrical revolute motors	Butterfass 2001
Tuat/Karlsruhe Hand	Tokyo and Karlsruhe Universities	2000	5 (Y)	24	1	Electrical revolute motors	Fukaya 2000
Ultralight Hand	Research Center of Karlsruhe	2000	5 (Y)	18	13	Pneumatic	Kawasaki 2001
Gifu Hand	Gifu Univeristy	2001	5 (Y)	20	16	Built-in DC Maxon servomotors	Jacobsen 1986 Kawasaki 1999
Shadow Hand	Shadow Robot Company Ltd.	2002	5 (Y)	23	23	Pneumatic muscles	Shadow hand webpage

From Table 2.6, the developing trend is clear, robotic hands must possess the functions as the human hands. To do this the numbers of joints on a robot hand and its' degrees of freedom must increase. Considering with the improvement of sensor

technology, robotic hands are capable of having more functions, and they work more precisely than human hands. Figure 2.12 shows the comparison of the 16 robotic hand design in size, contact surface and Kinematics.

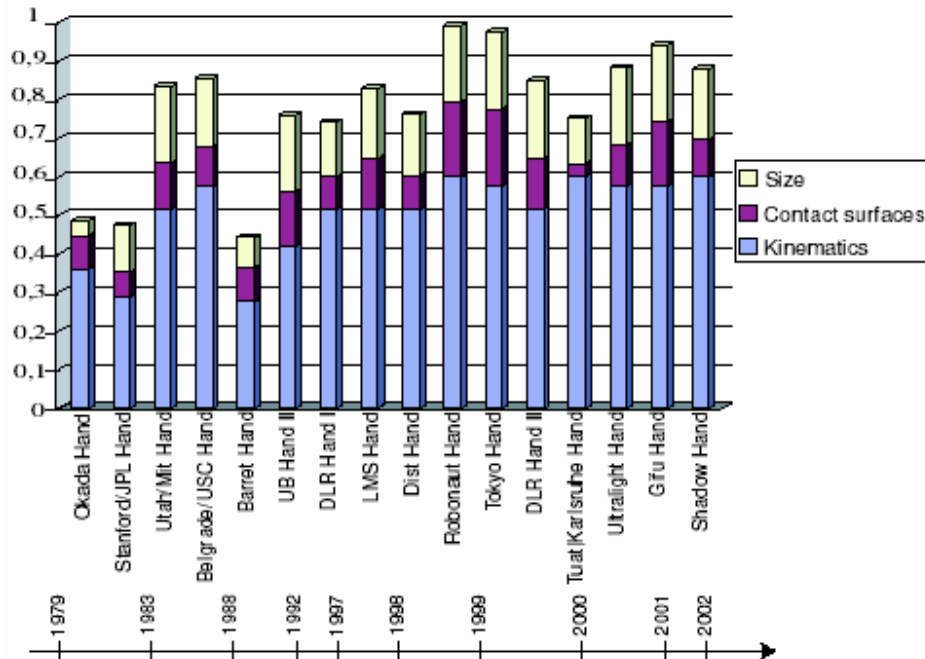


Figure 2.12 Comparison of Robotic Hand designs in last two decades

Three of these designs, the Utah/MIT Hand, the NASA Robonaut Hand and the Shadow Hand will be described in the following section.

2.6.1 Utah/MIT Hand

The Utah/MIT hand (figure 2.13) was developed by the Center for Engineering Design at the University of Utah and the Artificial Intelligence Laboratory at the Massachusetts Institute of Technology (MIT) in 1985. It was intended to function as a general purpose research tool for the study of machine dexterity (Jacobsen, etc, 1986).

The Utah/MIT hand has the same size as the human's hand. It has four fingers (three fingers and a thumb) in a very anthropomorphic configuration. Each finger has four degrees of freedom and can move at five times of human speed, including the grip of a firm handshake. There are totally 17 links (1 on the wrist, 4 on each of the 4 fingers) on the Utah/MIT hand. Among them, 16 joints on the fingers have degrees of freedom. Their bending and extension are controlled by cable driven by pneumatic pistons, which is integrated into the hand. By utilizing the finger tendon forces the grasp can react, to some degree, to the object being grasped. On the Utah/MIT hand, there are antagonistic tendons for each finger joint. The antagonistic tendons and the large amount of coupling between finger joints have complicated the work on the Utah/MIT hand (Jacobsen et al 1986). There are 4 kinds of sensors on the hand, motor position sensors, joint position sensors, tendon tension sensors and tactile array sensors. According to the signals detected, movement of the hand can be illustrated.

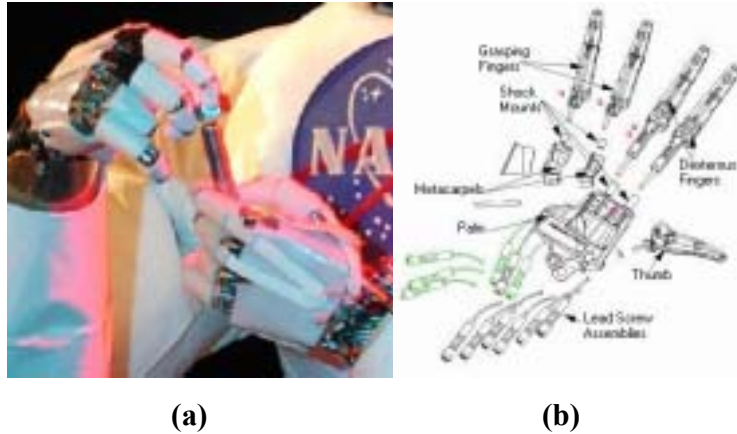


Figure 2.13 Utah/MIT hand

2.6.2 NASA Hand (Robonaut Hand)

The NASA hand was designed in 1999 by C.S. Lovchik in Robotics Technology Branch of NASA Johnson Space Center and M.A. Diftler in Automation and Robotics Department of Lockheed Martin Corporation. It was developed for space extravehicular activity (EVA) use. It is close in size and capability to a suited astronaut's hand (Lovchik 1999). This five finger hand combined with its integrated wrist and forearm has fourteen independent degrees of freedom. It consists of a forearm which houses the motors and drive electronics, a two degree of freedom wrist, and a five finger, twelve degree of freedom hand. The forearm, measures four inches in diameter at its base and is approximately eight inches long. It houses all fourteen motors, 12 separate circuit boards, and all of the wiring for the hand. The dexterous finger set consists of two 3 degree of freedom fingers (pointer and index) and a 3 degree of freedom opposable thumb. The grasping set consists of two, 1 degree of freedom fingers (ring and pinkie) and a palm degree of freedom. All of the fingers are shock mounted into the palm.

Overall the hand is equipped with forty-three sensors not including tactile sensing. Each joint is equipped with embedded absolute position sensors and each motor is equipped with incremental encoders (Lovchik 1999). The Utah/MIT hand has antagonistic tendons for each finger joint on the hand, but on NASA hand there is just one tendon sensor for each finger. This reduces the amount of coupling between finger joints which complicated the Utah/MIT hand. Figure 2.14(a) shows the working NASA hand, (b) shows an exploded diagram of the NASA hand.



(a) **(b)**
Figure 2.14 NASA Hand (Robonaut Hand)
(a) Hand is working (b) Components of the hand

2.6.2 Shadow Hand

Shadow hand (figure 2.15) is a product of Shadow Robot Company Ltd in 2002. Different from the DC motor used by NASA hand, Shadow hand is driven from a block of pneumatic artificial muscles mounted behind the hand on the "forearm". Air Muscles are used to provide compact light-weight compliant actuation for the system. These are packed into the forearm and jostle for space. This implementation strategy significantly reduces the design work necessary with the actuator mounting, and makes it relatively simple to, for example, upgrade a movement by replacing an actuator with a larger and more powerful one, as proved necessary for the wrist. Systems that have used other actuators seem to have had problems packing the actuators within the envelope of the robot or have used a reduced number of actuators and complex mechanical linkages to give the impression of more actuators. The use of muscles allows a very large number of actuators to be used; however, this requires a large valve manifold (Shadow Co. 2002). The inherent compliance of the muscles significantly reduces control issues for the hand, and has enabled the users to obtain impressive results with open-loop finger control.

Shadow hand has the maximum joints numbers and degrees of freedom in existing robotic hands. It has 4 fingers (4 degrees each), a thumb (5 degrees) and a wrist (2 degrees), which sum up to 23 degrees of freedom. It is equipped with hall-effect based joint position sensors and motor effort sensors. Table 2.7 shows the data about the Shadow Hand:

Table 2.7 Shadow Hand Range of Motion

Fingers	Thumb	Wrist
4 degrees of freedom. Distal & Middle: 0 - 90 degrees Proximal: -15 - 90 degrees Base: -15 - 15 degrees (one muscle)	5 degrees of freedom. Distal -10 - 90 degrees Middle: 0 - 90 degrees Middle2: -10 - 10 degrees Proximal: 0 - 90 degrees Base: 20 - 80 degrees	2 degrees of freedom. Flex: -90 - 45 degrees Palm ad/ab: -10 - 45 degrees



Figure 2.15 Shadow Hand

2.7 Literature Review Summary

Post-stroke rehabilitation is a very important area because stroke is the leading cause of impairment, especially for losing control of parts of the body. Traditionally, physicians and nurses help the stroke patients to rehabilitate through exercise. This is a common way for the body to recover, especially the arm and hand. Recently, it has been

shown that rehabilitation robots can help patients to exercise by themselves and improve their forearm and hand's flexibility and function step by step. Different rehabilitation gloves are available for this purpose. The application of virtual reality technology and simulation can also be used to help patients recover their hand and forearm functions and ADLs. Different actuators were compared for rehabilitation use. Although DC motors are the most popular actuators used, these have significant disadvantages for use in the rehabilitation of hands and forearms. Pneumatic muscles are introduced as a lightweight, flexible, compliant, safe actuator with smooth movement and it can give the combination of high force and low speeds, which is just suitable for the human body rehabilitation.

Chapter 3. Outline of System Design

3.1 Kinematics of the Hand

Kinematics is the science of motion. In human movement, it is the study of the positions, angles, velocities, and accelerations of body segments and joints during motion.

Hands and wrists are pretty complex structures. They rely on an intricate system of bones, tendons, muscles, nerves, joints and ligaments to provide the sensation and movement we need to touch, grasp, hold, pinch, press and do so much more. Individuals have 27 bones in one hand (eight carpals in the wrist, and five metacarpals though your palm, and 14 phalanges in your fingers and thumb). The two lower arm bones (the ulna and radius) meet at the beginning of the wrist where they are hinged to the other wrist bones. More than 60 different muscles coordinate the movement of these bones. Two large nerves run the length of the arm to send information to your brain and to create movement and sensation.

3.1.1 Finger and thumb kinematics

Of the 16 robotics hands introduced in chapter 2, the Shadow hand has the maximum degrees of freedom in its finger, thumb and wrist. It also has the most complicate finger kinematics among the 16 hands. The kinematics of Shadow hand is described and analyzed as follows. Figure 3.1 shows the finger and thumb model of the Shadow hand. According to the description of Shadow hand, a finger and the thumb both have 4 degrees of freedom. 3 degrees come from each 3 joints of the finger or the thumb

where it can do flexion and extension. Joints 4, 5 and 6 in figure 3.1 are these joints. The other degree is at the connection of the finger or thumb and the palm. It makes the finger or thumb move left and right, just like waving. Joint 3 is this kind of joint in figure 3.1.

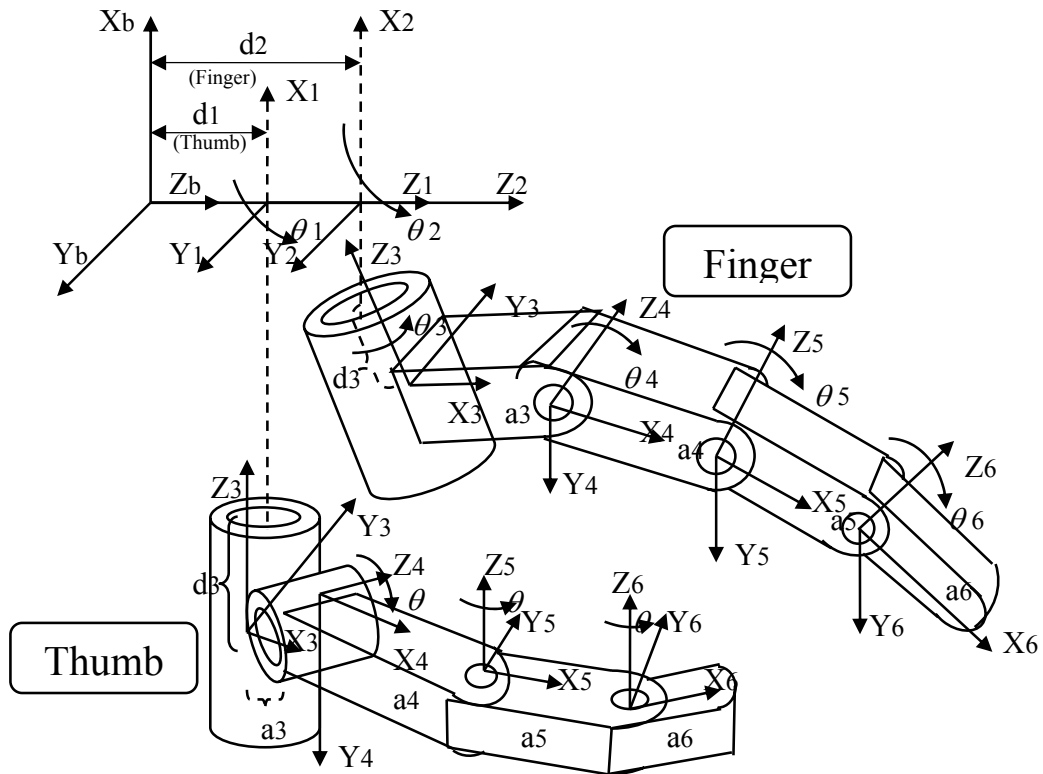


Figure 3.1 Shadow Hand's Finger and Thumb Kinematics

The hand has a thumb and four opposing fingers to the thumb. Each joint has a range of rotation which is larger than 90° and equivalent to that of a human hand. At least two of the fingers and the thumb can grasp an object. According to the Robot Kinemics description in Chapter 8, the finger and thumb transformation matrix of joint 4, 5 and 6 can be calculated by the equation 8.1 and 8.2. The link parameters are in Table 3.1

Table 3.1 Link parameters of finger and thumb

i	l_n	α_n	q_n	d_n
1 (thumb) or 2 (finger)	a_1 or a_2	0°	θ_1 or θ_2	0
3	a_3	90°	θ_3	0
4	a_4	0°	θ_4	0
5	a_5	0°	θ_5	0
6	a_6	0°	θ_6	0

Equation 8.1 Link transformation matrix

$${}^{n-1}T_n = T_n = T_z(l_{n-1})R_x(\alpha_{n-1})R_z(\theta_n)T_z(d_n) = \begin{bmatrix} c\theta_n & -s\theta_n & 0 & l_{n-1} \\ s\theta_n c\alpha_{n-1} & c\theta_n c\alpha_{n-1} & -s\alpha_{n-1} & -s\alpha_{n-1}d_n \\ s\theta_n s\alpha_{n-1} & c\theta_n s\alpha_{n-1} & c\alpha_{n-1} & c\alpha_{n-1}d_n \\ 0 & 0 & 0 & 1 \end{bmatrix}$$

Equation 8.2 System transformation matrix $K = {}^0T_1 \cdot {}^1T_2 \cdot {}^2T_3 \cdot \dots \cdot {}^{n-1}T_n$

3.1.2 Wrist Kinematics:

The wrist is a condyloid joint between the distal radius and the proximal row of carpal bones. It consists of 8 bones and 4 intrinsic and extrinsic ligaments which form complex interlocking shapes, 4 of the bones, navicular, lunate, triquetrum and pisiform, connect with the bones in the forearm which are radius and ulna. The other four bones, trapezium, trapezoid, capitate and hamate, connect with the bones in the palm, the metacarpals. The bones in forearm, wrist and palm are also connected by ligaments, volar radiocarpal ligament, dorsal radiocarpal ligament, radial collateral ligament and ulnar collateral ligament. To achieve this 3-D movement, the 8 bones produce a “link joint”

which can rotate freely. The proximal and distal form a row with scaphoid bone as a bridge. And three columns of bones make the normal movement. The center column has 3 bones: lunate bone, capitate bone and hamate bone. They control flexion and extension of the wrist. The lateral column has 3 bones: scaphoid bone, trapezoid bone and trapezium bone. They control the mobility of the wrist. The medial column has one bone named triquetrum bone. It can control wrist's rotation and the center of the rotation is the head of capitate bone.

Finger and thumb muscles are classified into two groups, extrinsic muscles and intrinsic muscles. Extrinsic muscles originate outside the hand and insert in the hand and intrinsic muscles originate inside the hand and insert in the hand. Table 3.2 shows the muscles in the wrist and their functions.

Table 3.2: Muscles deal with the movement of the wrist

Muscles	Functions
Flexor Carpi Radialis; Flexor Carpi Ulnaris	Flexes and abducts hand (at wrist)
Palmaris Longus	Flexes hand (at wrist)
Extensor Carpi Radialis Brevis; Extensor Carpi Radialis Longus	Extend and abduct hand at wrist joint
Extensor Carpi Ulnaris	Extend and abduct hand at wrist joint

*Table adapted from Upper Extremity Anatomy Webpage from University of Washington

With these connections on the wrist and muscles between the forearm and fingers, wrist's movements have flexion/extension/hyperextension, radial deviation/ulnar deviation and circumduction. Figure 3.2 shows the different movements of wrist.

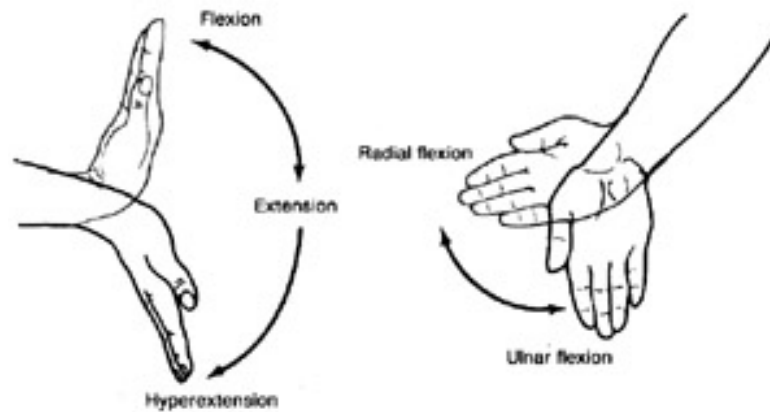


Figure 3.2 Movements of the human wrist

3.2 Hand Model in Hand Rehabilitation

According to the kinematics of the hand and previous robot hands, the human hand can be divided into palm, four fingers (index, middle, ring and pinky) and a thumb. Joints in the hand are used as the division indexes. The figure is the model of a left hand. The palm is named as l_hand . Each finger is connected with the palm at a joint. These joints are named after each finger as l_index1 or l_thumb1 . Then looking along the finger from the palm to the finger tip, the next joint after the l_index1 can be named as l_index2 , and so as the other four fingers. Lastly, the last joint in the index finger is named as l_index3 . All the joints on the hand now have their names for this model.

Then we define the segment between l_index1 and l_index2 is $l_index_proximal$, the segment between l_index2 and l_index3 is l_index_middle , the segment outside of the l_index3 is l_index_distal . This name method can be also used to other 3 fingers, middle, ring and pinky.

Thumb also has 3 joints, respectively. The segment between l_thumb1 and l_thumb2 is l_thumb_metacarpal. Segment between l_thumb2 and l_thumb3 is l_thumb_proximal and segment outside of l_thumb3 is l_thumb_distal.

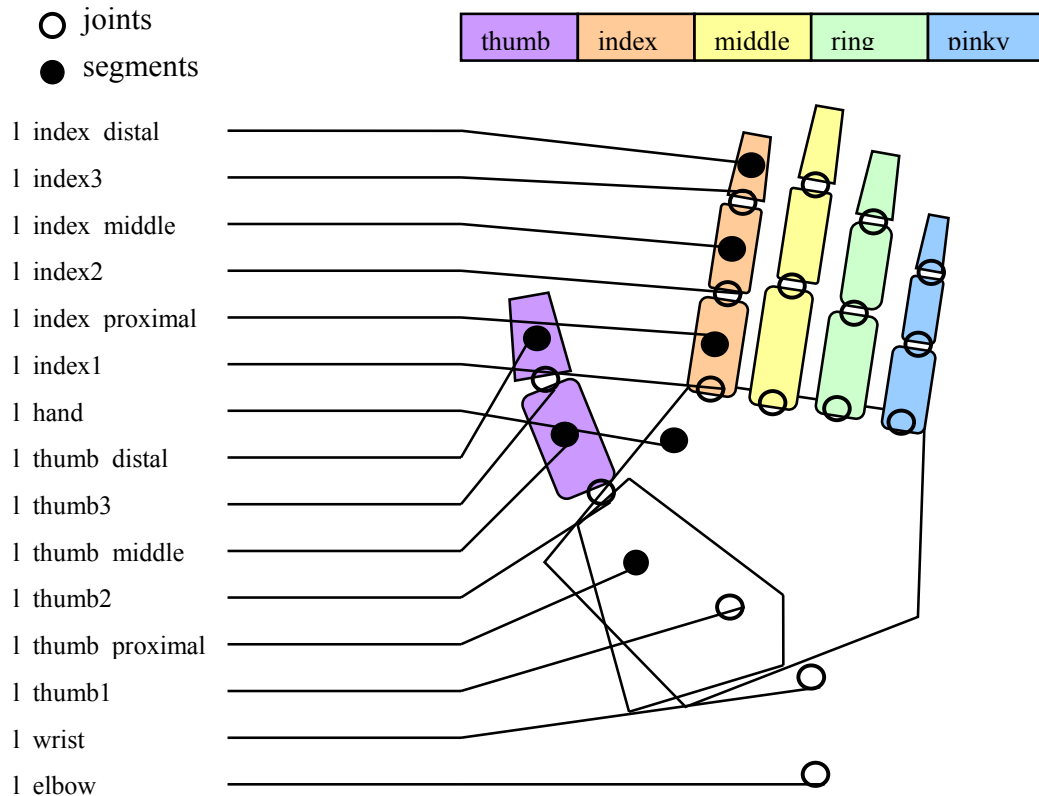


Figure 3.3 Model of Hand

In this model, the wrist is the joint that separates the forearm from the palm except for the fingers and the palm. Each segment is considered as a nonflexible surface having a certain thickness. Each joint on the fingers and thumb can be flexed from 0 to 90 in one degree. And wrist is a joint have two degrees. It can flex and extend on the palm surface, and also perpendicular to the palm surface, which is like waving one's hand.

In this research, a wooden hand mannequin, figure 3.4, is used to carry out the experiments. It has a flexible wrist, thumb and four fingers. The wrist has a fourth dimensional flexibility. It can rotate clockwise and anti-clockwise. The l_thumb2 and l_thumb3 joints can bend to 90 degrees, but the l_thumb1 joint is not flexible. All the 3 joints on the 4 fingers are flexible.



Figure 3.4 Hand Mannequin

3.3 Design of Brace, Glove and Muscles Attachment

The system design for the brace, glove and muscles attachment was derived from the overall goal or a design basis for this project in the future. The following section discusses the design basis for the design prototype and then describes the pneumatic and electronic hardware involved in the design.

3.3.1 Design Prototype Outline

Most of the current rehabilitative device for the hand use an external DC motor controlled robot as the manipulator of the human hand. But these devices have many

disadvantages: expensive, large, non-compliant, and they are not designed for the home rehabilitation, especially for the patients in their home recovery period. Our solution to designing a better rehabilitative device for the hand and forearm is to use a lightweight pneumatic actuator known as the McKibben Artificial Muscle or PPAM. Air muscles are lightweight, cheap, compliant, and are comparable to the human muscle. It is suitable to the desirability of the home based design. Instead of using an external device to house the air muscles we have chosen to design a brace attached at the elbow end of the radius and ulna, and a glove wearing on the patient's hand, to house the air muscles and allowing the patient to move freely and comfortably.

3.3.2 Design of the brace for elbow by Carey Merritt

The elbow brace is designed from an existing elbow brace called the IROM Elbow that was donated by dj Orthopedics, Inc (Merritt, 2003). Modifications were made to the elbow brace to allow for muscle connections to specific areas of the device, to allow elbow flexion and extension. The two main modifications to the device are the addition of two aluminum parts on the shoulder and elbow, shown in figure 3.5. Four air muscles connect the two aluminum parts and control the flexion and extension as biceps and triceps (Merritt, 2003).



Figure 3.5 Rehabilitation Garment designed by Carey Merritt

3.3.3 Design of the Brace, Glove and Air Muscles

The forearm and hand rehabilitation device consist of three parts: glove, brace and attached muscles. The brace is fixed with the rehabilitation elbow brace (the aluminum part at the elbow) designed by Carey R. Merritt (Merritt, 2003). The gloves are worn on the patients' hands. The air muscles attach both the brace and glove. This is inspired from the muscles attachment of the human being. Most of the muscles that control the fingers, thumb and wrist have their one ends on the bones of the forearm and the other ends on each controlled parts of the hand. The brace in our design functions as the bones of the forearms to connect one ends of the air muscles. The other ends of the air muscles will be attached to the each parts of the hand need to be controlled.

3.3.3.1 Design of forearm brace with the elbow brace

Most of the muscles control the movements of hand and fingers origin at from the elbow's end of the ulna and radius. Since the original end is inside of the human body, an

aluminum section was added around the joint of the elbow and forearm to act as the origin of the air muscles. The aluminum section is a thick plate bend as a circle with the middle flat. Two holes are drilled on the flat part to fix with the two holes of the elbow brace by $\frac{1}{4}$ " x $\frac{1}{2}$ " bolts. 4 holes are drilled on each end of the aluminum section to set the end of the air muscles. They function as the elbow's ends of ulna and radius. There is around 1 inch between the aluminum section and the forearm. Care is taken to ensure the air muscle does not rub on the skin of the patients. This will reduce the uncomfortable feeling of the patients and also reduce the wear of the air muscles. The other good effect is to make the air muscle works in a good position, help to draw the fingers in a good angle. The air muscle can exert big forces on the aluminum section, therefore the section need to have a strong structure to prevent the deformation under big force. One way to solve this is to add the width of the section.

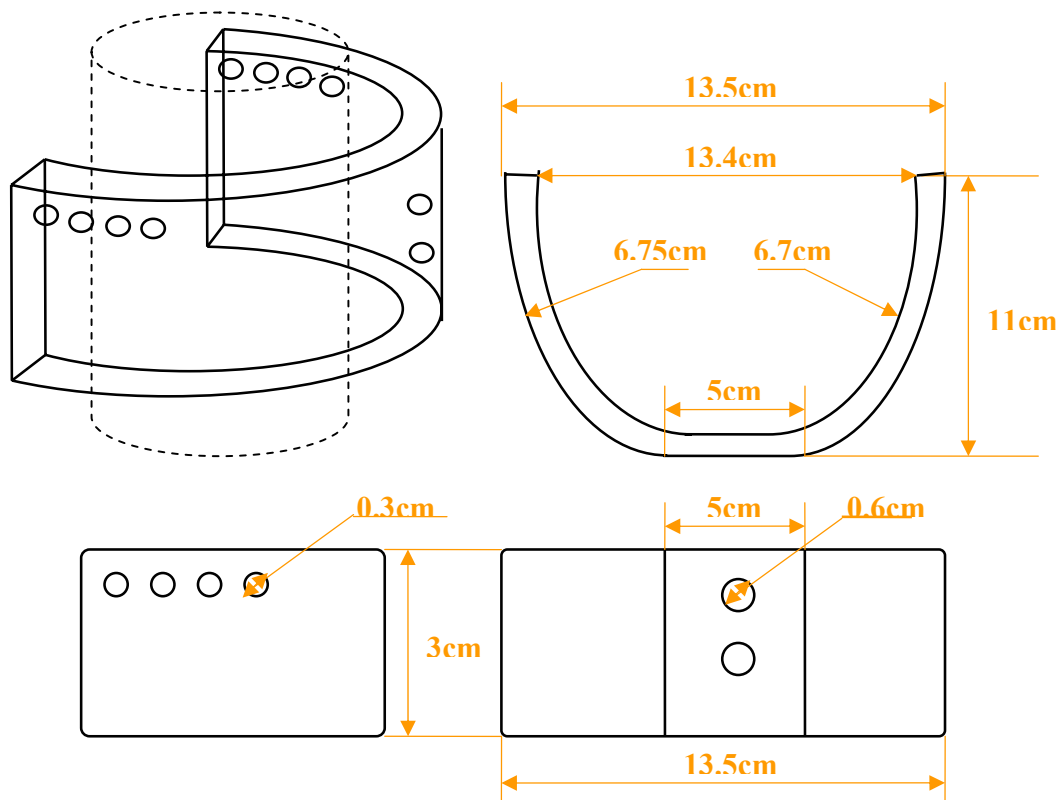


Figure 3.6 Drawing of Aluminum Elbow Section

3.3.3.2 Rehabilitation Glove

The rehabilitation glove is a glove that the patients can easily wear and have a good interface to the air muscles. It also provides the connection between the patient's hand and the air muscles. In the process of rehabilitation, patients will wear the garments and elbow braces. They will also wear the gloves to practice and recover their hand function and ability. The air muscle connects with the patient's hand through the glove and controls the movement of the hand. The rehabilitation glove can also give enough space for the patient to have different hand movement, such as grasp, stretch, wave and so on.

In order to attach air muscles on the glove and yet keep flexibility, we chose a golf glove was chosen as the prototype of the rehabilitation glove. The other reason for choosing this kind of glove is its elasticity. The patients have difficulty to moving their fingers and hand and it is not easy for them to wear a tight and rigid glove by themselves. The glove with a good elasticity can help the patients wear the glove easily and comfortably.



Figure 3.7 Rehabilitation Glove

In order to control each finger's movement, air muscles are connected to each finger. The connection methods must accommodate hand speed and flexibility. Since the metacarpophalangeal joints (MP), proximal interphalangeal joints (PIP) and distal interphalangeal joints (DIP) of the fingers flex and extend like a hinge, the control of these joints will also in a 2 dimensional phase. MP and PIP are the two joints used frequently in a finger. When PIP bends to 90° , the proximal segment of the finger will be perpendicular to the palm surface. When MP bends to 90° at the same time, the middle segment of the finger will be parallel to the palm. This flexion of PIP and MP is the most frequent movement of a finger. The DIP of a finger can also bend to 90° if needed, but normally DIP doesn't flex and extend in a same range as the other two joints. Considering

the ADL needs and the flexibility requirement, the primary goal of the controlled finger movements will concentrate on the PIP and MP and the DIP can be left free. In this way, the attachment points of the air muscles on the fingers are at the middle and proximal segments of the fingers and thumb. No muscle is used to control the distal segments. But the distal segment can also move with the adjacent middle segment. Figure 3.8 shows the primary controlled segments of the fingers and thumb.



Figure 3.8 Controlled Segments on the fingers and thumb

3.3.3.3 Muscle Attachment

In order to achieve flexion and extension of the fingers, air muscles were added to the brace to mimic the muscles that control hand and wrist motion. The end of the air muscle is a ring made from braided sleeve. In order to connect the finger segment and a ring, the nylon rope is used between the air muscle and the glove wearing the finger. The other benefit using the rope is to keep the air muscles away from the hand part in order to prevent the obstacle of the hand movements when muscles filled with high air pressure. And the rope is light and not elastic, which is a good to reduce the weight and increase the flexibility of the rehabilitation device.

Nylon rope with a 1/8" diameter was used to tie each muscle to the forearm brace and finger segments and act as a tendon. The rope was melted on both ends to avoid fraying and pushed through the air muscle's loop end. One end of the rope is connected to the rehabilitation glove. One each segment of the gloves need to be connected, several rubber rings are attached. These rings have the similar inner diameter as the diameter of the corresponding finger segments. The ropes are attached to the rubber rings around the fingers.

The other end of each muscle is attached to the aluminum sections of the brace also using nylon rope. This was achieved by drilling holes and tying the nylon rope through the holes. Three holes were drilled in the aluminum forearm section for each pair so that the muscle connection tubes could sit side by side. Each end of the rope was pushed through the two appropriate holes and a triple knot was tied behind the aluminum to hold the muscle in place. Finally, the muscles were tightened so that the fingers were fully stretched in the range of motion of the hand.

From the discussion on air muscles (section 4.4.1), one of the benefits of air muscles is that they can offer high force when operated at high air pressure. In our design, the force that needed to produce flexion and extension of each finger is less than half of the air muscle force range. To decrease the air muscles number in the device and increase the flexibility, one air muscle will control two of finger segments at the same time.

The actual views for muscle origin and insertion to the hand and brace are shown in figure 3.9.

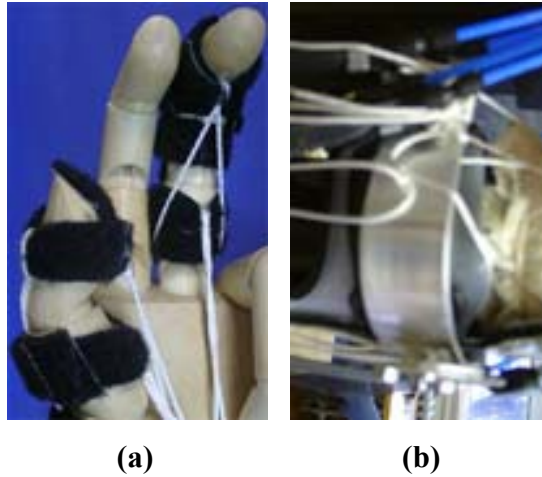


Figure 3.9 Insertions and origins of the air muscles
(a) Origin of air muscle connected rope on finger segments
(b) Insertion of air muscle on elbow brace

The lengths of the air muscles are determined by measuring the change of the displacement from the elbow brace to the finger segments when flexing and extending the fingers. The equation that determines the relationship between the length of air muscle and its displacement is as followed. It is based on the average percent contraction of these air muscles.

$$disp = L - C \cdot L \quad (3.1)$$

In the above equation, the parameter 'L' is the actual length of the muscle, 'disp' is the displacement, and 'C' is the average percent contraction for the type of air muscle used. The displacement of the air muscle is calculated by subtracting the stretched length by the contracted length in the following equation:

$$disp = L - C \cdot L \quad (3.1)$$

This is then rearranged to solve for the length of the muscle for a desired displacement.

$$L = \frac{disp}{1 - C} \quad (3.2)$$

The percent contraction, C , was calculated by measuring the contraction percentage of air muscles with various lengths. The average contraction percentage for the muscles developed for this thesis was 0.76 (76%). So for example, the contraction of the distance between the middle finger segments and the forearm brace is 7 cm, then use equation 3.2 would be:

$$L = \frac{6}{1 - 0.76} = 25cm$$

The contracted length was found by subtracting the desired displacement from the length, which equaled 25cm. Final lengths of the muscle are 25cm – 31cm for a muscle with a 6cm contraction. The lengths for the biceps and triceps were actually expanded to 28cm - 32cm to increase the chances of actually constructing a muscle with a 6cm contraction. The muscle was then constructed and the contraction was determined to be approximately 6cm. Finally, the air muscles were constructed, tested and placed on the device.

3.4 Artificial Muscles Design

Since air muscles are pneumatic, a pneumatic system was designed to control the air muscles required for the device. The following pneumatic components are required for the rehabilitative wearable arm's pneumatic system:

- Pneumatic Circuit
- Tubing and Connectors
- Pneumatic Air Muscles (PAMS)

- Valves
- Pressure Transducers

3.4.1 Pneumatic Circuit

The pneumatic circuit for the rehabilitative arm was designed to control the artificial muscles that are attached to the device using 2-way solenoid valves. Since solenoid valves are either on or off, two valves are required to control one artificial muscle. One valve lets air in the muscle causing it to contract while the other valve releases the air out to the environment causing it to extend and reach a resting position. In order to measure the air pressure in each muscle, a pressure transducer was placed in the circuit at each muscle inlet. A tank and an air filter were combined to provide the air supply to each muscle in the circuit. An example pneumatic circuit for two air muscles is illustrated in figure.

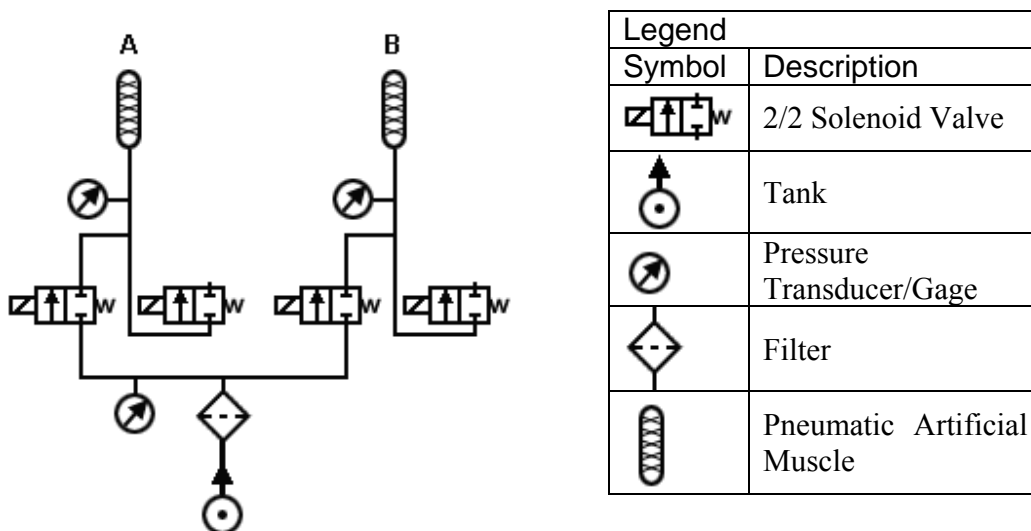





Figure 3.10 A Pneumatic Circuit for Pneumatic Artificial Muscles

3.4.2 Tubing and Connectors

The pneumatic circuit needed to be small and flexible so that the air muscles could be mounted on the device without being in the patient's way. Since the valves have 5/32" diameter inlets and outlets and most convenient and inexpensive push-fit connectors are no smaller than 5/32" diameter, the 5/32" tubing size for the circuit was chosen for all of the connectors and the tubing.

The tubing that was used to connect the pneumatic components for the device was 5/32" Nycoil tubing. Three push-fit connectors were also required for connecting the components together. One 5/32" Union "Y" was used to connect the inlet and exhaust valves to the air muscle. Also one unequal tee was used to connect the pressure transducer to the tubing that was directed to the air muscle. Since the pressure transducer required 1/4" tubing, the unequal tee's diameters were 1/4" for the unequal tube while the equal tube-to-tube diameter was 5/32" like the rest of the circuit. Finally, the tubing coming from the unequal tee was connected to an equal tube-to-tube connector, which plugged directly into the muscle's hose barb. The tubing and connectors used in the pneumatic circuit are listed in table 3.3.

Table 3.3 Tubing and Connectors used for pneumatic circuit

Graphic	Model Number	Item	Company	Unit Price
	65233	5/32" OD Flexible Nylon Tubing Blue	Nycoil	\$0.12 /ft
	3140-04-00	5/32" Union "Y"	Legris	\$1.83
	3104-04-56	5/32" – 1/4" Unequal Tee	Legris	\$2.89
	3106-04-00	5/32" Equal Tube to Tube Connector	Legris	\$1.90

3.4.3 Pneumatic Artificial Muscles (PAMs)



The actuator of choice for the device was the pneumatic artificial muscle known as the McKibben Air Muscle. The main reason for choosing this actuator over other actuators namely DC motors is because of their advantages and capabilities for producing a force that is similar to the human muscle. Instead of using a large gearbox and structure to convert a dc-motor's rotational motion into linear motion, air muscles were chosen to compliment the patient's own muscles by strategically attaching them to the device.

There are only a few air muscle manufacturers that exist so purchasing an air muscle is costly and difficult compared to custom making and designing them. For example, the most popular air muscle manufacturer, Shadow Robot Company, is located in the United Kingdom so shipping would be an additional expense. Prices for their air muscles are shown in table 3.4.

Table 3.4 Shadow Air Muscle Prices

Size	Stretched Length (mm)	Price
Small	150	\$10
Medium*	210	\$40
Large	290	\$100

* This is approximately the preferred size for the wearable device's muscles

The preferred muscle size for the wearable device is the medium size costing \$40. Unfortunately, there are over 15 muscles needed just for actuating the arm and shoulder so the cost for the muscles alone would be around \$600. Since one of the goals of this device is affordability for the patient, other alternatives must be considered.

Our alternative for obtaining inexpensive air muscles was to make them. Fortunately, the University of Washington Bio-Robotics Laboratory provides a simple guide to making air muscles. Their guide helped us to develop our own muscle design that enabled us to produce large numbers of muscles that are cheap, easy to make, and lightweight weighing only 11 g for a 180mm (≈ 7 ") length muscle. This new design of muscle, figure 3.11, for a 180mm air muscle costs only \$2.70. This cost is calculated from the price of the required materials, table 3.5, used in building a 180mm air muscle. The cost calculation is the following:

$$\frac{7''}{300''} \cdot \$31.00 + \frac{13''}{300''} \cdot \$8.75 + 2 \cdot \$0.61 + 2 \cdot \$0.19 = \$2.70$$

Table 3.5 Pneumatic Artificial Muscle Materials

Model Number	Item	Company	Diameter	Length/Quantity	Price
EW-95802-07	Platinum-Cured Silicone Rubber Tubing	Cole-Parmer	ID 5/32" OD 7/32" Wall Thickness 1/32"	25'	\$31.00
-	Protecto PE Braided Sleeving	Cable Organizer	1/2" Diameter	25'	\$8.75
3122-04053	Barbed Connector for Unequal Tube	Legris (Air Power Inc.)	Tube OD 5/32" Barb OD 1/8"	2	\$0.61
OE 10100008	7-9 Two-Sided Hose Clamp	Air Power Inc.	5/16"	2	\$0.19



Figure 3.11 New Air Muscle Design

3.4.3.1 Pneumatic Artificial Muscle Assembly

For an example of artificial muscle assembly, the actuator will have a resting length of about 14 cm and a stretched length of 18 cm and will be capable of producing forces up to 200N according to University of Washington Bio-Robotics Laboratory air muscle website. Air muscle assembly requires nippers, scissors, and a lighter. The materials for construction are listed in table 3.5 and shown in figure 3.12. The steps for assembly are listed below.



Figure 3.12 Materials required for new air muscle design

1. Cut a 16.0 cm piece of silicone rubber tubing for the inner bladder.
2. Cut a 30.0 cm piece of the braided sleeving for the outer braided shell.
3. Use the lighter to singe the ends of the braided sleeving to keep the ends from unraveling.
4. To make the plug take a barbed connector and cut about a ¼” off the tube end and melt the shortened end of the barb tube until the hole is closed.
5. Insert the plug and another barbed connector into both ends of the silicone rubber tubing.
6. Insert the silicone rubber tubing inside the braided sleeving.
7. Form a loop at the barbed connector end with the open tube and push the tube through the braiding.
8. Slide a 7-9 hose clamp on the other end of the braiding and slide it over the loop until it is flush with the middle of the barb where the barb stops and the barb tube begins. There should be a little ring or ridge to indicate this area. Clamp both sides of the clamp using a pair of nippers.
9. Slide the other 7-9 hose clamp on the other end

10. Slide the other end of the braiding up on the tubing a certain amount so when the tubing is stretched it goes to 18 cm and relaxes back to around 14 cm. Grab the middle of the barb connector when doing this making sure not to let go.
11. Form a loop on the end and slide the 7-9 hose clamp over the loop until the clamp is flush with the middle of the barb like in step 8. Clamp both ends of the clamp using the nippers. See figure 3.13 for end result.



Figure 3.13 Loop formed on plugged end of air muscle

3.4.4 Valves

The Mead Fluid Dynamics Isonic® 2-way solenoid valves, figure 3.14, were used for controlling the artificial muscles on the device. The main reasons for choosing this particular valve were because it was inexpensive, small and lightweight, and provides an easy connection to pneumatic circuit.



Figure 3.14 Isonic 2-way solenoid valve and manifold

Most solenoid valves prices range from \$30 to \$500 resulting in an expensive system especially when multiple valves are needed. Fortunately, Mead makes the Isonic® 1000 series for a little more than \$20 depending on the options selected like the optional LED. The cost of the 2-way Isonic® valve model V1B02RW1 that was used in this thesis was \$23.34. Due to the low cost of these valves the total cost for all the valves for the device was much lower.

Since these valves are made out of glass-impregnated Ultem thermoplastic they are extremely lightweight unlike the industrial valves made out of stainless steel. The dimensions of the device are about the size of a Zippo® cigarette lighter and are given in table 3.6. The small and lightweight characteristics of the valves allow for a lightweight device and possibly a belt of valves that could go around the patient's waist.

The easy connection of the built in push-in fittings eliminated the need for fasteners, adhesives, gaskets, and inserts. As a result, the 5/32" Nycoil tubing was plugged directly into the push-in fittings on the valve in one step and there were no additional costs for connectors.

Table 3.6 Specifications for Isonic® V1B02RW1

Voltage	5 VDC
Amps	320 mA
Resistance	18 Ω
Cycle Life	50,000,000 cycles
Orifice Size	0.90 mm
Flow	0.02 C _v
Max Pressure	120 PSI
Tubing	5/32"
Dimension (in)	1-9/32 x 1-3/4 x 5/8
Weight	1.5 oz
Response Time	10 ms

3.4.5 Pressure Transducers

The pressure transducer that was chosen for measuring the pressure of each muscle was the Motorola MPX5700GP-ND. The MPX5700 series is a piezoresistive monolithic silicon pressure transducer designed for use with a MCU with A/D inputs. The output signal is conditioned for a range of 0 – 4.7V and is proportional to the applied pressure. The main reasons for choosing this sensor over others are because of its low price, small size, minimum circuitry for interfacing with a MCU, and easy connection to pneumatic circuit.



Figure 3.15 Motorola Pressure MPX5700GP-ND Transducer

The prices of pressure transducers range generally from \$50.00 to \$1000.00. These high prices defeat the goals of this thesis to develop a device that is inexpensive for the patient. Extensive research on pressure transducers revealed the Motorola MPX5700 series, which is small and economical in comparison to most pressure transducers. The Motorola MPX5700GP-ND can be purchased from Digi-Key for \$18.19, which is more than a factor of 10 cheaper than most pressure sensors.

The Motorola pressure transducer is also small enough to be mounted on the device next to the air muscle. As a result, the pressure transducer takes up minimal space keeps the device design more mobile and lightweight. Also, connecting the transducer to the pneumatic circuit is simple because of the port extending from the package. This port fits approximately 1/4" diameter tubing allowing the device to be plugged into the pneumatic circuit via an unequal tube tee connector shown in table 3.3.

The specifications for the Motorola pressure transducer are given in table 3.7. These specifications comply with the 5V power supply and the Mitsubishi MCU, which has an ADC reference voltage of 5V and the pressure range of 0 – 101.5 PSI meets the requirements for the artificial muscles' range of 0 – 90 PSI.

Table 3.7 MPX5700GP-ND Specifications

Supply VDC	5 V
Pressure	0 – 101.5 PSI
Output	0 – 4.7 V
Response Time	1ms
Pressure Type	Gage

The equation given by the datasheet for output voltage related to pressure is:

$$V_{OUT} = V_S (0.0012858 P_{kPA} + 0.04) \pm \varepsilon \quad (3.3)$$

The following equations for Voltage in terms of PSI and ADC are derived below.

$$\begin{aligned}
 P_{kPA} &= \frac{P_{PSI}}{0.14504} \\
 V_{OUT} &= V_S (0.0088651407 P_{PSI} + 0.04) \pm \varepsilon \\
 V_{OUT} &= \frac{ADC \cdot V_S}{2^N}
 \end{aligned} \tag{3.4}$$

The equations for the A/D value in terms of PSI and vice-versa are derived below.

$$\begin{aligned}
 ADC &= \frac{V_{OUT}}{V_S} 2^N \\
 \frac{ADC \cdot V_S}{2^N} &= V_S (0.0088651407 P_{PSI} + 0.04) \pm \varepsilon \\
 ADC &= (0.0088651407 P_{PSI} + 0.04) 2^N \pm \frac{2^N \cdot \varepsilon}{V_S}
 \end{aligned} \tag{3.5}$$

$$P_{PSI} = \frac{\left(\frac{ADC \pm \frac{2^N \cdot \varepsilon}{V_S}}{2^N} \right) - 0.04}{0.0088651407} \tag{3.6}$$

$V_S = 5 \text{ V}$

$N = 10$ bits (10 bit analog to digital converter)

$\varepsilon =$ error offset (small value)

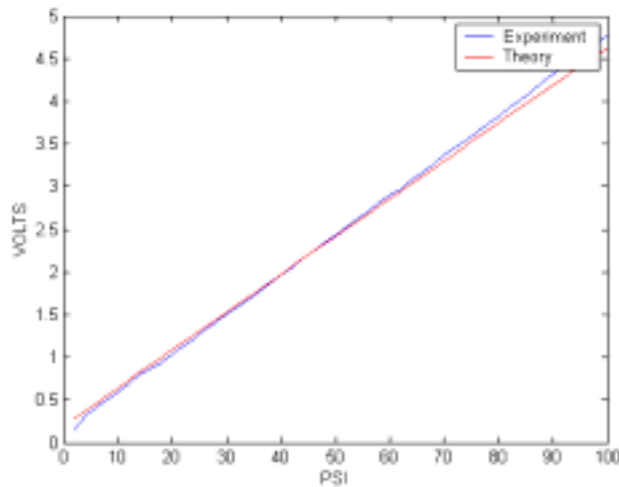


Figure 3.16 Pressure Transducer response to PSI

In order to show the linear response of the pressure transducer, voltage data was collected at 2-PSI increments from 0 – 100 PSI. The data was graphed in figure 3.16 along with data generated from the typical response data sheet equation 3.4. This figure shows that the pressure transducer’s response to pressure is extremely linear and fits the equation almost perfectly. There was a slight deviation at pressures 80-100 PSI but, fortunately, the air muscles typically operate between 0-75 PSI.

3.5 Hardware Design

The hardware required for controlling the pneumatic system consists of a micro-controller, solenoid valve driver circuit, and pressure transducer noise filtering circuit.

3.5.1 M32C/83 Micro-controller

The M32C/83 micro-controller (MCU) is a member of the Mitsubishi M16C platform. This 144-pin chip features:

- 20 MHz clock frequency

- 108 instructions
- 16 MB memory space
- 11 16 bit timer/counters
- 5 Serial I/O channels for UART, IE bus and I²C bus
- 34 A/D Pins
- 2 Independent 8-bit D/A Converters
- 4 Groups of Intelligent I/O for waveform generation, serial I/O, and IE bus
- 1 Channel CAN Module
- 4 Channel DMAC

Mitsubishi donated a single MSV1632/83 – SKP Starter Kit Plus™ shown in figure 3.17, which included the MCU, two serial ports, 16x2 LCD, push buttons, and a 150-Pin DIN header for easy access to the 144 pins on the MCU. This convenience of this kit made the M32C/83 easy to use and allowed all of its features to be exploited. The main features of attraction for the wearable device are the 20 MHz clock speed, 16 MB memory space, and abundant I/O for the sensors and control of the solenoid valves.

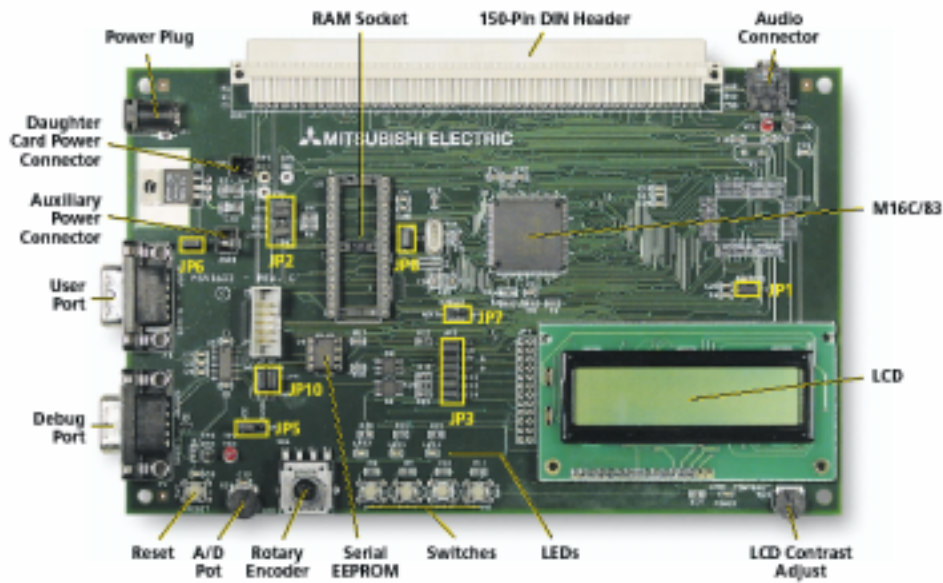


Figure 3.17 MSV1632/83 - SKP Starter Kit Plus™

Since control of each muscle required several sensors and the device required multiple muscles, the 34 A/D pins and fast sampling rate offered more than enough support for data acquisition. As a result, no extra data acquisition board was required for using this MCU for this application. Besides requiring A/D pins for the sensors, each muscle required a two output pins for control of the inlet and exhaust valves. Several pins are provided by the MCU and control possibilities are enhanced with the Intelligent I/O feature of the MCU. For example, the popular pneumatic control strategy PWM with the solenoid valves was possible through the use of Intelligent I/O waveform generation.

The serial channel debug port made programming the MCU simple and also allowed for outputting experimental data back to the computer for data collection. Also, the additional serial channels are appropriate for communicating data with a computer running a virtual reality environment for later use with the device.

3.5.2 Solenoid Valve Driver Circuit

The following circuit is used to switch the Mead Isonic® 2-way solenoid valve on/off via a MCU. A single NPN transistor switches the solenoid valve on/off by using a digital output pin from the MCU. A rectifier diode (1N4001) is connected across the valve leads to prevent any damage to the transistor due to inductance. The 4.7KΩ resistor is connected to the output pin to ensure that the output goes low while the RB resistor drops the current going through the base junction to reduce the current on the collector side. The Mitsubishi M32C/83 MCU has an I/O current of 5mA and voltage of 5V so that would give the solenoid a current of 5A. The RB resistor should drop this current down thus reducing power consumption. The solenoid driver circuit is illustrated in the following figure 3.18.

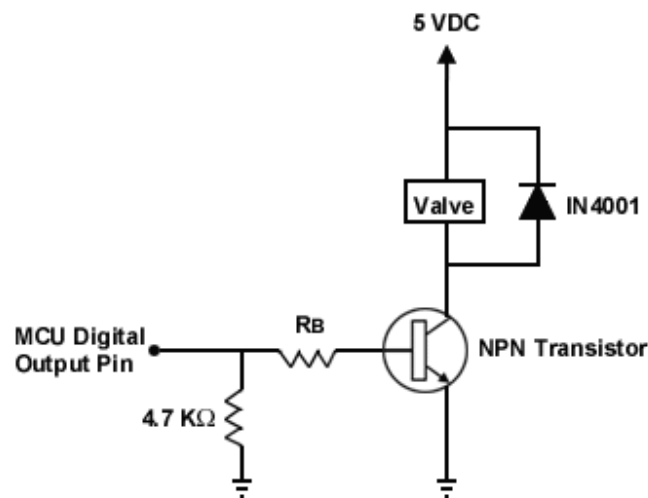


Figure 3.18 Mead Isonic® 2-way solenoid driver circuit

To solve for RB the following two equations were used.

$$I_C = h_{FE} I_B \quad (3.7)$$

When the digital output pin is raised high by the MCU the voltage is 5V. A KVL around the Base-Emitter loop results in the equation for RB in terms of IB.

$$-5V + I_B R_B + 0.7V = 0 \quad (3.8)$$

$$R_B = \frac{5V - 0.7V}{I_B} \quad (3.9)$$

$$R_B = \frac{(5V - 0.7V)h_{FE}}{I_C} \quad (3.10)$$

The current gain, hFE, for the NPN transistor is approximately 200 and the required IC for the solenoid is 320 mA according to their respective data sheets. Now RB can be solved for using equation (x-4)

$$h_{FE} = 200$$

$$I_C = 320mA$$

$$R_B = \frac{(5V - 0.7V)200}{320mA} = 2.69K\Omega$$

3.5.3 Pressure Transducer Circuit

The circuitry for interfacing with the MCU is a simple filter circuit using capacitors. Since the output is already conditioned to range from 0 – 4.7 V, the only work left to do is to filter the noise from the signal to achieve clear and accurate outputs. The recommended circuitry from Motorola's data sheet is given in figure 3.19. This circuitry was implemented for each pressure transducer connected to the pneumatic circuit.

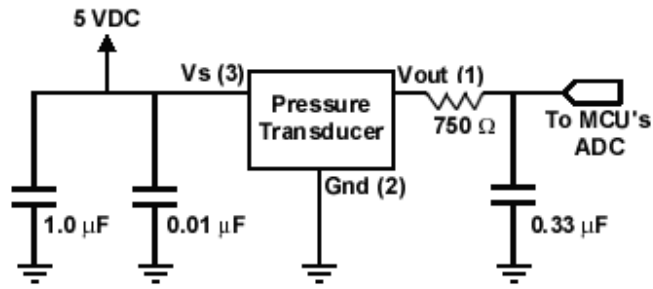


Figure 3.19 Recommended power supply decoupling and output filtering

3.6 Final Design

The design and experiment can be divided into two phases. In the first phase, the single finger and thumb experiments were made. Air muscles were attached to the middle finger and thumb to control all the segments and the joints, including the PIP, MP and DIP. Glove was not used at that phase. Velcro was used as the attachment of the nylon rope and the finger. In this phase, the relation between the air pressure in the air muscles and the angle of PIP and MP was tested.

In the second phase, the primary goal was changed from single finger to the whole hand. Rehabilitation glove was used and air muscles connected the hand by the rubber rings attached on the glove. The movement of the whole hand and its function is the concentration of this phase.

3.6.1 Phase I: Design for Experiment

In the design for experiment, middle finger and thumb are chosen to be the experiment subjects since middle finger is the longest finger and has the highest requirement of displacement among the 4 fingers in the hand. In the phase 1 design,

every segment of the fingers and joints are controlled by the air muscles. Three muscles are used to control a finger and two muscles are used to control the thumb.

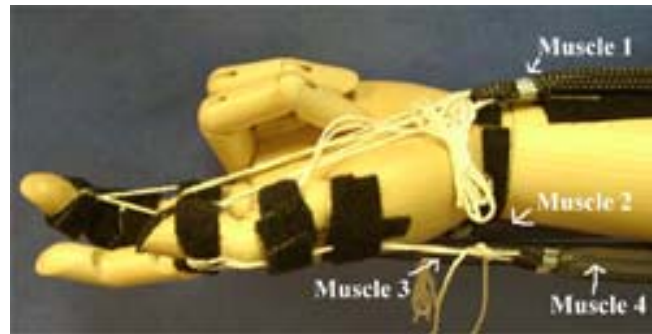


Figure 3.20 Muscle's Attachment in Phase I

In figure 3.20, there are four muscles along the forearm altogether. Their functions are listed in table 3.8.

Table 3.8 Muscle's Attachment Segments and Functions

Muscle No.	Attach Place	Functions
Muscle 1	Middle finger: proximal segment and PIP	Flexion of finger on PIP
	Thumb: distal segment and DIP	Flexion of thumb on DIP and MP
Muscle 2	Middle finger: proximal segment and PIP	Extension of finger
Muscle 3	Middle finger: Distal segment and DIP	Flexion of finger on DIP and MP
Muscle 4	Thumb: distal segment and DIP	Extension of thumb

When the muscle 1 and 3 were filled with high air pressure at the same time, both the middle finger and thumb will bend and joints PIP, MP and DIP will be close to the angles in their range of motion. When muscle 2 and 4 are filled with high air pressure and

1 and 3 have the air exhausted, the middle finger and the thumb will extent back to their original position.

There are two points in this design needed to be revised and improved. One is the Velcro attachment of the rope on the finger. The Velcro is not flexible enough to make adjustment to the attach place. It needs to have an alternative method which makes the rope tightly attached on the finger and easily adjusted to a new place. The other one is the friction between the forearm and hand and the air muscles. This will decrease the displacement the air muscles or even increase the blow up of them. When the inner tubing of the air muscle has friction with the arm, clothes or the Velcro, it has more chances to have wear/tear which could result in failure. The most frequent friction is at the PIP on the back of the palm. In order to extent the fingers, the rope always touch and move directly on the skin between the adjacent PIPs on the hand.

3.6.2 Phase II: Design for Function

In this phase, functions of the whole hand became the primary goal. All the four fingers and the thumb were connected with the air muscles. Forearm brace were added around the forearm, one ends of the air muscles are tied on the brace. Rehabilitation glove was introduced to the design and the air muscles attached the glove by rubber rings, figure 3.19. The rings are a good substitute to the Velcro. They are tightly attached with the fingers and it is easy adjusted to a new position.

In order to decrease the friction of the air muscles with the patient's body, a small distance is left between the forearm brace and the forearm. Then there is also a small distance from the air muscles to the forearm. For the most frequent friction on the PIP

joint back on the palm, 5 small pulleys are added in this design. They are attached on the back of the glove where the PIPs are. The rope travels on the pulley when the air muscles change with the air pressure. Figure 3.21 are the pulley on the design.

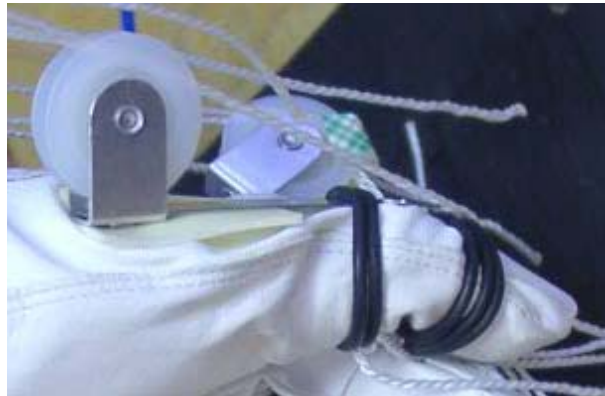


Figure 3.21 Pulley and the Rubber Rings on Thumb

We have totally 8 muscles to control the phase 2 design. For one of the four fingers, two muscles are attached to the front side of the finger, on the proximal and middle segments separately, to make the finger flex. The other muscle is attached to the middle segment on the back side of the finger to make the finger extent. And two adjacent fingers will share the common three muscles. Then the index finger and middle finger have three muscles attached and the ring finger and pinky have the other three muscles attached. Two muscles are connected with the thumb on the two side of it separately. The front one makes the thumb flex and the back one make it extent back.

From figure 3.22, phase 2 shows that:

- One ends of the muscles connect with the forearm brace
- The other end of the air muscles connect with the rehabilitation glove by the rubber rings

- There is a pulley attached on each of the PIP joint back of the palm
- There are more space between the muscles and the body to decrease the friction.

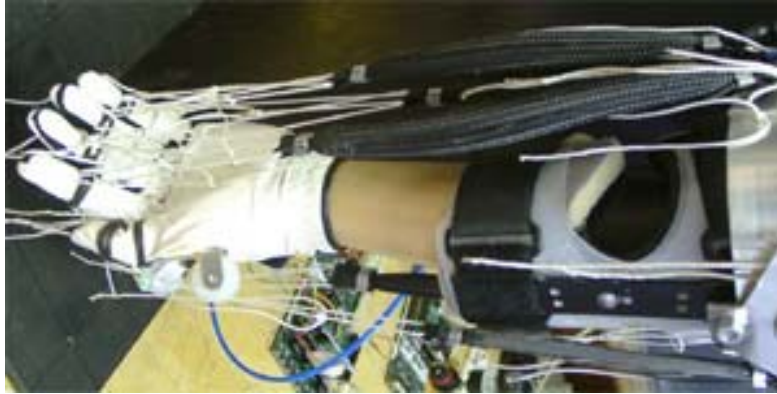


Figure 3.22 Design of Rehabilitation Device on Phase II

Chapter 4. Air Muscle Control and Characters

4.1 Air Muscle Overview

Controlling an air muscle with solenoid valves deserves special attention because extra work must be done to make the muscle respond smoothly and achieve a desired length. Currently there are two popular types of control for an air muscle with two solenoid valves: PWM and Bang-Bang control.

4.1.1 PWM Control

Recently the most popular type of control for a valve controlling an air muscle is PWM. PWM for an on/off valve uses a fixed frequency from and varies the duty cycle of a binary waveform in order to control the pressure in an air muscle. Since an air muscle requires two valves for operation, the duty cycles of each valve must coordinate so that air fills the muscle when desired. The duty cycle generally works within a range given the response time of the valve to open and close i.e. if the duty cycle is smaller than the valve response time then the valve will never open or close (van Varseveld et al. 1997, p. 1197). These duty cycles generally increase to achieve a faster rate of airflow into the muscle. Since the duty cycle determines the flow in an air muscle, air muscles can be easily controlled in a smooth fashion by using small duty cycles that are larger than the response times of the valves.

4.1.2 Bang-Bang Control

Bang-Bang control is an extremely simple control algorithm that uses only the sign of the error to determine whether to make a change to the system. This type of control for air muscles uses the sign of pressure error to decide from three possible types of states: In, Exhaust, Leak. The In state, where the inlet valve is opened, is called when the pressure error is positive. The Exhaust state, where the exhaust valve is opened, is called when the pressure error is negative. When this error is zero or within a preset dead-band region then the Leak action is called in which both the valves are closed.

Cham has offered a modified version of bang-bang control added a Flow state to the three existing types of states. Since the air muscle requires two valves, there are a total of four possible states for the air muscle (Cham 1999). Table 4.1 shows the binary representation of each state. Each bit is attributed to each valve so if the binary value is '0' then the valve is off and if the value is '1' then the valve is on.

Table 4.1 Four States of control for an air muscle using two solenoid valves

Inlet	Exhaust	State
0	0	Leak
0	1	Exhaust
1	0	In
1	1	Flow

Cham uses an estimate of the current state and a model of the delays for each state and predicts the future errors for each transition. The controller finally picks the transition with the smallest predicted error.

4.1.3 Antagonistic Muscle Pair

Another important means for controlling the position of a joint like and elbow is the use of an antagonistic pair of muscles. An antagonistic pair like a human muscle can provide the power to achieve a specified angle and also restore the device to an initial angle in a controlled fashion.

The antagonistic pair of air muscles in figure 4.1, works by varying the pressure in both muscles to achieve a desired angle. Ideally, when both pressures are the same ($P_1 = P_2$) in two identical air muscles the forces exerted by them should cancel out and the angle should be zero (Daerden 2001b, p.1961). However, if the pressure in one muscle is greater than the pressure in the other muscle then the angle will increase in its favor and vice versa if the pressure decreases.

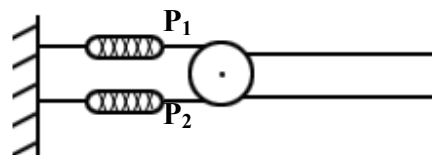
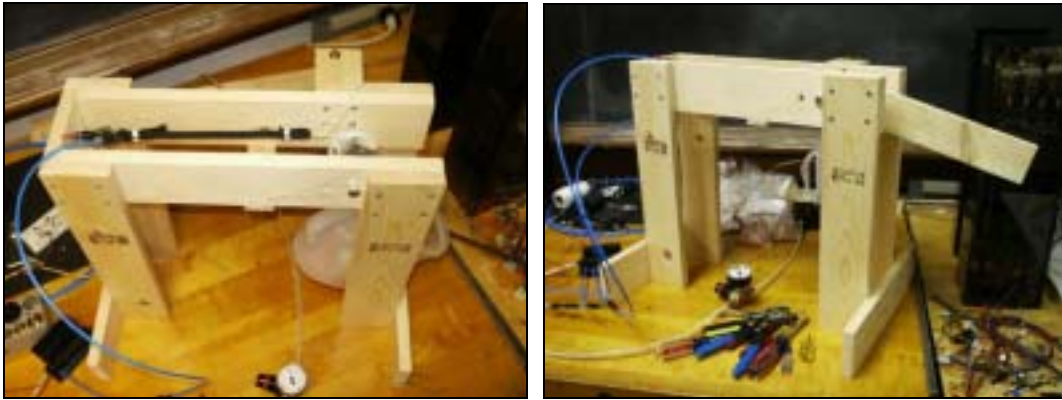


Figure 4.1 Antagonistic Pair

4.2 Test Platform

A test platform, figure 4.2, was developed to run several experiments on the air muscles to determine their characteristics. This platform can be used for hanging weights on a single air muscle and for balancing a wooden arm with one or two air muscles. The steps and materials for the construction of the test platform are outlined in the appendices.



(a)

(b)

Figure 4.2 Test platform (a) setup for lifting a mass (b) setup for positioning an arm with either one or two muscles

4.2.1 Experimental Operation

The test platform was designed to be flexible so that it could support a variety of experiments. In order to support several experiments with one test platform the platform was designed for two different configurations. This test platform can be configured for hanging a mass for force or it can be configured for positioning a wooden arm with one or two muscles. A graphical representation of these options is illustrated in figure 4.3.

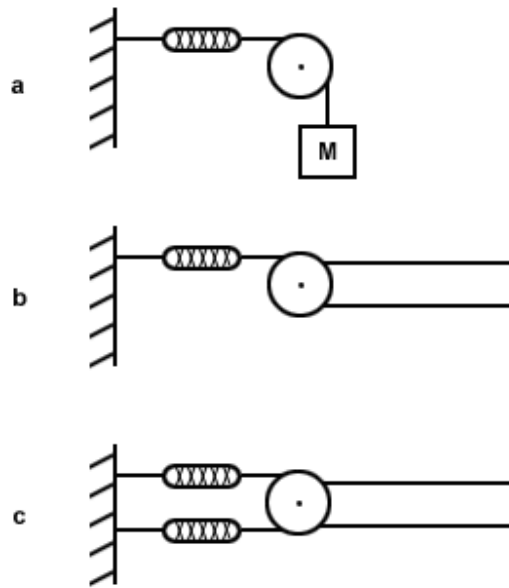


Figure 4.3 Test Platform Options (a) hanging mass (b) single muscle with arm (c) antagonistic muscles with arm

4.2.2 Single Muscle Pulling a Constant Mass

Option ‘a’ in figure 4.3 allowed for experiments with a single air muscle in order to measure the relationship between length, force, and pressure. This configuration was also useful for determining the characteristics of the air muscle during the four different pressure states: in, exhaust, flow, and leak. For example, recorded pressures when opening the in valve for two seconds revealed both the response time to fill the air muscle and confirmed the response time of the valve. Besides using this configuration for determining the response time of the air muscle, this configuration was also used to determine the damping coefficient of the muscle under test.

Instead of using expensive conventional weights, bee-bees were used to provide incremental weight to the single air muscle. This incremental unit of weight was 1 lb so 15 zip-lock bags were filled with 1 lb of 0.4g bee-bees, figure 4.4. As a result, tests were

done with a 0 – 15 lb range weight by simply adding or removing 1 lb bags of bee-bees. These bags were placed in a plastic lightweight pitcher and hung from the nylon string that usually connects to the second muscle. Figure 4.4 shows the pitcher with several 1 lb bags being lifted by an air muscle.



Figure 4.4 1 lb zip-lock bag of bee-bees

4.2.3 Air Muscle Positioning a Wooden Arm

Option ‘b’ and ‘c’ in figure 4.3 allowed for control experiments with one or two air muscles. For example, the potentiometer measured the angle of the arm while the pressure transducer measured the pressure in the muscle to provide two error terms for both determining the duty cycle when using PWM and determining pressure states when using Bang-Bang control. Figure 4.5 shows two muscles controlling the weight of bee-bees.

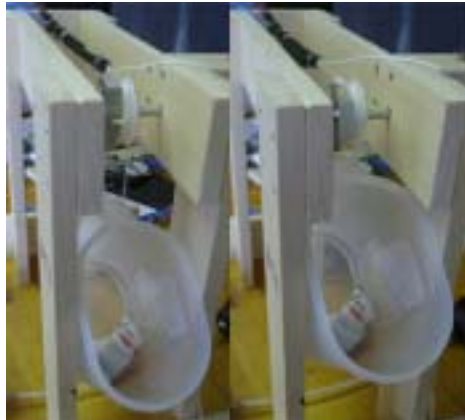


Figure 4.5 Antagonistic muscle pair controlling the weight of bee-bees

4.3 Test Platform Experiments with Air Muscles

Several experiments were set up for determining the characteristics of the air muscles that were built for the rehabilitative wearable arm. Since the response times of the valves and the air muscles are important for both Bang-Bang control and PWM control, tests were executed to measure the response times of both the valves and the air muscles. Experiments were also designed to measure the static and dynamic characteristics of the air muscles to understand the nature of these custom made air muscles.

4.3.1 Response Time

Response time tests were done by using the test apparatus set up for hanging weights of 0 lb, 1 lb, and 5 lb on a single air muscle at pressures of 20-70 PSI in 10 PSI increments. The single air muscle was connected to an inlet valve, an exhaust valve, and a pressure regulator. The M32C/83 was programmed to open the high-pressure valve for one second and record the pressure transducer values during that time. Figure 4.6 shows

the test results for response times for a 7 ¼" - 11" air muscle. In the figure, the solid black lines are drawn through the 90% steady-state values to determine the response time of filling the air muscle. The response time for filling the air muscle was approximately 610 ms \pm 20ms and was independent of the load on the muscle.

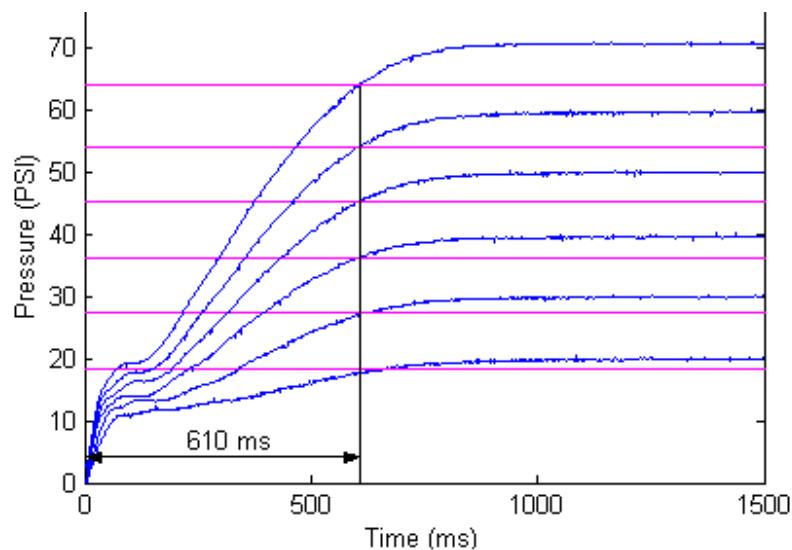


Figure 4.6 Response Time to Fill Muscle at 0 lb

A Response time experiment was also done on two muscles connected in parallel to the same two valves. This experiment was intended for the doubled muscles that were later used on the device for improving the strength of the device for flexion and extension. Since the response time was independent of the load the experiment only used a 1 lb weight. The results, figure 4.7 show that the response time increases by nearly double. Fortunately, the flexion and extension must be slow and controlled for rehabilitation and requires times greater than 1080 ms between each motion. As a result, both single and double muscles have response times that are fast enough to handle the slow rehabilitation of the elbow.

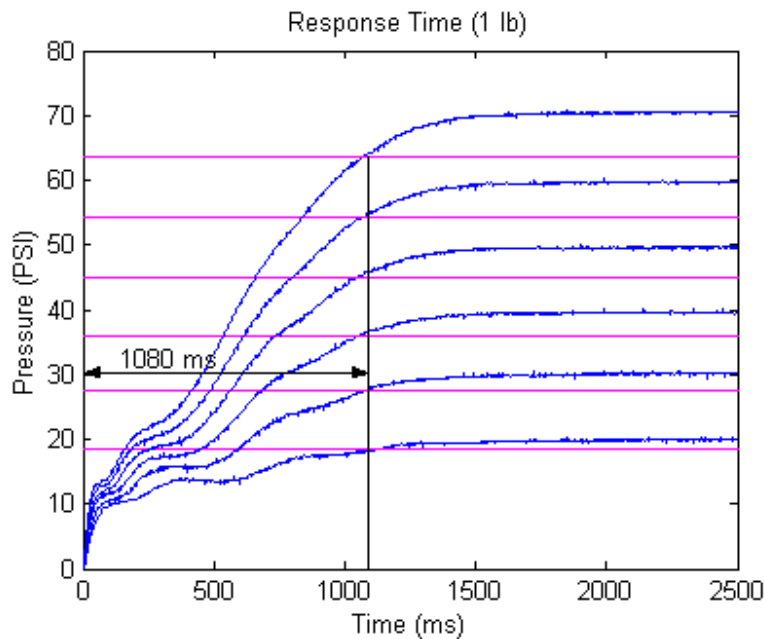


Figure 4.7 Response time for doubled 7 1/4" - 11" air muscles

4.3.2 Valve Response Time

The same data that was collected for figure 4.6 was analyzed to estimate and confirm the factory response time for opening the solenoid valve. According to the Mead specifications on the Isonic® 1000 valves the response time of the valve is 10 ms. The valve's approximate 10 ms response time is also shown in the previous data collected by zooming in on the plot for the first 20 ms. Results for the valve response time at various pressures is shown in figure 4.8. According to figure 4.8 the response time of the solenoid valve lies between 8 ms and 10 ms.

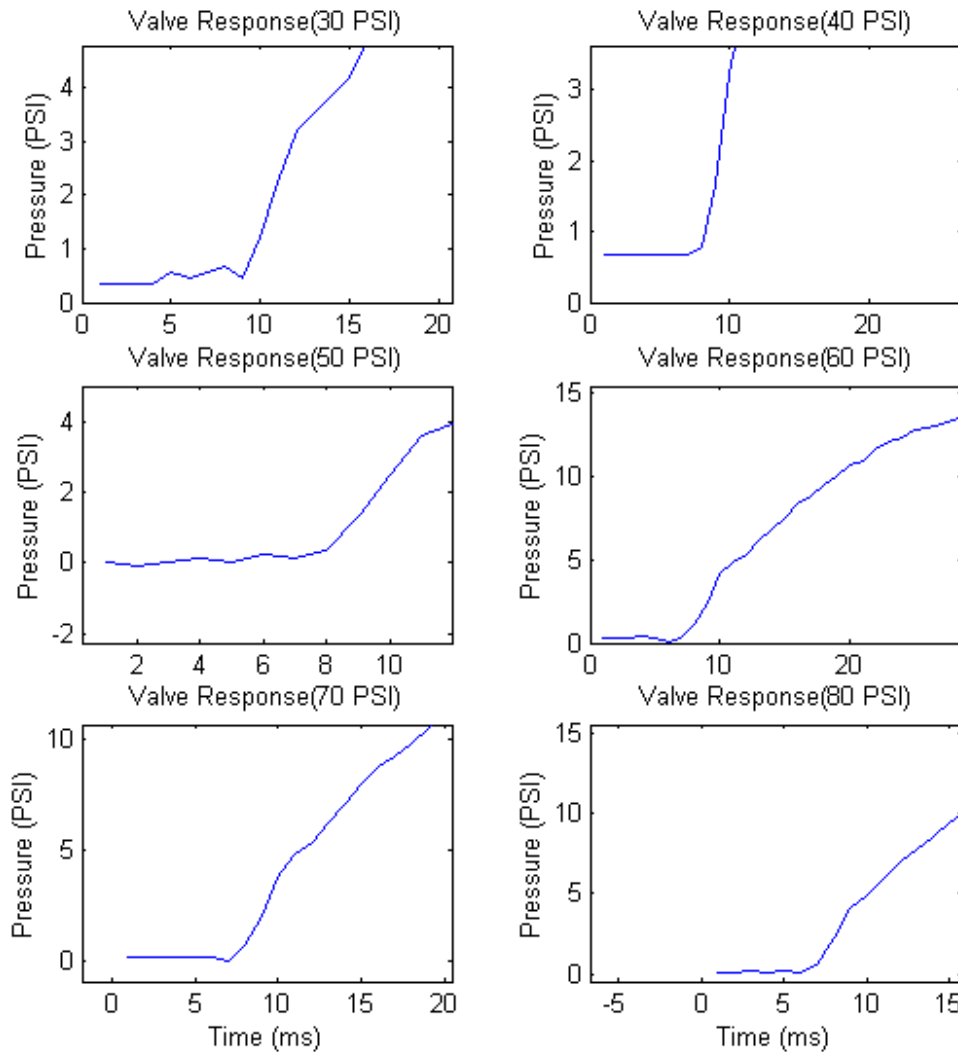


Figure 4.8 Valve response time \approx 8 – 10 ms for various pressures and a zero load.

4.3.3 Leakage

Another important characteristic of the air muscle is the amount and rate of leakage during the leakage state when all the valves are closed and the air muscle is full of air. Several experiments to observe the leakage were conducted using 0 lb, 1 lb, and 5 lb loads each at set pressures from 20-70 PSI. First, the inlet valve was opened for two

seconds to fill the muscle completely with the specified pressure. After two seconds the inlet valve was closed and half-second pressure samples were taken for two minutes from the Motorola pressure transducer to measure the air leakage from the air muscle and its connections to the pneumatic circuit. These results were collected and plotted in figure 4.9.

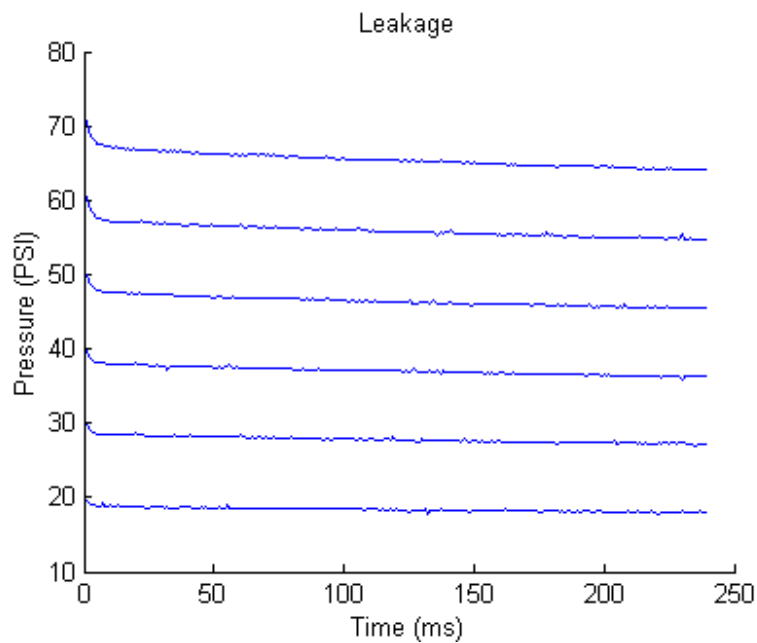


Figure 4.9 Average Leakage from air muscle with a 0 lb, 1 lb, 5 lb load over ½ second samples for 2 minutes

The results from these figures show that for higher pressures there is a small 2-3 PSI pressure drop approximately 10ms when the inlet valve closes. Fortunately, there is little concern over the leakage of the system because the pressure drops slowly over these two minutes. Leakage also appears to be independent of the load on the air muscle. These results indicate that maintaining a constant pressure in the air muscles should not be difficult.

4.3.4 Exhausting the valve

The third possible state when using a two-valve circuit with an air muscle is the exhaust state. When the air muscle is exhausted from a nominal pressure to 0 PSI, the time for exhausting the muscle completely is important for developing a control scheme. As a result, experiments similar to the inlet valve response time experiments were done to capture the response time and nature of the system when the air muscle is depleting. First, the inlet valve was opened for two seconds to fill the air muscle completely. The inlet valve was then closed and 5 ms later the exhaust valve was opened for two seconds while values were read from the pressure transducer.

The results that are shown in figure 4.10 indicate that the higher the initial pressure the longer it takes for the muscle to deplete. Each pressure level tends to take the same response curve except time shifted to the right with increasing pressure. The rate of pressure decrease appears to slow down around 10 PSI, which is the max pressure for the silicone tubing. After reaching 10 PSI the tubing forces the air at a faster rate due to the tubing taking its natural form.

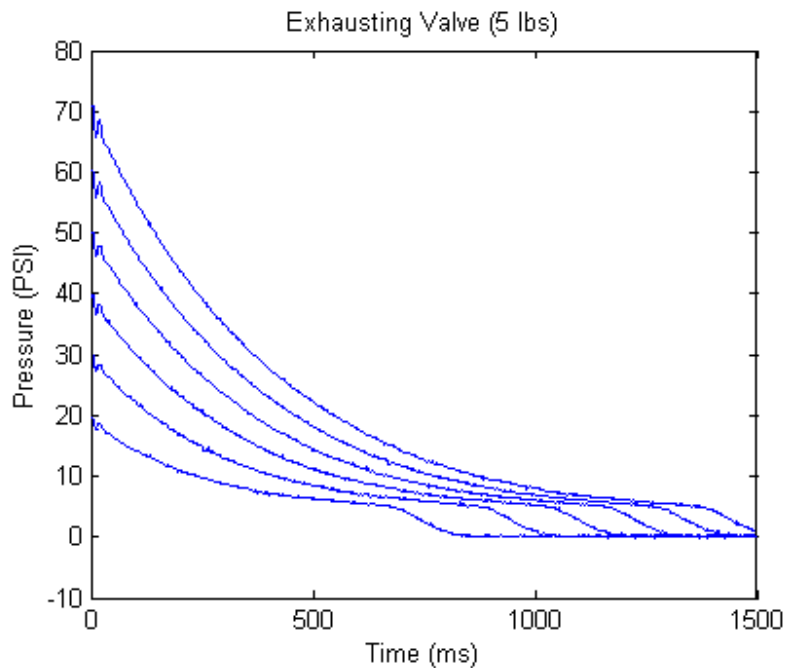


Figure 4.10 Exhausting a 7 ¼" - 11" air muscle

Figure 4.10 also indicates that the time to exhaust the air muscle is between 750 and 1500 ms. One possible way to speed this up may be to take 10 PSI as fully exhausted since the muscle does not contract with pressures equal to or less than 10 PSI. Another possible way to speed up exhausting the valve may be to either increase the exhaust port size or to add additional exhaust valves.

Figure 4.11 shows the trend when exhausting the air muscle from 40 PSI and 70 PSI with various loads. As the load increases the exhaust time decreases at times after the 10 PSI mark. This change in time is due to the weight stretching the tubing, which causes the diameter of the tubing to contract and force the air out faster. However, before the 10 PSI mark the curves are approximately the same for what this thesis is concerned with.

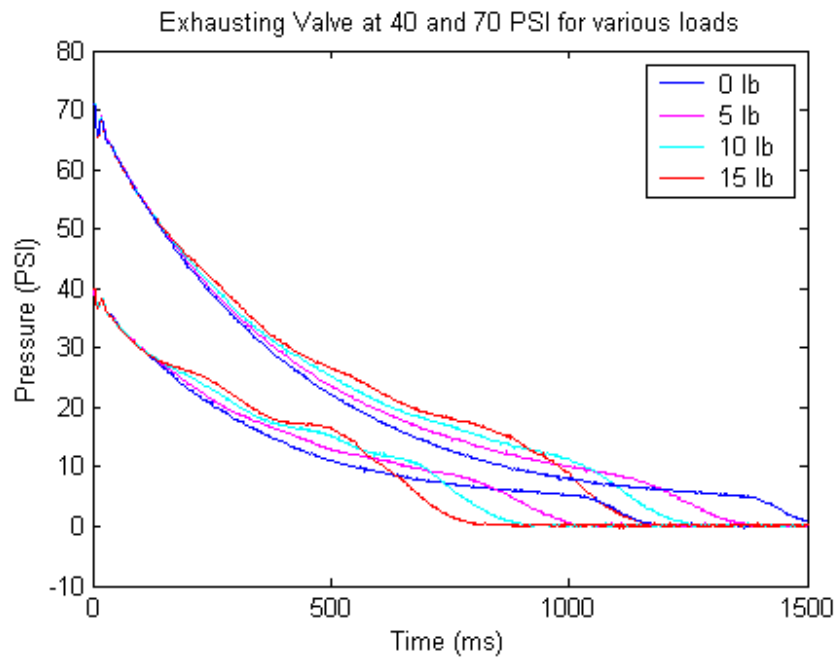


Figure 4.11 Exhausting a 7 ¼" - 11" air muscle at 40 and 70 PSI with different loads.

An Exhaust experiment was also conducted on the doubled muscles that were used on the device for increasing the strength and improving the angles achieved by the device. This experiment was the same as the previous exhaust experiments except the only weight tested was a single 1 lb weight. The results for this experiment, shown in figure 4.12, reveal that the exhaust time for two muscles is around 1700 ms for the 70 PSI source if the 10 PSI mark is considered the fully exhausted state. Otherwise the time response for exhausting the muscle is around 2500 ms, which is almost a second later. As a result, the 10 PSI mark may be better suited for exhausting the double air muscles unless flexion and extension is really slow.

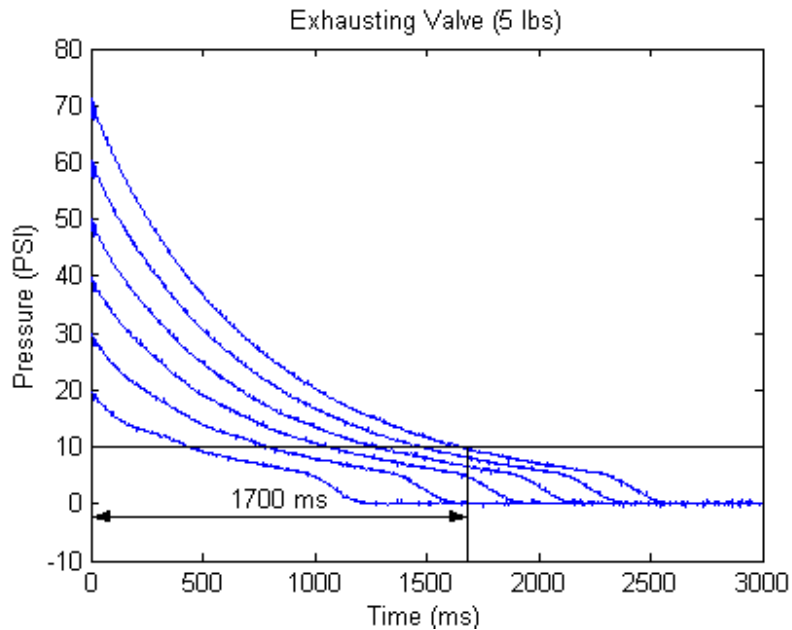


Figure 4.12 Exhausting doubled 7 ¼" - 11" muscles

4.3.5 Flow Experiments and Results

The final possible state (flow) for a two-valve system is when both valves are open. When both valves are opened with a preset pressure in the air muscle the pressure in the muscle drops by an amount dependant on the pressure level. Experiments were designed to measure the flow state's response over a two second time period with a 1 ms sample time. The MCU was programmed to open the inlet valve for two seconds to all the set pressure to fill the air muscle. After two seconds the inlet valve was left open while the exhaust valve was turned on and the pressure was measured from the Motorola pressure transducer. Results for the flow experiments are shown in figure 4.13. Figure 4.13 shows the tests for 0 lb at different set pressures as well as the tests for 1 lb and 5 lb. According to this plot the pressure change is independent of the load on the air muscle. Another observation is that the higher the initial pressure the larger the pressure drops in

the system. For example, the pressure drops 20 PSI from 70 PSI to 50 PSI and drops only 10 PSI from 20 PSI to 10 PSI. Also, the response time of the plots appears to converge to approximately 550 ms.

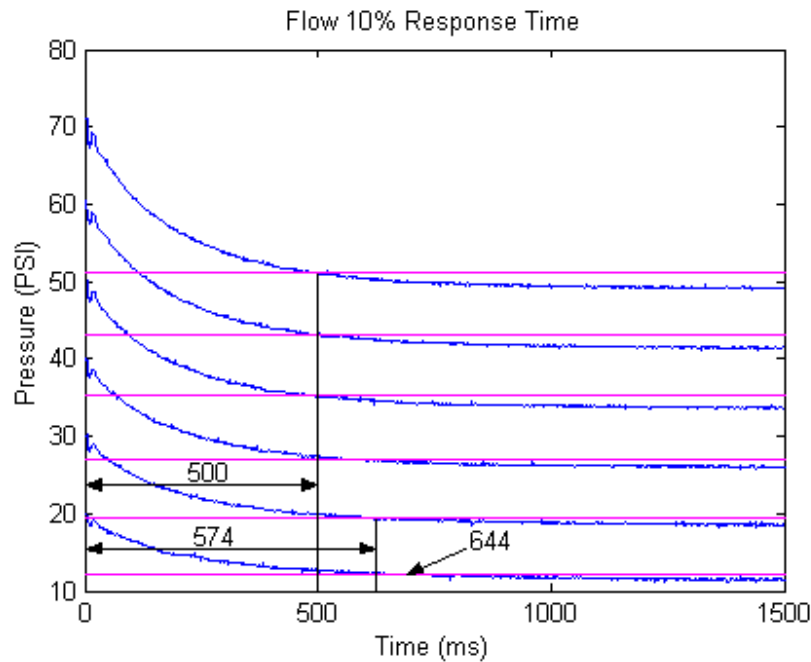


Figure 4.13 Flow response curves combined (0 lb, 1 lb, 5 lb)

4.4 Characteristics of the Air Muscle

4.4.1 Static Characteristics

Experiments were done to determine the force-length relationship of the muscles and to measure the hysteresis of the air muscles. Separate tests at 20 PSI increments from 20 PSI to 80 PSI were done with weight increments of 1 lb ranging from 0 lb to 15 lbs. For each test a pressure regulator that was connected to the air muscle was set to the desired pressure and weights were added starting from 0 lb to 15 lb and then removed from 15 lb to 0 lb. The length and pressure were recorded at each increment using the

pressure transducer and potentiometer connected to the pulley wheel. Since the angle was measured on the potentiometer the change in length had to be calculated by first measuring the circumference of the pulley wheel and then finding the radius of the wheel.

$$\begin{aligned} C &= 2\pi r \\ r &= \frac{C}{2\pi} \end{aligned} \quad (4.1)$$

The change in length was measured by taking the angle at 0 lb as the initial angle and subtracting the measured angles to get the change in angle from the start. Then the formula for calculating arc length was used to find the change in length from the starting 0 lb.

$$S = r(\theta_i - \theta_0) \quad (4.2)$$

Since the angles are converted from voltage to a 10-bit number the angle must be converted back to an angle in radians. This conversion takes place by multiplying the resolution (k_R) in radians per bit by the ADC change in values.

$$\begin{aligned} S &= r[k_R(ADC_i - ADC_0)] \\ k_R &= \frac{Span}{2^N} \cdot \frac{\pi}{180} \end{aligned} \quad (4.3)$$

Results for tests on a 5 5/16" – 7 1/2" sized muscle and a 7.25" – 11" sized muscle are shown in figures 4.14 and 4.15 respectively. Figure 4.24 indicates that the hysteresis for the air muscles is between 0.19" and 0.25". This value is poor compared to the same experiments using the Shadow muscles and could easily be observed by simply pulling on the muscle while it was attached to a mass. The reason for this hysteresis is due mostly to the friction between the braiding and the inner bladder. Figure 4.15 also shows even more hysteresis, 0.25" - 0.40" for the longer muscles that were actually used on the pneumatic brace. This leads to the conclusion that longer muscles give worse hysteresis

because there is more braiding and tubing to creating more friction when inflated. Based on this hysteresis the elbow brace will exhibit larger angles for weights after the brace is flexed or extended without weights vs. flexing and extending with the weight simultaneously.

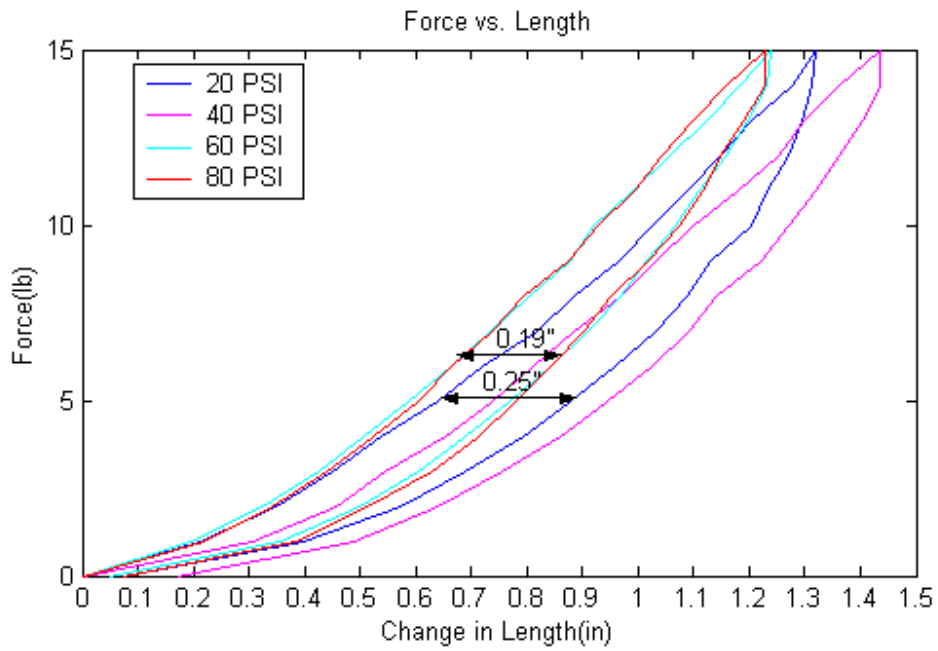


Figure 4.14 Force vs. Length for 5 5/16" – 7 1/2" air muscle

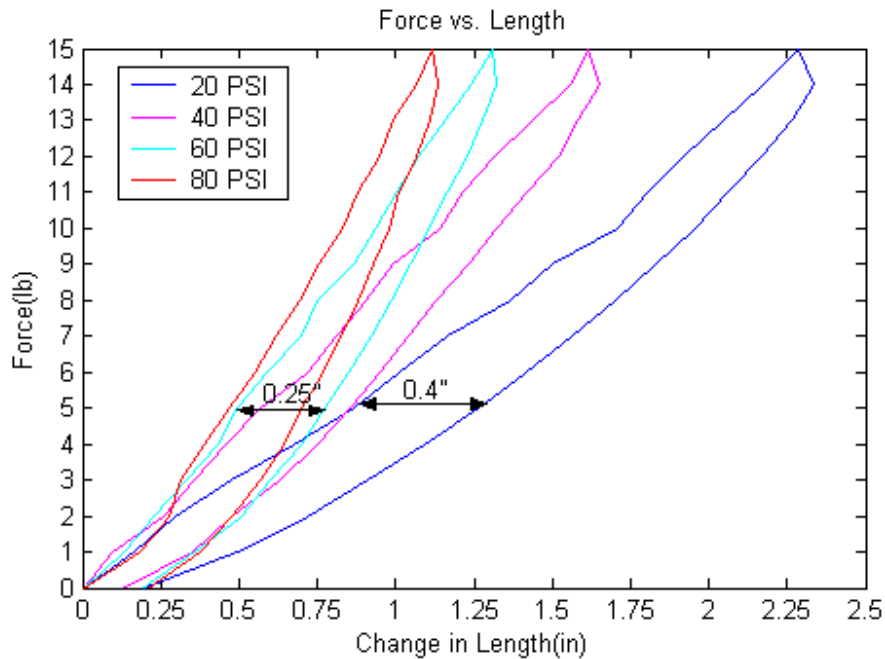


Figure 4.15 Force vs. Length for 7.25" – 11" muscle used on pneumatic brace

4.4.2 Dynamic Characteristics

An experiment was designed to measure the damping of the air muscles that were made for the pneumatic brace. This experiment consisted of hanging a mass from an air muscle that is filled with a constant pressure and displacing the mass to cause the muscle to oscillate until it reaches a steady state. During this time the potentiometer connected to the pulley wheel recorded the angles so that the change in length could be plotted versus time. Figures 4.16 – 4.17 show the results for the experiments, which use various constant pressures and weights from 5 lb, 10 lb, and 15 lb. According to each of these figures the damping increases with respect to an increase in load. Therefore, damping is not constant but could possibly be averaged since the change in damping for 5 lb increments is small.

These plots reveal that the muscles made for this project are much more damped compared to the Shadow's air muscles that were tested in Colbrunn's thesis (Colbrunn 2000). One possible reason for more damping is because the selected rubber tubing is silicone rubber instead of latex rubber, which is used in the Shadow air muscles. This silicone tubing is supposedly more durable and longer lasting than the latex rubber, but the friction between the braiding and the silicone rubber may be greater. The braiding may also be the difference that is causing the damping instead of the tubing but this is an uncertainty. Another possible reason for this additional damping may be attributed to the friction on the pulley wheel bolt that rotates through two wooden holes on the test frame. This type of friction could cause more damping but is not expected to be significant since the pulley wheel rotates freely.

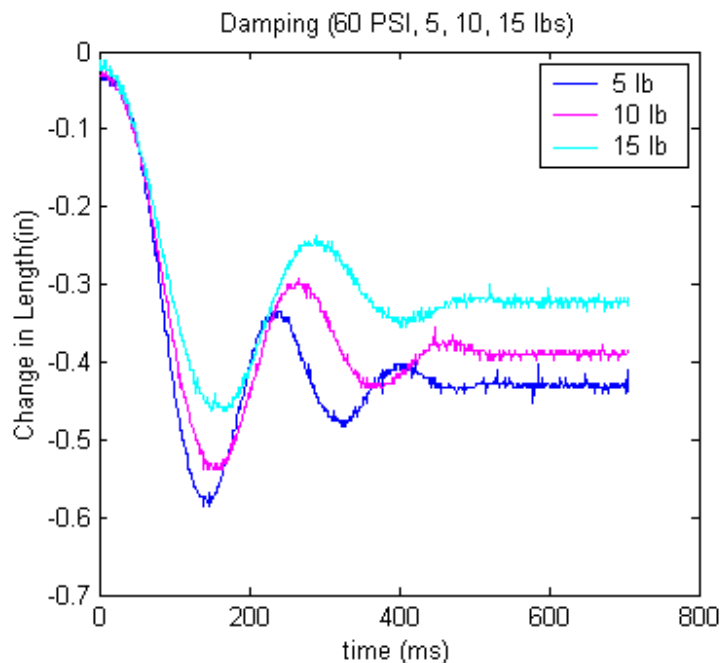


Figure 4.16 Damping for 60 PSI with 5 lb, 10 lb, 15 lb loads

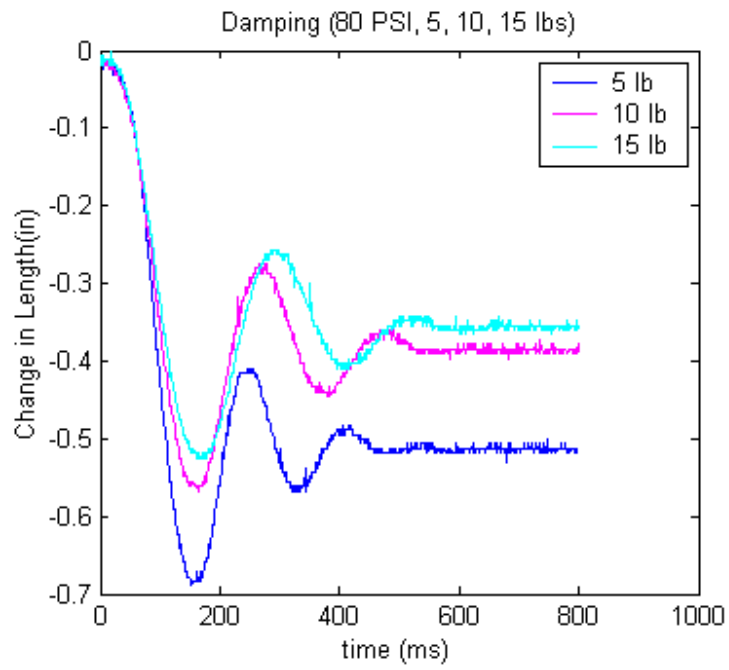


Figure 4.17 Damping for 80 PSI with 5 lb, 10 lb, 15 lb loads

Chapter 5. Rehabilitation Glove Experimentation

5.1 Experiment Design and Set Up

The experiments use the hand mannequin bought from Jerry's Artarama art supply store and a mannequin forearm donated from North Carolina State University's Department of Textile and Apparel, Technology and Management (TATM), which was cut at the elbow to allow the two sections of the arm to move freely. For the elbow rehabilitation garment experiments, the shoulder-elbow portion of the arm was attached to a 1x4 block so that the shoulder could be fixed at desired angles. The 1x4 block was then drilled into the side of a table to hold the arm in position. A screw was also drilled in the top of the block so that a rope could be added to hold the brace up since the dummy arm has a slick hard surface unlike that of the human arm. The brace was then added to the shoulder-elbow section and connected from the aluminum shoulder section to the screw in the block with nylon rope.



Figure 5.1 Wooden block with screw in the top

The hand mannequin has part of the forearm, which is only 10cm long. The hand connects with the mannequin forearm and does not have flexible fingers. The solution was to attach the hand mannequin take place of the rigid hand on the mannequin forearm. The new upper extremity has a 30cm forearm and a hand as big as an adult man's hand, which will require the maximum air muscle displacement.

The experiments used the goniometer to measure a finger joint angles being produced by the air muscles. The angle is measured by relating one finger segment to its corresponding segment. Figure 5.2 shows an example of the angle measurement, here the angle (PIP joint angle) between palm and proximal segment (angle 1) and the angle (MP joint angle) between proximal segment and middle segment (angle 2) are measured.

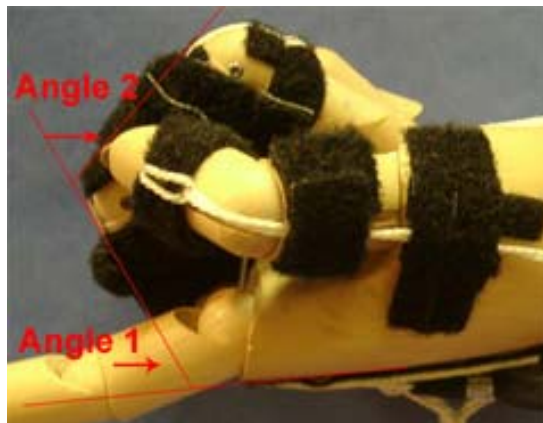


Figure 5.2 Angle measurements

Several experiments were undertaken using this setup. The new forearm and hand determined the effectiveness of the air muscles and where to effectively position the muscles on the device. Two experiments were designed to test flexion and extension, which are shown in figure 5.3. The first experiment tested the flexion and extension of

the middle finger. The second experiment tested the combined middle finger and thumb movement, which is “pinching”.



(a)



(b)



(c)

Figure 5.3 Experiments for testing flexion and extension (a) Middle finger flexion testing (b) Combined fingers testing pinching (c) Combined fingers testing extension

5.2 Experiment Results

Because the middle finger is the longest finger on the hand it gives the largest displacement, so it was chosen to be the finger that makes the single finger experiment.

Two experiments were conducted to test the middle finger. Only the muscles that controls the middle finger was being controlled during these experiments.

First, the response time test. This test used incremental increases on the air pressure, every 10 PSI from 0 to 70 PSI. At certain air pressures, the valve was turned on and the muscles are filled with air in a short period of time. The muscles contract and make the middle finger flex. The process ends when the air pressure in the muscles, reaches a quiescent state as the same as the air pressure set before.

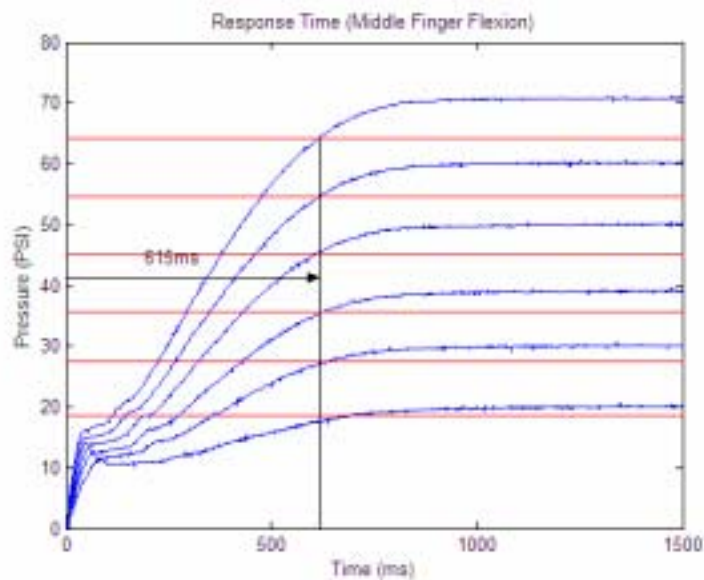


Figure 5.4 Single Finger Test – Response Time

The second experiment tested the range of motion of single finger flexion, which is related with the function fingers could have. Two muscles are connected with two joints of the middle finger, the joint between palm and the proximal segment (PIP) of middle finger and the joint between the proximal and middle segments (MP) of middle finger. The angle is defined as in figure 5.2. During the test, at different pressures from 0

to 80 PSI, the finger segments positions and the two angles are recorded at the end. Finally there comes a graph shows the relation between the set air pressure and the final angles of the PIP and MP joints.

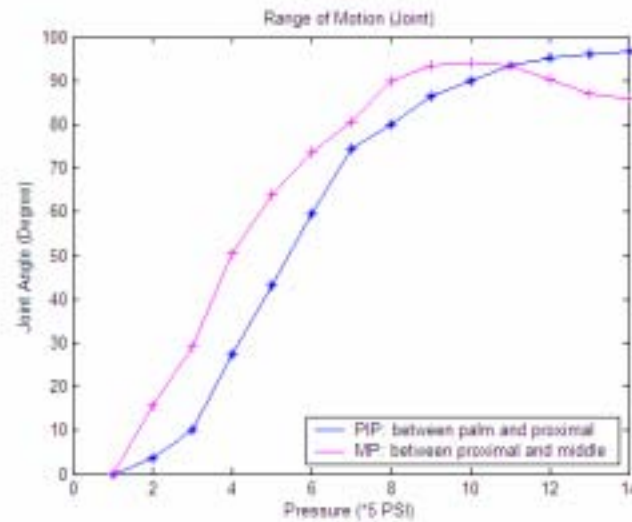


Figure 5.5 Single Finger Experiment – Range of Motion

From the results, we see that the angle of finger joints can be adjusted by the incoming air pressure. For the stroke patient hand rehabilitation, their finger practice can also be adjusted by adjusting the air pressure. The experiment showed that 60 PSI was the pressure that gave the maximum finger movement and control, since both of the joint angles were nearly 90 degrees, which are also the ROM of human's finger joints. When the air pressure is less than 60 PSI, the finger does not flex to a full range of motion. This ensures the patients move their finger smoothly and accurately, to allow movement such as the Franzblau Eye Hand Tracing System. If the air pressure is higher than 60 PSI, joint 3 (MP joint) will decrease instead of increase and joint 2 (PIP joint) will increase to an angle higher than 90°. This region of the air pressure helps the patients flex and extent

their finger in the largest range of motion, which will prevent the ligament and muscle in the hand from atrophy from disuse.

5.3 Control of Pneumatic Brace

The pneumatic brace utilized an antagonistic pair of air muscles that required varying the pressure in each muscle to flex and extend the elbow. Since the air muscles work in an antagonistic way, the pressure in the muscles is also antagonistic because they follow opposite paths. For example, when the desired angle is at a maximum, the pressure in one muscle is at the maximum pressure while the pressure in the opposite muscle is near zero. As a result, the waveform in figure 5.6 was derived to map out the paths that each pressure would take during flexion and extension. In this figure t_{FE} is the time for the device to completely flex or extend and t_D is the time between flexion and extension. The two pressures are represented as P1 and P2, which are the pressures for the biceps and the triceps respectively.

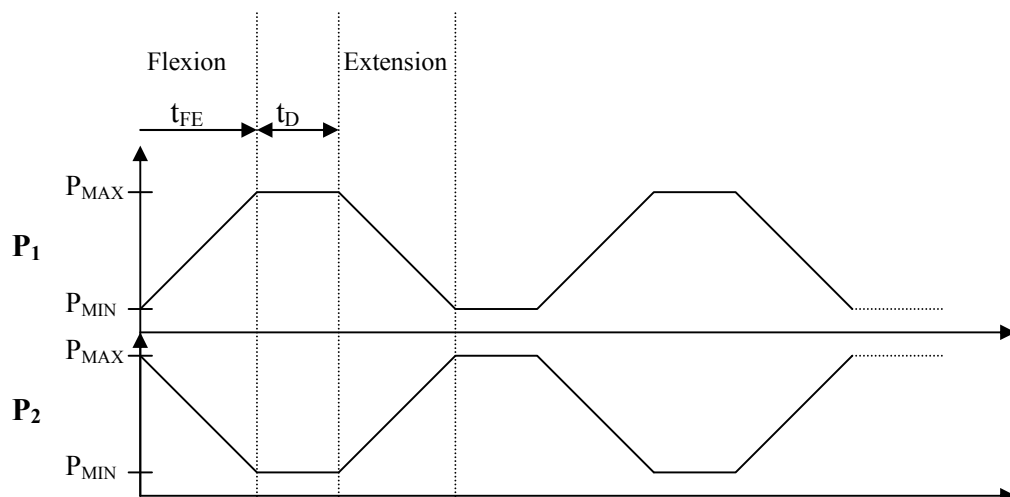


Figure 5.6 Pressure changes during flexion and extension

Examples of the brace angles accomplished for these pressure paths are shown in figure 5.7. Figure 5.7a describes the device fully extended where the pressure in the bicep, P_1 , is at a minimum pressure while the pressure in the triceps, P_2 , is at a maximum. Figure 5.7b shows the brace halfway flexed where the pressures are equal in both muscles while figure 5.7c shows the brace fully flexed where the pressure in the bicep is at a maximum and the pressure in the triceps is at a minimum.

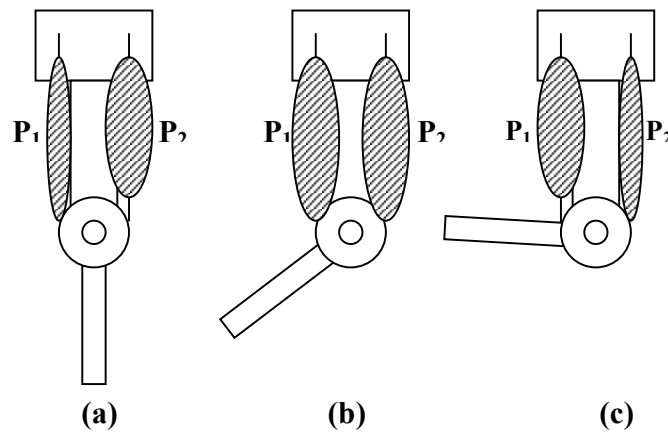


Figure 5.7 Brace angles using antagonistic pair (a) Fully extended [$P_1 = P_{MIN}$ $P_2 = P_{MAX}$] (b) Flexion at approx. 50° [$P_1 = P_2$] (c) Fully flexed at approx. 110° [$P_1 = P_{MAX}$ $P_2 = P_{MIN}$]

A control scheme was designed to force the pressures in each muscle follow the paths depicted in figure 5.6. This control scheme, figure 5.8, used bang-bang control instead of PWM as the means for controlling the pressure in each muscle with a cycle time of 7ms. The controller begins with a signal generator, which either increases in value or decreases in value depending on whether the user pressure button one, B1, or button two, B2. Button one is reserved for flexion of the elbow while button two is

reserved for extension of the elbow. If the user presses button one to flex the elbow then the signal generator increases the pressure in increments of the ADC value of the on board potentiometer divided by 100. As a result, the potentiometer could be used to set the speed of flexion by increasing the pressure increments. If button two for extension is pressed then the signal generator sets the pressure at a max value and decreases this value with the same potentiometer value, which is divided by 100. The output of this signal generator is always signal conditioned for both pressure paths. For the P1 pressure path the signal conditioner uses the same value of the signal generator except that it forces the pressure to conform to equal no less than the minimum pressure and be no more than the maximum pressure. The P2 pressure path takes the signal generator output and subtracts this value from the maximum pressure value and then ensures that it is no greater or less than the maximum and minimum pressures respectively. The signal-conditioned outputs, which are interpreted as desired pressures, are then sent to the bang-bang portion of the controller that calculates the errors between these outputs and the actual pressures read in from the Motorola pressure sensors.

The bang-bang controller for each muscle finally makes a decision on which valves to open and closed based on the sign of the error and if it is outside of a 3-PSI threshold.

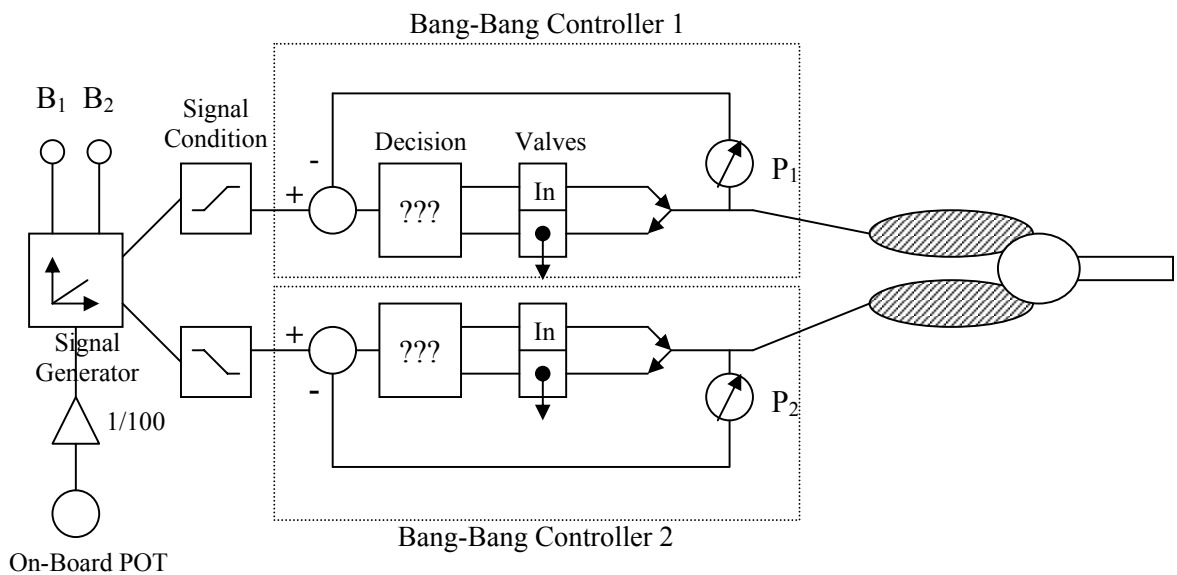
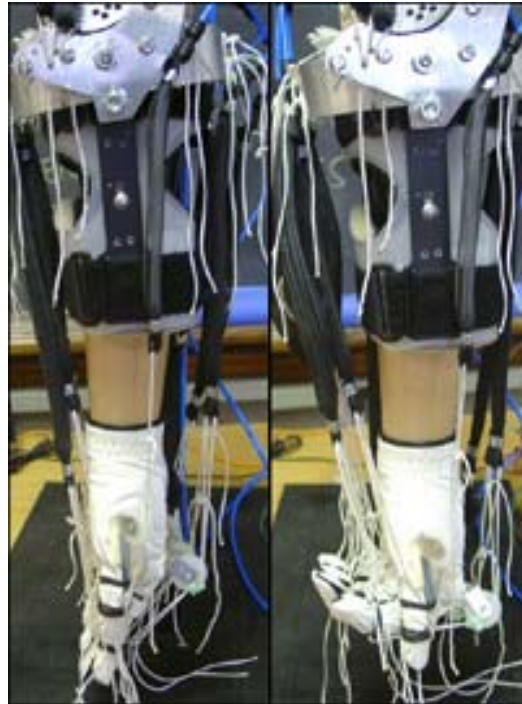


Figure 5.8 Antagonistic Controller Schematic

Values for P_{MAX} and P_{MIN} were 60 and 10 PSI respectively. P_{MIN} was set to 10 PSI instead of 0 PSI because the muscle was considered inflated or deflated at the 10 PSI mark that is indicated in the exhaust graphs in chapter 4. Besides, the time to exhaust the valve from 10 PSI to zero results in a longer settling time according to figure 4.19. This minimum pressure also makes the movement of the muscles more stable for both flexion and extension because the tubing does not have to continue to break the 10 PSI maximum pressure barrier of the tubing. t_{FE} was determined by the analog potentiometer and t_D depended on the time between the user pressing the flexion and extension buttons. Figure 5.9 shows the final results of pressing the flexion and extension buttons on the M32/83C board.



(a)

(b)

Figure 5.9 Flexion and extension using control scheme (a) Extension (b) Flexion

Chapter 6. Conclusions and Suggestions for Future Research

6.1 Conclusions

Experiments with the pneumatic actuated glove and forearm device shows that the pneumatic brace prototype was potential uses and for stroke rehabilitation, demonstrates the capabilities of air muscles for achieving tasks that would normally require a large, external, expensive and dc-motors. Only a glove and a forearm brace are worn by the patient. In addition to the lower cost, the designed air muscles are light weight and will reduce patient fatigue. The usage of air muscle will also reduce the price of the rehabilitation device and affordable and convenient to the home based rehabilitation. The connection of the air muscle in the device is flexible. As a result, if one muscle is damaged, replacement will be easily achieved.

Controlled by MCU and other auxiliary circuits, the device can help the patient make flexion and extension with each finger. One button on the MCU board can achieve the flexion and another button can do the extension. The device can help the patient keep the stationary gesture of the hand, which may benefit the patient to keep the ROM capabilities.

The design of this prototype will lead to the further research on developing a complete upper extremity stroke rehabilitation device. Such devices will hopefully become a reality in the near future to aid the overwhelming and increasing number of stroke sufferers.

6.2 Suggestions for Future Research

There are several possibilities for future research on this device. They are adding goniometers to measure the angles of the finger joints, new rehabilitation glove design and manufacture, more tests on the healthy people and stroke patients and virtual reality training system as the interface between patients and computer.

The angle of a finger is one of the most important characters describing the control range of the rehabilitation device. We currently only measured the final stable angles of the finger joints MP and PIP. For the dynamic joint angle measurement, strain gauges are suggested as a potential measurement device of the goniometer of finger joint angle (Merritt, 2003). This could provide dynamic measurements of the fingers angle.

Currently the design consists with different components from multiplied sources. The gloves and air muscles are connected with rubber rings, nylon ropes. Some pulleys are attached to the gloves to decrease the friction. But these connections may become loose or unstable after the frequent hand movement. The rope is left outside of the glove at present. If there is a twist between different ropes, errors will occur during the control of the finger movement. A new integrated glove is proposed for future research. The glove will have two layers. The inner layer is similar to the rehabilitation glove now. The rubber rings are substituted by some small rings at the finger joints between the two layers. The muscles are connected to the rings by the rope that hidden in the space between the layers. This will prevent ropes from interfering. The outer layer can be opened to make adjustment or maintenance.

More research could be done to measure the performance and characteristics of the air muscles. Besides the wear/tear between the air muscle and the glove, friction between the silicone tubing and braided sleeving is also a reason of the explosion of the air muscle. We found the tubing near the two ends of the air muscle have more possibility to explode. The reason is both tubing and sleeving have irregular shape near the clamps and more friction happens in these areas. Also the contraction percentages of the muscles are only 76%, but the real muscles have contractions closer to 50%. If we could decrease the contraction percentages of the air muscles further, shorter muscles can be used in the design and smaller range of hand motion can be simulated by the rehabilitation device. One of the research suggestions is to find the relationship between the contraction percentages and the components parameters of the muscle, such as diameter ratio and length ratio of the braided sleeving and silicon tubing. The design of the air muscles can follow the parameters that have the best contraction ratio. The other suggestion is to use the pleated muscle discussed in the literature review section (section 2.5.3).

Besides increasing the functions and stability of the hand rehabilitation device, a virtual environment could be developed to increase the interactivity of the stroke patient and the rehabilitation device. It can also create fun for the patient and increase the rehabilitation efficiency potentially. Geometric Forms or Pursuit Patterns in the Franzblau Eye Hand Tracing System can be introduced in the interactivity generated by the virtual environment. One possible inexpensive virtual reality programming environment is Sun's Java 3D (Carey, 2003). A simple example of a possible GUI using Java 3D was created and is shown in figure 6.1. It uses a standard GUI layout with a file menu, figure 6.2, for selecting an existing patient's profile or starting up a new patient's

profile. The GUI also has an options menu, figure 6.3, for setting the individual patients preferences, viewing statistics to see if the patient has improved, and establishing a serial connection, figure 6.4, with the rehabilitative device. The most important feature of the GUI is the Java3D view where the patient can play games and select different games by choosing for the tree in the right hand column.



Figure 6.1 JRehabilitor GUI using Java3D

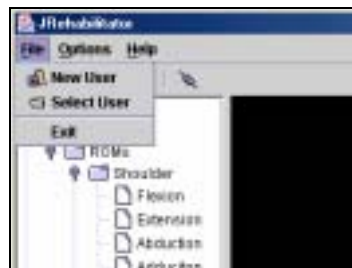


Figure 6.2 File Menu

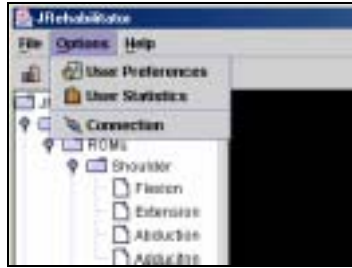


Figure 6.3 Options Menu



Figure 6.4 Connection Dialog

Finally, more tests should be made to the real human hand instead of hand mannequin. In the experiment, the rehabilitation device should be comfortable to the subject. No fatigue should happen other than the normal tiredness in the rehabilitation. Results will be needed to collect and analyze on different stroke patients with different size hands or in different rehabilitation phases. Information from these tests will help the researchers improve comfort and usefulness of the pneumatic rehabilitation hand design.

Chapter 7. Reference

Ambrose, R.O., Aldridge, H., Askew, R.S., Burridge, R.R., Bluethmann, W., Diftler, M., Lovchik, C., Magruder, D. and Rehnmark, F., Robonaut: NASA's Space Humanoid, *IEEE Intelligent System*, 2000.

Barret Hand Webpage:

<http://www.barrettechnology.com/robot/products/hand/handarfr.htm>

Bekey, G.A., Tomovic, R. and Zeljkovic, I., Control Architecture for the Belgrade/USC Hand, *Dexterous Robot Hands*, Springer-Verlag, 1990.

Bonivento, C. and Melchiorri, C., Towards Dexterous Manipulation with the UB Hand II, *12th IFAC World Congress*, Sydney, Australia, 1993.

Bouzit, M., Popescu, G., Burdea, G. and Boian, R., The Rutgers Master II-ND Force Feedback Glove, *Proceedings of IEEE VR 2002 Haptics Symposium*. Orlando, FL, March 2002.

Butterfass, J., Grebenstein, M., Liu, H. and Hirzinger, G. (2001), DLR Hand II: Next Generation of a Dextrous Robot Hand, *IEEE International Conference on Robotics and Automation*, ICRA01, Seoul, Korea, 2001.

Butterfass, J., Hirzinger, G., Knoch, S. and Liu, H. (1999), DLR's Multisensory Articulated Part I: Hard and Software Architecture, *IEEE International Conference on Robotics and Automation*, ICRA98, 1999.

Caffaz, A. and Cannata, G., The Design and Development of the DIST Hand Dextrous Gripper, *IEEE Int. Conf. on Robotics and Automation*, ICRA98, 1998.

Carey, J.R., Kimberley, T.J., Lewis, S.M., Averbach, E.J., Dorsey, L., Rundquist, P. and Ugurbil, K., Analysis of fMRI and Finger Tracking Training in Subjects with Chronic Stroke, *Brain*. 2002(125): 773-788.

Cerullo, L.J., *Stroke Rehabilitation*, Butterworth Publishing, Stoneham, MA, 1986.

Cham, Jorge, Jorge Cham's Qualifying Exam Technical Talk: "Control of a Linkage with Embedded Components". 1999, Available:

http://www-cdr.stanford.edu/biomimetics/documents/cham_qual/.

Chase, T.A. and Luo, R.C., A Capacitive Tri-axial Tactile Force Sensor Design, *IEEE/ASME International Conference on Advanced Intelligent Mechatronics*, 1997.

Colbrunn, R., Design and Control of a Robotic Leg with Braided Pneumatic Actuators, M.S. Thesis, Case Western Reserve University, Cleveland OH, 2000.

Daerden, F., Lefeber, D., Verrelst, B. and Van Ham, R. (2001a), Pleated Pneumatic Artificial Muscles: Actuators for Automation and Robotics, *2001 IEEE/ASME International Conference on Advanced Intelligent Mechatronics*. July 8 - 12, 2001, vol. 2, pp. 738 – 43.

Daerden, F., Lefeber, D., Verrelst, B. and Van Ham, R. (2001b), Pleated Pneumatic Artificial Muscles: Compliant Robotic Actuators', *Proceedings of the 2001 IEEE/RSJ International Conference on Intelligent Robots and System*. Oct. 29 - Nov. 3, vol. 4, pp. 1958 – 63.

DIST Hand Webpage:

<http://www.graal.dist.unige.it/research/activities/DISThand/DISThand.html>.

Fearing, R.S., Some Experiments with Tactile Sensing during Grasping, *IEEE International Conference on Robotics and Automation, ICRA87*, 1987.

Franzblau Tracing Pattern Sheets Webpage:

http://www.keystoneview.com/Products/DiagnosticTrainingProducts/Pattern_Sheets.asp.

Fugl-Meyer A.R, Post Stroke Hemiplegia Assessment of Physical Properties, *Scan J of Rehab Med*. 1980(7): 85-93.

Fukaya, N., Toyama, S., Asfour, T. and Dillmann, R., Design of the Tuat/Karlsruhe Humanoid Hand. *IEEE/RSJ Int. Conf. on Intelligent Robots and Systems, IROS'00*, 2000.

Gazeau, J.P., Zegloul, S., Arsicualt, M. and Lallemand, J.P., The LMS Hand: Force and Position Controls in the Aim of Fine Manipulation of Objects, *IEEE International Conference on Robotics and Automation, ICRA01*, Seoul, Korea, 2001.

Immersion Corporation - 3D Technologies Hardware, (Immersion Corporation), Available: <http://www.immersion.com/3d/products/>.

Jacobsen, S.C. et al, Design of the Utah/MIT Dexterous Hand, *IEEE International Conference on Robotics and Automation, ICRA86*, 1986.

Johnston, D., Zhang, P., Hollerbach, J.M., and Jacobsen, S.C., A Full Tactile Sensing Suite for Dexterous Robot Hands and Use in Contact Force Control, *IEEE Int. Conf. Robotics and Automation, ICRA96*, Minneapolis, 1996.

Kawasaki, H., Shimomura, H. and Shimizu, Y. (2001), Educational-industrial Complex Development of an Anthropomorphic Robot Hand 'Gifu hand', *Advanced Robotics*, 15(3), 2001.

- Kawasaki, H., Komatsu, T., Uchiyama, K. and Kurimoto, T. (1999), Dexterous Anthropomorphic Robot Hand with Distributed Tactile Sensor: Gifu Hand II, *IEEE SMC '99 Conference on Systems, Man and Cybernetics*, 1999.
- Krebs, H.I., Williams, D.J. and Hogan, N., A Robot for Wrist Rehabilitation, *Proceedings of the 23rd Annual International Conference of the IEEE Engineering in Medicine and Biology Society*. Oct. 25 – 28, 2001, vol. 2, pp. 1336 – 9.
- Lee, K. and Shimoyama, I., A Skeletal Framework Artificial Hand Actuated by Pneumatic Artificial Muscles, *IEEE International Conference on Robotics and Automation, ICRA99*, Detroit, Michigan, 1999.
- Liu, H., Butterfass, J., Knoch, S., Meusel, P. and G. Hirzinger, A New Control Strategy for DLR's Multisensory Articulated Hand, *IEEE Control Systems Magazine*, 19(2), 1999.
- Lovchik, C.S. and Diftler, M.A., The Robonaut Hand: A Dexterous Robot Hand for Space, *IEEE International Conference on Robotics and Automation, ICRA99*, 1999.
- McCammon, I.D. and Jacobsen, S.C., Tactile Sensing and Control for the Utah/MIT Hand, *Dexterous Robot Hands*, Springer-Verlag, 1990.
- Melchiorri, C. and Vassura, G. (1993), Mechanical and Control Issues for Integration of an Arm - Hand Robotic System, *Experimental Robotics II, the 2nd Int. Symposium*, Springer-Verlag, 1993.
- Melchiorri, C. and Vassura, G. (1992), Mechanical and Control Features of the UB Hand Version II, *IEEE/RSJ Int. Conf. on Intelligent Robots and Systems, IROS'92*, 1992.
- Merritt, Cary R. and Grant, Edward, A Pneumatically Actuated Brace Designed For Upper Extremity Stroke Rehabilitation, M.S. Thesis, North Carolina State University, Raleigh NC, 2003
- Okada, T., Computer Control of Multi-jointed Finger System for Precise Object Handling, *International Trends in Manufacturing Technology - Robot Grippers*. 1986.
- Pedretti, L.W., *Occupational Therapy: Practice Skills for Physical Dysfunction*, 2nd ed., C.V. Mosby Co. St. Louis, Missouri, 1985.
- Reddy, M.P and Reddy, V, Stroke Rehabilitation, *American Family Physician*. vol. 55, no. 5, pp. 1742 – 8.
- Reinkensmeyer, D.J., Pang, C.T., Messler, J.A. and Painter, C.C. (2002a), Web-Based Telerehabilitation for the Upper Extremity after Stroke, *IEEE Transactions on Neural Systems and Rehabilitation Engineering*. June 2002 (10) 102-108.

Reinkensmeyer, D.J. (2002b), Rehabilitators, in: Kutz, M., *Biomedical Engineer's Handbook*, McGraw-Hill.

Reinkensmeyer, D.J., Pang, C.T., Messler, J.A. and Painter, C.C., Java Therapy: Web-based Robotic Rehabilitation: Integration of Assistive Technology in the Information Age, *Proceedings 7th International Conference on Rehabilitation Robotics*, April 25-27, 2001, IOS Press, Amsterdam, pp. 66-71.

Robonaut Webpage: <http://robonaut.jsc.nasa.gov/>.

Post-Stroke Rehabilitation, U.S. Dept. Health and Human Services, Public Health Service, National Institutes of Health. Bethesda, Maryland, 2000.

Rowland, L.P., Stroke, Spasticity and Botulinum Toxin, *N Engl J Med.* 8 Aug, 2002, 347(6): 382-383.

Salisbury, K.S. and Roth, B., Kinematics and Force Analysis of Articulated Mechanical Hands, *Journal of Mechanisms, Transmissions and Actuation in Design*, 105, 1983.

Shadow Hand Webpage: <http://www.shadow.org.uk/products/newhand.shtml>.

Shadow Robot Company: Air Muscles (2002, Sept. 10 – last update), (Shadow Robot Company), Available: <http://www.shadow.org.uk/products/airmuscles.shtml>.

SportRAC Webpage: http://www.performancehealth.com/rac_home.html.

Stroke Rehabilitation Information, (2001, July 1 – last update), (National Institute of Neurological Disorders and Stroke), Available: http://www.ninds.nih.gov/health_and_medical/pubs/stroke_rehabilitation.htm.

Townsend, W.T., MCB - Industrial Robot Feature Article - Barrett Hand Grasper, *Industrial Robot: An International Journal*, 27(3), 2000.

Upper Extremity Anatomy Webpage: <http://www.rad.washington.edu/atlas/>.

van Varseveld, R.B. and Bone, G.M., Accurate Position Control of a Pneumatic Actuator Using On/Off Solenoid Valves, *Proceedings of the 1997 International Conference on Robotics and Automation*. April. 1997, Albuquerque, New Mexico, pp. 1196 - 1201.

Woldag H. and Hummelsheim H., Evidence-based Physiotherapeutic Concepts for Improving Arm and Hand Function in Stroke Patients, *J Neurol.* 2002: 518-528.

Chapter 8. Appendices

8.1 Robot Kinematics

Robot kinematics is the analytical study of the geometry of motion of a robot. It is:

- With respect to a fixed reference co-ordinate system
- Without regard to the forces or moments that cause the motion.

8.1.1 Homogeneous Transform Matrix

The homogeneous transform matrix is used on the relationship between two frames. It is effective on a translation and a rotation. Suppose there is a frame transformation as figure 8.1, then the transform matrix between the two coordinate is as figure 8.2.

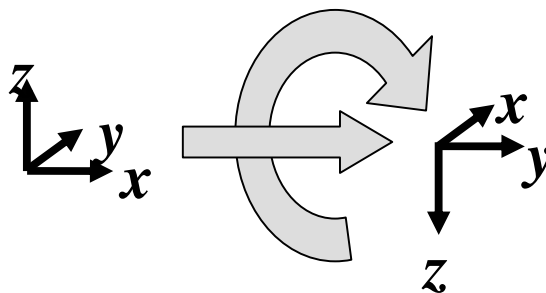


Figure 8.1 Frame Transformation

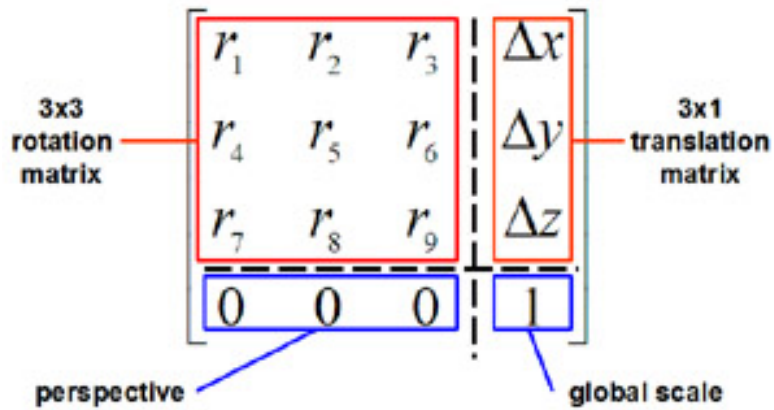
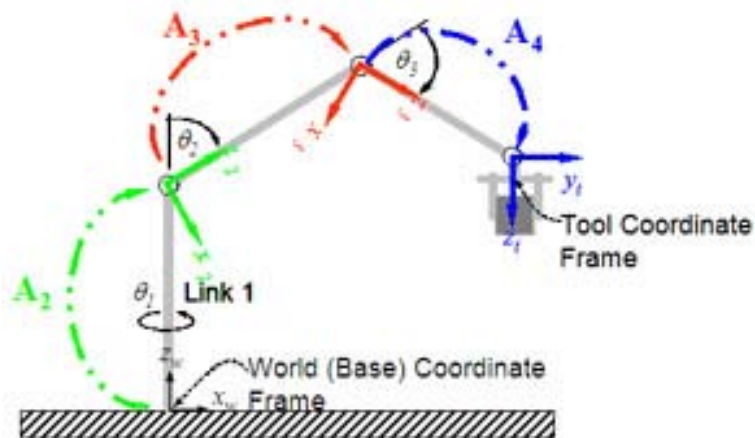


Figure 8.2 Homogeneous Transform Matrix

8.1.2 Link Transformation

For a robot with several segments and each adjacent segments are connect by a rotatable link, the overall transformation matrix K is equal to the product of the link transformation in sequence. In figure 8.3, the tool coordinate frame is equal to the world coordinate frame multiply the transformation matrix K of the whole system.



$$K = A_1 A_2 A_3 \dots A_n$$

Figure 8.3 System transformation matrix K

For each pair of adjacent segments, the link that connects them has the following parameters and the graph is shown in figure 8.4

Table 8.1 Link parameters

Parameters	Description
l_n	The length of the link (the distance along the common normal between the joint axes)
α_n	The twist angle between the joint axes
q_n	The angle between the links
d_n	The distance between the links (the displacement, along the joint axes between the links)

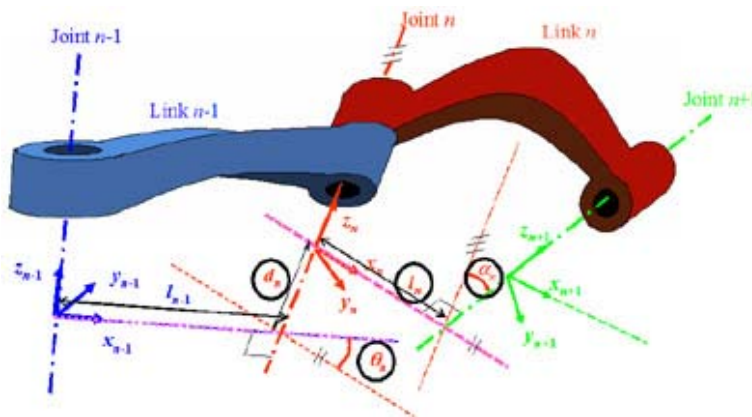


Figure 8.4 Link of two adjacent segments

In figure 8.4, the z_n axis points along the n^{th} axis. The origin of the n^{th} frame is on the n^{th} axis at the point of the common perpendicular with the $n+1$ frame. The x_n

axis points along the perpendicular, or if the axes intersect, x_n is normal to the plane containing the two axes. The y_n axis completes a right-handed coordinate system.

l_n = the distance from z_n to z_{n+1} measured along x_n .

α_n = the angle between z_n and z_{n+1} measured about x_n .

d_n = the distance from x_{n-1} to x_n measured along z_n .

q_n = the angle between x_{n-1} to x_n measured about z_n .

Translate along x_{n-1} a length l_{n-1} .

Rotate about x_{n-1} the twist angle α_{n-1} .

Rotate about z_n an angle q_n .

Translate along z_n a distance d_n .

Then the link transformation matrix is as figure 8.5:

$${}^{n-1}T_n = T_n = T_z(l_{n-1})R_x(\alpha_{n-1})R_z(\theta_n)T_z(d_n) = \begin{bmatrix} c\theta_n & -s\theta_n & 0 & l_{n-1} \\ s\theta_n c\alpha_{n-1} & c\theta_n c\alpha_{n-1} & -s\alpha_{n-1} & -s\alpha_{n-1}d_n \\ s\theta_n s\alpha_{n-1} & c\theta_n s\alpha_{n-1} & c\alpha_{n-1} & c\alpha_{n-1}d_n \\ 0 & 0 & 0 & 1 \end{bmatrix} \quad (8.1)$$

Figure 8.5 Link transformation matrix

And the system transformation matrix is: $K = {}^0T_1 \cdot {}^1T_2 \cdot {}^2T_3 \cdots {}^{n-1}T_n$ (8.2)

8.2 Controller and Experiment Code

8.2.1 Main.h and Main.c

8.2.1.1 Main.h

```
// Main.h
// author Carey Merritt

void main(void);
void buttons_init(void);
void bang_flexion(void);
void bang(void);
void sampleLength(void);
void samplePressure(void);
void sampleLeakage(void);
void sampleExhaust(void);
void sampleFlow(void);
void wait(unsigned long t);
```

8.2.1.2 Main.c

```
// main.c
// author Carey Merritt

#include "sfr83v100.h"    /* SFR register definition */
#include "main.h"        /* main.c definition */
#include "timer.h"
#include "ad.h"
#include "board.h"
#include "serial1.h"
#include <stdio.h>

#define v1IN p12_0        // inlet valve for muscle 1
#define v1EX p12_1        // exhaust valve for muscle 1
#define v2IN p12_2        // inlet valve for muscle 2
#define v2EX p12_3        // exhaust valve for muscle 2

volatile unsigned long system_counter = 0;
volatile unsigned int ad0_value = 0, ad4_value = 0, ad6_value = 0;
volatile unsigned int ad7_value = 0;

volatile unsigned char button_1;        // Button 1 pressed flag
volatile unsigned char button_2;        // Button 2 pressed flag
volatile unsigned char button_3;        // Button 3 pressed flag

unsigned const char clear[] = "                \0";
unsigned const char UART_NOFLICKER1[] = {'\r', ' ', '[', '1', 'A', 0};
unsigned const char UART_NOFLICKER2[] = {'\r', ' ', '[', '2', 'A', 0};

unsigned int pressure[6000];
char out[80];
unsigned int test = 0;

void main(){

    float degreeF;
    int degreeI;
    float m = 0.342787f;    // slope of rotary pot degrees per ad_value
```

```

// for rotary pot there is a dead zone from 335 - 360 degrees so the
// rotary pot should be offset from zero to calibrate. The degree offset
// from zero should be subtracted from the calculation to shift the value
// back. This way we can avoid the deadzone.

// Set BCLK to divide by 1 (Full Speed) from the default divide by 8
prc0 = 1;      // Unlock the System Clock Control Register
mcd = 0x12;    // Set the divide ratio to 1.

prc0 = 0;      // Lock the System Clock Control Register

// Start the 32Khz crystal sub clock
prc0 = 1;      // Unlock the System Clock Control Register
cm04 = 1;     // Start the 32KHz crystal
prc0 = 0;     // Lock the System Clock Control Register

ta0_init();    // Initialize Timer TA0 (Tick Clock)
buttons_init();
ad_init();     // Initialize the A/D Converter
init_uart();

// initialize on board LED's and set data direction for output
pd8_0 = 1;     // set green led4 for output
pd7_4 = 1;     // set up port P7_4 as output (Yellow LED/ LED)
pd7_2 = 1;     // set red led for output
LED2 = 0;
LED3 = 0;
LED4 = 0;

// set data direction for pins to control pneumatic solenoid valves
pd12_0 = 1;    // set data direction register for pin12_0 output
pd12_1 = 1;    // set data direction register for pin12_1 output
pd12_2 = 1;    // set data direction register for pin12_2 output
pd12_3 = 1;    // set data direction register for pin12_3 output
v1IN  = 0;     // A38 on 150 DIN (P120/OUTC30)
v1EX  = 0;     // B38 on 150 DIN (P121/OUTC31)
v2IN  = 0;     // C38 on 150 DIN (P122/OUTC32)
v2EX  = 0;     // A39 on 150 DIN (P123/OUTC32)

// The Pressure sensor 1 is on AN6/P106 and A34 on 150 DIN
// The Pressure sensor 2 for the triceps is located on AN4/P104
// The Rotational sensor is on AN7/P107 and B34 on 150 DIN

while(1){

    // button handler
    LED2 = !p8_2;
    v1IN = !p8_2;

    LED3 = !p8_3;
    v1EX = !p8_3;

    //LED4 = !p8_4;
    //v2IN = !p8_4;

    v2EX = !p9_7;

    // if button 3 pressed then run test routine
    if(!p8_4){
        //bang();
        bang_flexion();
        //flexion();
    }
}

```

```

        //bicepTest();
        //sampleExhaust();
        //samplePressurePWM();
        //samplePressure();
        //sampleLeakage();
        //sampleFlow();
        //generateSquareWave();
        //sampleLength();

        // output length and pressure
        /*
        if(test == 0){
            sprintf(out, "%d %d \r\n", ad7_value, ad6_value);
            writeString(out);
            test = 1;
        }
        */

        //bicepTest();

    }
    else {
        test = 0;
    }

    //writeString(UART_NOFLICKER1);

    //pressure = ((float)ad6_value - 40.96f)/9.0779f;
    //if(pressure < 0.0f)
    //    pressure == 0.0f;
    //sprintf(out, "%d %d\r\n", ad4_value, ad6_value);
    //writeString(out);
    //bang();
    wait(101);

    //display_ad(0, ad6_value, "AD6=\0"); // display pressure
    //display_ad(0, ad0_value, "AD0=\0");
    //display_ad(64, ad7_value, "AD7=\0"); // display angle
}
}

// bang_flexion is the main control algorithm presented in the thesis
void bang_flexion(){
    int error;
    int pmax = 585; // maximum of 60 psi converted to adc
    int pmin = 91; // maximum of 10 psi converted to adc
    int pldesired, p2desired;
    int pinc = 2;
    int desired = 40;
    unsigned char bltoggle = 0;
    unsigned char b2toggle = 0;

    // while button 4 has not been pressed
    while(p9_7){
        // toggle between flexion and extension modes based on
        // button presses on button 1 and 2
        if(!p8_2){
            if(!bltoggle){
                LED2 = 1;
                LED3 = 0;
                bltoggle = 1;
                b2toggle = 0;
                desired = 40;
            }
        }
    }
}

```

```

    }
}
else if(!p8_3){
    if(!b2toggle){
        LED2 = 0;
        LED3 = 1;
        b1toggle = 0;
        b2toggle = 1;
        desired = pmax;
    }
}
pinc = ad0_value/100;    // set increment based on on-board pot value

// signal generator based on button 1 or 2
if(b1toggle)
    desired = desired + pinc;
else if(b2toggle)
    desired = desired - pinc;

    // signal conditioner to make sure desired is less
    // than max psi and greater than min psi
if(desired > pmax){
    desired = pmax;
    p1desired = pmax;
    p2desired = pmin;
}
else if(desired < pmin){
    desired = pmin;
    p1desired = pmin;
    p2desired = pmax;
}
else {
    p1desired = desired;
    p2desired = pmax - desired;
    if(p2desired < pmin)
        p2desired = pmin;
}

    // calculate the error for the bicep
error = p1desired - (int)ad6_value;

// use the error to decide which valves to open
// and allow for a 3 PSI threshold
if(error < -30){
    v1IN = 0;
    v1EX = 1;
}
else if(error > 30){
    v1IN = 1;
    v1EX = 0;
}
else {
    v1IN = 0;
    v1EX = 0;
}

    // calculate the error for the tricep
error = p2desired - (int)ad4_value;

// use the error to decide which valves to open
// and allow for a 3 PSI threshold
if(error < -30){
    v2IN = 0;

```

```

        v2EX = 1;
    }
    else if(error > 30){
        v2IN = 1;
        v2EX = 0;
    }
    else {
        v2IN = 0;
        v2EX = 0;
    }
    wait(71);
}
}

// bang() is a similar control algorithm to bang_flextion
// that converts the angle of the potentiometer to a
// desired pressure for the bicep.
void bang(void){
    int error;
    int desired;
    int pmax = 585;          // maximum of 60 psi converted to adc
    int pmin = 91;         // maximum of 10 psi converted to adc
    int pldesired, p2desired;

    while(1){
        desired = ad0_value + 40;          // set desired to pot value plus 40
                                           // (0 PSI) to make sure that the value
                                           // is a pressure value

        // make sure angle is less than max psi
        if(desired > pmax){
            pldesired = pmax;
            p2desired = pmin;
        }
        else if(desired < pmin){
            pldesired = pmin;
            p2desired = pmax;
        }
        else {
            pldesired = desired;
            p2desired = pmax - desired;
            if(p2desired < pmin)
                p2desired = pmin;
        }

        error = pldesired - (int)ad6_value;

        // use the error to decide which valves to open
        // and allow for a 3 PSI threshold
        if(error < -30){
            v1IN = 0;
            v1EX = 1;
        }
        else if(error > 30){
            v1IN = 1;
            v1EX = 0;
        }
        else {
            v1IN = 0;
            v1EX = 0;
        }

        error = p2desired - (int)ad4_value;
    }
}

```

```

        // use the error to decide which valves to open
        // and allow for a 3 PSI threshold
        if(error < -30){
            v2IN = 0;
            v2EX = 1;
        }
        else if(error > 30){
            v2IN = 1;
            v2EX = 0;
        }
        else {
            v2IN = 0;
            v2EX = 0;
        }

        wait(71);
    }

}

// waits for a time t in ms
void wait(unsigned long t){
    unsigned long waitTime = system_counter + t;
    while(waitTime > system_counter);
}

// sample length for 6 seconds
void sampleLength(void){
    int i;
    unsigned long waitTime;
    system_counter = 0;           // reset system counter

    for(i = 0; i < 6000; i++){
        pressure[i] = ad7_value; // sample angle
        // wait 1ms
        wait(11);
    }

    // output to uart
    for(i = 0; i < 6000; i++){
        sprintf(out, "%d %d \r\n",i,pressure[i]);
        writeString(out);
    }
}

// sample pressure from 0 to max PSI when opening the valve
void samplePressure(void){
    int i;
    unsigned long waitTime;
    system_counter = 0;           // reset system counter
    v1IN = 1;
    for(i = 0; i < 2000; i++){
        pressure[i] = ad6_value; // sample angle
        // wait 1ms
        wait(11);
    }

    v1IN = 0;
    v1EX = 1; // exhaust valve
    wait(20001); // wait 2 seconds
    v1EX = 0; // close exhaust valve
}

```

```

    // output to uart
    for(i = 0; i < 2000; i++){
        sprintf(out, "%d %d \r\n",i,pressure[i]);
        writeString(out);
    }
}

// sample pressure after filling up the muscle with air and closing the valve
void sampleLeakage(void){
    int i;
    unsigned long waitTime;
    system_counter = 0;           // reset system counter
    vLIN = 1;
    wait(1000l);    // open valve and wait for 1s for it to fill up
    vLIN = 0;      // turn off valve and measure leakage - output every 1/2
(500ms) sec

    for(i = 0; i < 240; i++){    // (60*2)*2 -> 2 mins of half second samples
        // output to uart
        sprintf(out, "%d \r\n",ad6_value);
        writeString(out);
        wait(500l);             // wait half a second
    }

    vLEX = 1;
    wait(1500l);    // wait 1.5 seconds for the air muscle to exhaust
    vLEX = 0;
}

// sample pressure from a max PSI after filling up the muscle with
// air and exhausting the muscle
void sampleExhaust(void){
    int i;
    unsigned long waitTime;
    system_counter = 0;           // reset system counter
    vLIN = 1;
    wait(3000l);    // open valve and wait for 1s for it to fill up
    vLIN = 0;      // turn off valve and measure leakage - output every 1/2
(500ms) sec
    wait(5l);
    vLEX = 1;
    for(i = 0; i < 6000; i++){
        pressure[i] = ad6_value;
        // wait 1ms
        wait(1l);
    }
    vLEX = 0;

    // output to uart
    for(i = 0; i < 6000; i++){
        sprintf(out, "%d %d \r\n",i,pressure[i]);
        writeString(out);
    }
}

// samples the flow state when both valves are open
// measurements begin after the muscle is filled with air
void sampleFlow(void){

```



```

    int i;
    unsigned long waitTime;
    system_counter = 0;           // reset system counter
    vLIN = 1;
    wait(20001);                // open valve and wait for 1s for it to fill up
    vLEX = 1;                    // turn on exhaust valve for flow state and measure
pressure
    for(i = 0; i < 1500; i++){
        pressure[i] = ad6_value;
        // wait 1ms
        wait(11);
    }
    vLIN = 0;
    vLEX = 0;

    // output to uart
    for(i = 0; i < 1500; i++){
        sprintf(out, "%d %d \r\n",i,pressure[i]);
        writeString(out);
    }
}

// initializes the 4 on board buttons
void buttons_init(void)
{
    asm("FCLR I"); // Disable all interrupts

    pu24 = 1;        // Turn on the pullups for ports 8_0 through 8_3
    pu25 = 0;        // Turn on the pullups for ports 8_4, 8_6 and 8_7
    pd8_2 = 0;       // Set port 8_2 (button 0) to an input
    pd8_3 = 0;       // Set port 8_3 (button 1) to an input
    pd8_4 = 0;       // Set port 8_4 (button 2) to an input
    int0ic = 0x03;   // Set button 0's interrupt level to 3
    int1ic = 0x03;   // Set button 1's interrupt level to 3
    int2ic = 0x03;   // Set button 2's interrupt level to 3

    // Set the initial values of the button flags and debounce timers
    button_1 = 0;
    button_2 = 0;
    button_3 = 0;

    asm("FSET I"); // Enable all interrupts
}

```

8.2.2 Serial1.h and Serial1.c

8.2.2.1 Serial1.h

```

/*****
*
*   File Name:      serial1.h
*
*   Content:       Header file for the RS232 Serial Port driver for UART0 of
*                 the M32C/80's MCU.
*****/

#ifndef MAIN_CLOCK
#define MAIN_CLOCK      (unsigned long)20e6 // Main clock crystal speed 20MHz
#endif
#define BAUDRATE      115200 // UART0 baud rate
#define DIV_RATE      0 // Valid entries are 0, 1, 2... Where:

```

```

        // 0 = clock divide rate of 1,
        // 1 = clock divide rate of 8,
        // 2 = clock divide rate of 32

#define XMIT_BUFFER_SIZE      80    // Transmit buffer size in bytes.
#define RECEIVE_BUFFER_SIZE  80    // Receive buffer size in bytes.

// Calculate Bit Rate Register Value
// Setting UART0 bit rate generator for 9600 baud
// example: 129 = 20MHz / (16*(n+1)*9600) - 1      :   f1 => n=0
#if DIV_RATE == 0
#define BRG_REG_VALUE (unsigned char)((MAIN_CLOCK/(BAUDRATE*16*1))-1)
#elif DIV_RATE == 1
#define BRG_REG_VALUE (unsigned char)((MAIN_CLOCK/(BAUDRATE*16*8))-1)
#elif DIV_RATE == 2
#define BRG_REG_VALUE (unsigned char)((MAIN_CLOCK/(BAUDRATE*16*32))-1)
#endif

//
//          Some                      handy                      MACROS
//          *****
#define TXEMPTY  0x8          /* transmit register empty */
#define TE       0x1         /* transmit enable          */
#define TI       0x2         /* transmit buffer empty   */
#define RE       0x4         /* receive enable          */
#define RI       0x8         /* receive complete        */

#define ACK      0x40
// #define BUSY   0x20
#define FAULT    0x10
#define RESET    0x8
#define STROBE   0x4
/*****
**/

// Interrupt Processing Functions
#pragma INTERRUPT rcev_isr      // Receive Interrupt Handler.
void rcev_isr(void);

#pragma INTERRUPT xmit_isr     // Transmit Interrupt Handler.
void xmit_isr(void);

void init_uart(void);          // Initial Serial UART0 of M32C/80's MCU.
int  char_rcev(void);          // Test for presence of char in receive queue.
char rcev_char(void);          // Receive single char from receive serial
queue.
void writeString(char * str);
void uart_xmit(char c);

```

8.2.2.1 Serial1.c

```

//serial1.c
#include <string.h>
#include "sfr83v100.h"          /* SFR register definition */
#include "serial1.h"
#include "board.h"

// QUEUE STRUCTURES
char Ser_RCEV_q[RECEIVE_BUFFER_SIZE];
int  SRECV_IN, SRECV_OUT;

void init_uart(void){

```

```

int trash;
ps0_7 = 1;                // set port 6_7 to TxDO function page

ulmr = 0x05;              // 8 bits, Internal clock, one stop bit,
Parity disabled, sleep mode deselected.
//ulbrg = BRG_REG_VALUE;  // bite rate generator register - 0 (n+1)
ulbrg = 10;               // 10 is for 115000bps baud
ulc0 = 0x10;              // f1(main clock), no CST/RST, TXD is CMOS
output, transmit on falling edge, MSB first.

// Initialize Queues
//SXMIT_IN = 0;           // Init queues indexes.
//SXMIT_OUT = 0;
SRECV_IN = 0;
SRECV_OUT = 0;

ultb = 0;                 // clear transmit buffer register
ulc1 = u0c1;

ulc1 |= RE;               // receive enable
trash = ulrb;             // clear receive buffer by reading it
ulc1 &= 0x0b;             // receive disable

_asm("fclr i");           // disable interrupts

slric = 0x02;             // UART1 receive interrupt control register -
priority = 2

ulc1 |= RE;               // receive enable
ulc1 |= TE;               // transmit enable

_asm("fset i");           // enable interrupts
}

//Interrupt handler for the receive buffer
void rcev_isr(void){
    static char received;
    LED3 ^= 1;             // toggle yellow LED3
    received = ulrb;
    Ser_RCEV_q[SRECV_IN] = received;
    if(++SRECV_IN >= RECEIVE_BUFFER_SIZE)
        SRECV_IN = 0;
    ulc1 |= RE;           // receive enable
}

void xmit_isr(void){

}

void writeString(char * str){
    int temp;
    temp = strlen(str);
    while(temp--){
        // wait for data to be grabbed by remote connection i.e. data is still
on the transmit buffer
        while(( ulc1 & 0x02) == 0);
        ultb = (unsigned short) *str++;
    }
}

// transmit a single character
void uart_xmit(char c){

```

```

    // wait for data to be grabbed by remote connection i.e. data is still on
the transmit buffer
    while(( ulc1 & 0x02) == 0);
    ultb = c;
    LED4 ^= 1;
}

//Receive single char from receive serial queue.
char rcev_char(void){ // Receive single char from receive serial
queue.

    char data;
    if(SRECV_OUT != SRECV_IN){
        data = Ser_RCEV_q[SRECV_OUT];
        if(++SRECV_OUT >= RECEIVE_BUFFER_SIZE)
            SRECV_OUT = 0;
        return data;
    }
    else
        return 0xff;
}

//returns 1 if received data is in the receive queue. Checks queue buffer for
receive data.
int char_rcev(void){
    if(SRECV_OUT == SRECV_IN)
        return 0;
    else
        return 1;
}

```

8.2.3 adc.h and adc.c

8.2.3.1 adc.h

```

// ad.h
// author: Carey Merritt

#pragma INTERRUPT ad_int // define ad_int() to be an interrupt routine
void ad_int(void); // AD conversion interrupt routine

void ad_init(void); // initialize the A/D converter

```

8.2.3.1 adc.c

```

// ad.c
// author: Carey Merritt

#include "sfr83v100.h" // SFR register definition
#include "main.h" // Include the ain header file for any
definitions
#include "ad.h" // Header definitions for this file

extern unsigned int ad0_value;
extern unsigned int ad4_value;
extern unsigned int ad6_value;
extern unsigned int ad7_value;

unsigned char channel;

```

```

/*****
Name:      AD_init
Parameters: None
Returns:   None
Description: Initializes the A/D converter to a single mode 10 bit conversion
            using the sample and hold circuit and using the fAD/2
conversion
            clock. Also set up the A/D converter to convert channel AN0
*****/
void ad_init(void)
{
    //_asm("fclr i");
    ad0con0 = 0x80; // Set the AD to AN0 input, One shot Mode,
                  // Software trigger
                  // and a fAD/2 conversion clock

    ad0con1 = 0x28; // Connect Vref and set the AD to a 10bit conversion
    ad0con2 = 0x01; // Enable the Sample and hold circuit
    ad0ic = 6;     // Set the interrupt priority level to 6

    pd9_7 = 0;    // Set the A/D pin to an input //for ADTRG

    channel = 0;
    adst_ad0con0 = 1;

    //_asm("fset i");
}

//This is that ad completion interrupt routine.
void ad_int(void){

    switch (channel){
        case 0:
            ad0_value = ad00;           // onboard pot
            channel = 4;
            break;
        case 4:
            ad4_value = ad04;
            channel = 6;
            break;
        case 6:
            ad6_value = ad06;
            channel = 7;                 // next channel is channel 7
            break;
        case 7:
            ad7_value = ad07;
            channel = 0;                 // next channel is channel 0
            break;
        default: break;
    }

    ad0con0 = 0x80 | channel;
    adst_ad0con0 = 1;                   // start next conversion
                                        // clear interupt flag is handled by hardware
}

```

8.2.4 Board.h

```

// board.h
// author Carey Merritt

```

```

/*****
 *
 *   File Name:    board.h
 *
 *   Content:     Macros for access to items on the M32c/83 evaluation board
 *****/

#define LED2 p7_2
#define LED3 p7_4
#define LED4 p8_0
#define LED5 p15_1

```

8.2.5 Timer.h and Timer.c

8.2.5.1 Timer.h

```

// timer.h
// author Carey Merritt

#pragma INTERRUPT ta0_int      // define ta0_int() to be an interrupt routine
void ta0_int(void);          // Timer A0 interrupt routine

void ta0_init(void);

```

8.2.5.2 Timer.c

```

// timer.c
// author Carey Merritt

#include "sfr83v100.h"      // SFR register definition
#include "main.h"          // Include the main header file for any definitions
#include "timer.h"         // Header definitions for this file

// Redefine the variables that these routines need to use but are defined
// in another module
extern volatile unsigned long system_counter; // background counter

int time_cnt = 0;

/*****
Name:      ta0_int
Parameters: None
Returns:   None
Description: This is the timer A0 interrupt routine. It updates the timer count
              every timer a0 interrupt (every milisecond).
 *****/
void ta0_int(void){
    system_counter++;
}

/*****
Name:      TA0_init
Parameters: None
Returns:   None
Description: Initializes the timer A0 interrupt
 *****/
void ta0_init(void){
    _asm("fclr i");
    ta0mr = 0x40;      // Set Timer A to a Timer operating at f8
    //ta0 = 1999;     // Set the timer to fire every lms

```

```
    ta0 = 2499;          // Set the timer to fire every 1ms
    ta0s = 1;           // Start the timer
    ta0ic = 2;          // Set the interrupt Priority level to 2
    _asm("fset i");
}
```